UNIVERSITY OF TWENTE

MSC THESIS REPORT

Unveiling the Implications of Schematisation Choices in Fluvial Flood models

Dike breach induced floods in Betuwe Tieler en Culemborgerwaarden

---

Author:
Ruben den Hertog

Supervisors:
Dr.Ir. Martijn Booij
Ir. Max Leummens
Ir. Marcel van den Berg
P. Khorsandi Kuhanestani

August 10, 2024
Final version

UNIVERSITY OF TWENTE.

Royal HaskoningDHV

Preface

During my studies, I developed a deep interest in modelling studies and hydraulic models in general. Flood safety in the Netherlands and large floods were topics that captivated me. When Isabelle Schippers completed her thesis, she shared her insights, sparking the idea for more exciting research into this topic. This idea was quickly embraced and supported by Marcel van den Berg, leading to this master thesis. I was fortunate to be part of the Flood Protection team at Royal HaskonigDHV during my thesis project. Their attention, knowledge and resources not only enabled me to start and complete my thesis but also made me feel a part of the organisation. A big thanks to my colleagues in the Flood Protection team.

I want to express my gratitude to my daily supervisors at Royal HaskoningHDV, Marcel van den Berg and Max Leumens. Our numerous discussions about the interpretation of my results, flood risk context, or just ways of schematising or executing something have inspired me and significantly contributed to the quality and relevance of my research. I want to extend the same gratitude to my supervisors from the University of Twente, Parisa Khorsandi Kuhanestani and Martijn Booij. Your guidance in the set-up and structuring of my research and writing my report was not only necessary but has greatly helped in the quality, too.

I want to thank Marcel van de Waart of Water Board Rivierenland for providing me with the models I used. Your input at the start of my research helped me immensely in the set-up and finding interesting subjects for my research. I thank Sam Westerhof for providing me with tips and guidance when I tried to comprehend the workings of Delft-FLS at the start of my research. I often opened your thesis report for reference or inspiration during my own thesis project. Finally, I want to thank Rineke Hulsman for taking the time to help me with some small modelling things and providing me with the insight that meant a breakthrough in my indefinite struggles with my models.

My hope is that my research will not only contribute to an increase in practical knowledge in the application of hydraulic models for fluvial flood simulations, but also to the improvement of Dutch flood models. I see this research serving as a guide to modellers in the policy domain for future fluvial flood model schematisations, paving the way for more effective and accurate flood simulations. I am optimistic about the potential impact of this research and I hope it inspires others in the field.

Ruben den Hertog
August 10, 2024
Enschede

Email address:

Phone:
LinkedIn:

Summary

Since 2017, the Netherlands adopted a new risk-based flood safety assessment. Currently, voices are raised to advocate for an integral area assessment. Next to the assessment of primary flood defences, measures can be designed within the area that achieves the same safety requirements as strengthening dikes by looking at the impact of a flood. Reliable flood models and detailed flood simulations are needed to carry out such an area assessment. Modelling software is constantly updated and new software is designed like D-HYDRO. Flood models are complex, and their accuracy depends on many modelling choices and schematisation possibilities. The goal of this research is to unveil the implications of the use of D-HYDRO and its different schematisation possibilities for the computation of dike breach flow and water distribution in fluvial flood models. Doing so provides a future guide for modellers in their model schematisation for current and future goals of fluvial flood models.

For this, comparative analyses between models with different schematisations have been used. Firstly, the implications of the D-HYDRO software as opposed to the Delft-FLS software are analysed. This is done by rebuilding a Delft-FLS model in D-HYDRO using the same schematisation. This has shown no significant differences between the two software packages in the computation of water distribution. Differences only arise when newer schematisation techniques are added to the D-HYDRO model. However, the computation of dike breach flow is largely different between Delft-FLS and D-HYDRO. Delft-FLS uses a simple weir equation, while D-HYDRO uses the 2D-shallow water equations. This makes the flow through a breach in D-HYDRO dependent on the energy conservation upstream of the breach. It accounts for friction around the breach, velocity gradients and streamlines on the river. In D-HYDRO, significant differences in breach discharge can be found at locations with similar water levels but different flow directions, flow velocities, bottom slope or channel width. In general, D-HYDRO will compute much lower breach discharges than Delft-FLS. These findings have practical implications for flood risk assessments, potentially leading to more accurate predictions of flood scenarios.

Secondly, the effect of alternative river schematisations as opposed to a detailed 2D river schematisation are analysed. Because of the dependence on upstream energy conservation, breach flow in D-HYDRO is sensitive to local water level decreases around the breach, local flow velocities in flood plains, bed friction, dry areas, and local elevations around the breach. A 2D river schematisation can capture all these local influences. However, using a water level boundary or a 1D river schematisation can result in significantly lower runtimes. By comparing results from these schematisations with a detailed 2D river model, this research has shown that these approaches significantly overestimate breach discharge. Using a water level boundary at the river axis causes a main flow direction towards the dike breach because river flow is not computed. It also reduces water level drawdown. The values of a 1D simulation are averaged over a cross-section. Main channel hydraulic conditions have a more significant and direct effect on breach discharge in this schematisation. The effects of a breach on the main channel flow can far upstream depending on the river's slope. It is, therefore, essential to schematise the area around the breach location using a detailed 2D grid and place boundary conditions at least 20 km upstream of the breach location for breach locations in the Waal.

Thirdly, this research compared breach initiation moments and growth equations using a detailed 2D river model. Next to the computation of upstream hydraulic conditions, breach initiation moment and breach growth are important schematisation choices in modelling breach flow. This research has unveiled considerable implications of the Verheij-vdKnaap equation and has introduced promising alternative breach growth equations. The Verheij-vdKnaap equation does not consider underlying developments in flow velocities, flow height and upstream energy level. This makes the final breach width insensitive to the moment of breaching, which hides the possible devastating effect that a breakthrough before peak water level can have. This research shows that breach growth formulations based on flow velocity and flow height in the breach are increasingly sensitive to the moment of breaching and the computed hydraulic conditions in the breach. Using the Verheij-vdKnaap equation in D-HYDRO limits the computed breach width and can significantly underestimate the actual breach width. The alternative breach growth equations shown in this research are proven to better relate breach growth to hydraulic conditions computed by the model.

Finally, the implications of two essential aspects of a fluvial flood model area are analysed. These aspects are the schematisation of elevated elements and waterways. Elevated elements can be schematised in D-HYDRO by introducing fixed weirs on the grid. By comparing a schematisation without fixed weirs and a schematisation with fixed weirs, this research has shown the implications of this schematisation technique for flood model results. Comparing schematisations with an overestimated waterway and an accurate waterway has shown the significant influence of waterways on flood simulation results. Implementing fixed weirs means much lower flow velocities over elevated elements are computed. These lower flow velocities cause higher water depths upstream of the elevated element and a delay in the flood wave. However, for maximum inundation, it is more critical to schematise the elevated line's dimensions accurately. Waterways have a significant influence on the propagation of a flood wave and the discharge of water to lower areas. Locations around waterways inundate far before the actual flood wave reaches that location. A waterway must be sufficiently large relative to the magnitude of the flood wave and the storage capacity of the surrounding area to have a significant impact. Waterways with enough discharge capacity relative to the flood wave can significantly lower maximum inundation depths and maximum rise rates.

This research has unveiled the implications of breach flow computation in D-HYDRO on breach discharge as opposed to Delft-FLS. It has identified prominent influencing factors in breach flow computation and has shown that alternative river schematisations have significant effects that can vastly overestimate breach discharge. This research has revealed flaws in the Verheij-vdKnaap equation for breach growth. It has shown that this approach can underestimate breach width and does not reflect computed hydraulic conditions. Effects of breach flow computation, breach growth computation, and local effects or fixed weirs and waterways can be translated to other areas in the Netherlands and fluvial flood simulations in general. However, global effects are primarily dependent on area characteristics. River or coastal areas with tidal influences might result in different quantifications of the effects of varying breach growth schematisation on dike breach discharge. Qualification of 1D, water level boundary or Verheij-vdKnaap approaches might differ in these areas. Therefore, this research topic should be extended to an international context, to smaller dike rings in the Netherlands and areas with prominent tidal influences. Further research should also focus on developing a new breach growth equation. Extensive field experiments that represent actual breach conditions in the upper river area (prolonged periods of high water, increasing water level after breakthrough, significant flow velocity upstream, oblique main flow direction and large breach width) can significantly contribute to this.

Contents

List of Figures

List of Tables

Glossary

Concept	Defenition/Explanation
3Di	Hydrodynamic modelling package developed by Nelen & Schuurmans
Advection	The transport of a substance or quantity by bulk motion in a fluid.
Amsterdam Rijn Kanaal (ARK)	Canal in the Netherlands
Arrival time	Moment in time when water depth reaches 10 centimer
Bathymetry	Underwater depth or bedlevel
Bernoulli's principle	Principle stating that an increase in the speed of a fluid occurs simultaneously with a decrease in static pressure or a decrease in the fluid's potential energy.
Compartementalise	The process of dividing something into sections. Blocking flow in flood models
Culvert	A structure that allows water to flow under a road or similar obstruction
D-HYDRO	Hydrodynamic model developed by Deltares. characterised by its flexible mesh
Delft-FLS	A hydrodynamic model widely used in the Netherlands for flood simulation. Developed by Deltares
Deltares	An independent institute for applied research in the field of water and subsurface, based in the Netherlands.
Deltaprogramma	Dutch government program that aims to protect the Netherlands against the impact of climate change, including sea level rise and river discharge
Digital elevation model	A 3D representation of a terrain's surface created from terrain elevation data.
Hydraulic conditions	Water depth, flow direction and flow velocity
Kinetic energy	The energy of an object or fluid due to its motion
Maximum inundation	Maximum water depth of a grid cell at any point in time reached in a simulation [m]
Maximum Rise rate	Highest rise rate of a grid cell over the first 1.5 meters of water depth [m/h]
Momentum	A property of a moving object that the object has by virtue of its mass and motion
Navier stokes equations	Set of equations that describe the motion of fluid substances
Python	An interpreted, object-oriented, high-level programming language
Rijkswaterstaat	The Dutch government body responsible for the design, construction, management and maintenance of the main infrastructure and water bodies in the Netherlands
Schematisation	Building blocks of a hydraulic model. For instance a grid, boundary conditions, dambreaks, bed elevation, roughness
SOBEK	Hydrodynamic model that couples 1D and 2D flow, developed by Deltares
Sub-critical flow	State of flow in open channels associated with a Froude number less than one, indicating slower, deeper flow.
Super critical flow	State of flow in open channels associated with a Froude number greater than one, indicating faster, shallower flow
Trachytope	Name of complex roughness formulations in D-HYDRO
Tygron	Engineering modelling package developed by Maxim Knepfle en Florian Witsenburg
Upper River Area	River area in the Netherlands characterised by high discharges and negligible tidal influences. Area east of Hagenstein, Tiel and Lith
VNK1	Abbreviation for the first phase of the "Veiligheid Nederland in Kaart" project
VNK2	Abbreviation for the second phase of the "Veiligheid Nederland in Kaart" project
Wall shear stress	The shear stress in the layer of fluid next to the wall of a pipe or channel
Water Board	Government responsible for water management in a specific region of the Netherlands
Water level boundary	Defined water level in time at certain location in a hydraulic model
Weir	A barrier across a river designed to alter its flow characteristics. Pooling water behind them while also allowing it to flow steadily over their tops.

1 Introduction

1.1 Background

For many countries worldwide, flooding is a severe potential risk; a country like the Netherlands is no exception. Its location in the Rhine and the Meuse River delta makes 59% of its land surface susceptible to flooding (PBL, 2007). Dike rings enclose these flood-prone areas. In the 21st century, the Dutch government started two large water safety projects. An overview of the consequences of flooding had to be provided for the entire country. This research is called "Veiligheid Nederland in kaart" or VNK (Arcadis et al., 2005). This is the predecessor of the larger project VNK2 (Ministerie van Infrastructuur en Milieu et al., 2011). Policymakers had to assess the impacts of large-scale flooding with "what if" scenarios. As large-scale experiments are not feasible, these "what if" scenarios are approximated by careful simulations of dike breaches and flood wave propagation. These simulations use computer models that predict inundation patterns based on solutions to the Navier-Stokes equations. The model used is called Delft-FLS (Stelling et al., 1998). Later in the project, updated models based on Delft-FLS, like SOBEK1D2D (Verschelling, 2000), were used. The VNK2 project was concluded in 2014.

Since 2017, the Netherlands adopted a new multi-layer risk-based flood safety assessment (ENW, 2017). This means that, besides decreasing flood probability (layer 1), policymakers should look at a sustainable layout of areas (layer 2) and crisis management (layer 3). Although the focus is still mainly on decreasing flood probability (strengthening dikes), failure to mitigate climate change may make a more integral approach inevitable (OECD, 2014;Kaufmann et al., 2015). Van den Berg, Westerhof and Huting advocate for an integral area assessment (Havermans, 2024). Next to the assessment of primary flood defences, measures can be designed within the area that achieves the same safety requirements as strengthening dikes by looking at the impact of a flood. This can be combined with nature and housing development and can have profound economic benefits. Reliable flood models and detailed flood simulations are needed to carry out such an area assessment. Flood models are complex, and their accuracy depends on many modelling choices, making knowledge of their application essential.

As computational power and technical possibilities constantly advance, models are updated, and newer models are developed. A prime example of this is the recently developed hydrodynamic modelling package, D-HYDRO (Deltares, 2023a). This package, now widely used amongst engineering companies and Water Boards, has significantly increased the possible schematisation choices compared to Delft-FLS and SOBEK1D2D. By implementing these newer possibilities in flood modelling, different results are achieved as opposed to those from older software (Schippers, 2023). The absence of field measurements in dike breach situations makes evaluating model performance in the real world hard to do. Model results are only validated based on expert judgement. Validation could also be achieved through cross-comparison with other widely available modelling software. When different schematisation choices are made in a newer model instead of schematisation decisions of an older validation model, it is essential to understand the impact of these other choices. Studies into the consequences of floods and dike breaches use various modelling software worldwide. This makes a significant contribution to scientific proficiency in the application of complex hydraulic models for flood simulations and assessment of flood adaptation measures of global significance. Practical knowledge among engineers, researchers, and policymakers on the application of these flood models must be augmented constantly. This is emphasised by the publication of an updated guideline on inundation modelling in 2018 (De Bruin, 2018) and recent research into breach modelling (Verbeek, 2019;Van Damme, 2020).

This research specifically focuses on applying hydraulic models for fluvial flooding, using a case study in the Netherlands. The study involves a comparison between flood simulation results achieved with an older schematisation used in Delft-FLS and results obtained with the newer modelling software D-HYDRO. Furthermore, the research compares the results of different schematisations in D-HYDRO. By unveiling the consequences of schematisation choices for dike breach flow and water distribution, this research aims to increase practical knowledge in the application of hydraulic models in fluvial flood simulation, increase the applicability of model cross-validation, reduce uncertainty in risk assessment due to modelling choices, improve Dutch flood models and guide modellers in the policy domain in a shift to the latest developed modelling possibilities.

1.2 State of the art in flood modelling

The two VNK projects have mapped the flood safety of the entire Netherlands. Flood modelling was the most important tool (De Bruin, 2018). Flood modelling is used in flood risk assessments, crisis management, spatial planning and spatial adaptation projects. For different project goals, different flood output variables are essential. Fast runtimes are very important for flood forecasting, while accurately representing flood and inundation patterns is more important for risk assessment (Teng et al., 2017). When a flood simulation is done in the context of evacuation planning, the arrival time of the water is the most crucial output variable. Table 1.1 overviews project goals and the most critical output variables.

TABLE 1.1: Important project goals and output variables

Project goal	**Important output variables**
Flood risk assessment	Maximum inundation depth Maximum rise rate Maximum flow velocity
Crisis management	Arrival time Rise rate
Spatial planning	Inundation pattern Inundation depth Flow velocity Rise rate Arrival time
Spatial adaptation	Inundation pattern Inundation depth Flow velocity Rise rate Arrival time

Flood modelling software can generate all these variables for analysis and further calculations. To guide modellers and increase consistency in all these flood modelling projects with different goals, Deltares and Rijkswaterstaat developed a guideline (De Bruin, 2018). This guideline advises on the choice for flood scenarios, schematisation and reporting. The flood pattern, calculated with a flood simulation, is determined by two factors: the volume of water that flows into the area and the distribution of water across the region (De Bruin, 2018). The former depends on how hydraulic conditions outside the dike ring and the dike breach are modelled, and the latter depends mainly on the schematisation choices and area characteristics. The schematisation of a flood model is not straightforward and has changed over the last 20 years.

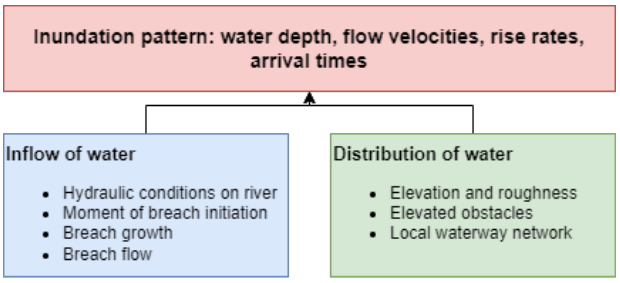

FIGURE 1.1: Factors determining inundation pattern

1.2.1 Different models

Several software packages have been developed and used in the past 20 years. It started with Delft-FLS in 1998 (Stelling et al., 1998), a 2-dimensional model. Grid cells were square, and elevated obstacles like railway dikes or highways had to be incorporated into the grid by elevating grid cells. A predefined linear height decay for specific grid cells controlled the dam breach size. In 2000, this model was connected with the SOBEK 1D flow module. This created a coupled 1D2D overland flow model (Verschelling, 2000). In

the new combined model, it was possible to schematise waterways in 1D inside the 2D grid. This method of schematising detailed parts of the model was necessary because grid cells had to be kept square and rather large. It became possible to model dike breaching as a 1D channel, which allowed the modeller to define breach growth more accurately. This version of SOBEK was the standard for the VNK1 project (Arcadis et al., 2005). As computational power increased, SOBEK Overland Flow was constantly under development. The use of the Verheij-vdKnaap equation for modelling breach growth was introduced (Verheij, 2003), and it became possible to schematise elevated obstacles as 1D weirs. This version of SOBEK was the standard for the VNK2 project (Ministerie van Infrastructuur en Milieu et al., 2011).

One of the developers of Delft-FLS and SOBEK, Herman Kernkamp, started in 2007 with developing a new generation of hydrodynamic models called D-Flow FM. D-Flow FM is the calculation core of D-HYDRO (Deltares, n.d.). The most significant difference with the old generation is that grid cells, called flexible mesh, can now be of different sizes and shapes. With this flexible mesh, many new possibilities in the schematisation of a study area arise. All these models mentioned above are developed by or in cooperation with Deltares. Other models that are widely used in flood modelling are 3Di, created by a consortium consisting of Nelen & Schuurmans, Deltares, TU Delft EWI (prof Elmar Eisemann) and Stelling Hydraulics (em. prof. Guus Stelling) (Nelen en Schuurmans, n.d.) and HEC-RAS developed by the US Army Corps of Engineers (USACE Hydrologic Engineering Center, 2024). These models are, however, not considered in this research.

1.2.2 Dike breach flow

One of the largest sources of uncertainty in flood modelling is the inflow of water through a breach in the dike (De Bruin, 2018;Westerhof et al., 2023). The schematisation of the dike breach can be divided into two parts. The growth of the breach and the computation of the flow through the breach. After the first collapse, water flows through the opening in the dike and erodes the bed and the sides. This results in a growing breach size over time.

In the past century, extensive research has been done into the breaching of earthen dams. Simple parametric analytical formulas have been derived to estimate outflow and breach growth as a function of various dam parameters. These relations are primarily based on straightforward regression techniques from databases of dam failures (Wahl, 2004) and simple weir flow theory. Wahl (2004) concludes that these models should be treated with caution and engineering judgment because of significant errors and uncertainties. Next to the parametric models, more process-based models have been developed. An extensive overview of parametric and process-based models is given by West et al. (2018). Process-based models are based on a combined calculation of the flow through a dike, primarily based on weir formulas and erosion relations. The most recently developed models are the ones of Verbeek (2019) and Van Damme (2020).

In the Netherlands, first, models like BRES (Visser, 1998) and BREACH (Fread, 1988) were used. These are self-standing models which are, although perceived as very accurate, not integrated into a larger flood model. This decoupled way of estimating breach growth mainly resulted in one generic growth pattern for all possible breach locations in a dike ring. Later, a parametric equation was developed. This equation models breach growth as a function of the head over the breach, the dike material's critical flow velocity, and time. This new Verheij-vdKnaap formula was implemented in the SOBEK models in 2003 (Verheij, 2003). In Dutch flood modelling, the standard is still to use the Verheij-vdKnaap formula to model breach growth. This was used in the VNK and VNK2 projects and is also the recommended approach for D-HYDRO (Deltares, 2023a) and the guideline for flood modelling (De Bruin, 2018). The Verheij-vdKnaap equation states:

$$B = c\frac{g^{0.5}(h_{outside} - h_{inside})^{1.5}}{u_c}\log\left(1 + \frac{0.04g}{u_c}t\right) \tag{1.1}$$

Where, B = width of the breach [m], g = gravitational acceleration [m/s^2], h = water height [m], u_c = critical flow velocity of the dike material [m/s], c = a coefficient which can be used to calibrate for sand or clay dikes, t = time [s].

Van Damme (2020) presents a process-based breach-widening formulation. It is derived from the weir flow equation and process-based erosion equations. As the weir flow equation is incorporated in D-HYDRO, using this new model instead of the Verheij-vdKnaap equation might be an interesting option for modellers. A comparison shows that the new model has improved accuracy over the Verheij-vdKnaap method when comparing the predictions against the output of experiments (Van Damme, 2020).

Breach flow can be schematised in several different ways. In literature, dike breach flow is mainly described using a simple weir equation. These equations are based on Bernoullie's principle. Although breach flow in Delft-FLS and D-HYDRO are based on this principle, the implementation is different. In Delft-FLS, the weir flow equation for a sharp-crested weir in equation 1.2 is directly used.

$$Q = wh_w\sqrt{2gH_u - h_d} \tag{1.2}$$

Where w is the width of the channel [m], h_u is the upstream water level [m], h_d is the downstream water level [m] with the upstream point being an inlet grid cell and the downstream point being an outlet grid cell. In D-HYDRO, the discharge over the weir is not calculated using a stage-discharge relationship. Instead, using a sub-grid numerical method, the velocities, flow area, and, thus, discharges are computed using the 2D-shallow water equations with a particular discretisation of the advection terms in the momentum equation. This is explained in section 6.7.1 of the technical reference manual (Deltares, 2023b).

Computation of breach flow and growth requires a computation of upstream flow conditions. The guideline for flood simulations stresses the importance of an accurate computation of upstream water levels (De Bruin, 2018). This can be done using a full river model (1D or 2D) or by schematising only a part of the river. When only a part of the river is schematised, a water level boundary on the river axis can be used.

1.2.3 Distribution of water

The schematisation of the elevation grid and the 2D overland flow is the basis of every flood model. Any surface where water flow is present causes friction between the surface and the water. This causes the water to lose energy. In hydraulic modelling, it is necessary to parameterise roughness through a friction coefficient. One of the terms in the momentum equation governing the flow of water is the bed friction or roughness of the bed. Vegetation and other objects on the Earth's surface strongly influence the flow. The roughness thus determines a large part of the flow velocity. This influences the extent of inundation, arrival times and rising rates in a study area. The calculation core of the flood model can use different types of roughness coefficients like the Chezy or Manning coefficient. In Delft-FLS and SOBEK, the friction definition is always translated to a Chezy value (Deltares, 2024). However, how a roughness value is applied to the calculation grid can differ. In Delft-FLS, SOBEK and D-HYDRO, the modeller can choose to use a uniform friction value for the entire grid or specify a friction value per grid cell. Today's standard in Dutch flood modelling translates a land use map to a single roughness value per grid cell. This is, for instance, done with look-up tables provided in the guideline (De Bruin, 2018). These tables translate land use to a single Nikuradse roughness value, which can easily be translated to a Chezy value.

Next to the overland flow, several objects can be added to the grid to increase accuracy at elevated elements or local waterways. Elevated obstacles are elements that can substantially obstruct flow. Examples are elevated highways, railway dikes, or regional dikes. These elements can obstruct the flow so that inundation patterns are influenced. They can influence arrival times in areas beyond and inundation depths around the obstacles. In the Delft-FLS and early SOBEK models, these elements had to be incorporated in the elevation of the grid cells. This means a railway dike resulted in a line of elevated grid cells (Deltares, 2024). In the later versions of SOBEK and D-HYDRO, it is possible to schematise these elements in 1D. This means that a 1D weir element can be added to the grid with a certain crest level, which obstructs the flow between grid cells and reduces the total wet area of the grid cells (Deltares, 2023b). With the possibility of local grid refinement in D-HYDRO, it is also possible to schematise these elevated obstacles accurately by using small elevated grid cells.

The discretisation of the 2D shallow water equations does not always produce realistic velocity values at sudden elevation changes. Flow can be overestimated if the elevated line is only one grid cell wide in the flow direction (Stelling et al., 1998). Several updated methods for advection computation increase the accuracy, although this might lead to a decrease in possible time steps. An elevated element will produce energy losses in the system, which can be approximated by moment-conserving advection schemes. Schematising elevated elements as 1D fixed weirs in D-HYDRO changes the advection scheme in the flow computation. In flood modelling, the stability and reliability of these obstacles are essential. If the water rises above the obstacle height, the obstacle will overflow. How the flow is modelled (weir flow equations, special advection schemes, or continuity) can significantly influence the through-flow over the obstacle.

Waterways can accelerate the flood wave (De Bruin, 2018). In old Delft-FLS models, before the coupling with SOBEK, regional waterways could not be taken into account. Grid cell sizes were in the order of 50mx50m or 100mx100m. A waterway of five meters wide could not be schematised using this grid (Stelling et al., 1998). Larger waterways were incorporated by artificial lines of grid cells, which could overestimate their discharge capacity. After the coupling with SOBEK, small waterways could be schematised using 1D flow links (Verschelling, 2000). This results in two overlapping models. A model simulates water flow in the 1D waterways, and a 2D model simulates water flow over land. The flow in the 1D channel below the 2D grid level is treated as 1D flow, while the flow above the 2D Grid level is treated as 2D flow with the area of the 2D grid cell (Verschelling, 2000).

For the modelling of a waterway network in 1D, a lot of information about the waterways is needed. Because the influence of a waterway tends to decrease with decreasing size, it is often chosen to model only waterways with a specific size. With the D-HYDRO software, different shapes and sizes of grid cells can be specified. A curvilinear grid of a local waterway can be incorporated into a more coarse grid. As detailed information on waterways is not always available, waterways can be schematised as refinements in the grid. This ensures that overflowing waterways are uniformly simulated with the surrounding cells and that the storage capacity of waterways is more accurate.

1.3 Knowledge gap

The Dutch flood safety standards established in 2017 are primarily developed with flood simulations used in the VNK projects. The models used often have limitations in schematisation and coarse structured grids. Significant uncertainties in assessing flood risk concerning the modelling of fluvial floods are shown by Westerhof et al. (2023), who used the Delft-FLS software. Uncertainty in mortality calculations is strongly related to breach development and the dike breach flow. Furthermore, Schippers (2023) has shown significant differences between risk assessments using Delft-FLS and D-HYDRO. Different schematistations of line elements and waterways caused differences in the distribution of water in a flooded area. Uncertainty in fluvial flood simulations is embedded in the different schematisations of flood model aspects and the modelling software used. This leads to a need for comprehensive research into the implications of schematisations in D-HYDRO as opposed to the older schematisation of Delft-FLS. Next to that, the implications of different schematisation choices on flood simulation results in D-HYDRO itself need to be quantified.

The newest guideline on flood simulations has been adjusted to the latest insights and practical experiences in flood modelling (De Bruin, 2018). It acknowledges the importance of computing water levels on the river for an accurate computation of dike breach flow. However, this can be schematised in multiple ways. While breach discharge has been a variable in sensitivity and uncertainty analyses in fluvial flood modelling, less research has been done into factors influencing breach flow itself in 2D flood models. The implications of different schematisation techniques are unknown. The guideline advises on breach initiation moment and using the Verheij-vdKnaap equation for breach growth. Research has been done into different breach growth formulations. However, these schematisation options often need more detailed data or increased runtime, while the possible extent of their improvement in a broader flood modelling context is unknown.

Research into the implications of different schematisation choices in the distribution and dike breach flow in fluvial flood models leads to focus and direction in standardising flood model schematisations and improving fluvial flood simulations in general.

1.4 Research goal and research questions

The guideline on flood modelling shows several aspects of flood modelling in which practical experiences form the basis of the followed procedure. The guideline advises on specific choices that can be made in the schematisation of dike breach flow and water distribution aspects of flood models. The D-HYDRO software offers a wider range of schematisation possibilities than the established Delft-FLS software. These different schematisations can have a significant impact on simulation results and cause differences between Delft-FLS and D-HYDRO. There are also schematisation possibilities which are not discussed in the guideline. Impacts are uncertain and complex to quantify. This research will unveil the impact of several choices in the schematisation of fluvial flood models in D-HYDRO and find the root causes of differences between Delft-FLS and D-HYDRO models. As inundation patterns and depths are determined by a combination of inflow (dike breach flow) and distribution of water (De Bruin, 2018), this research focuses separately on dike breach flow and the distribution of water in a fluvial flood simulation.

The research goal and research questions are formulated as follows:

To unveil the implications of the use of D-HYDRO and its different schematisation possibilities for the computation of dike breach flow and water distribution in fluvial flood models

---

Dike breach flow

1. *What implications does the use of the D-HYDRO software have for the computation of dike breach flow, as opposed to the established Delft-FLS software?*
2. *What are the effects of alternative river schematisations on dike breach flow, as opposed to a full 2D river schematisation in a fluvial flood model?*
3. *What are the effects of different breach initiation moments and growth equations on breach growth and dike breach flow in a fluvial flood model?*

Distribution of water

4. *What implications does the use of the D-HYDRO software have for the computation of water distribution, as opposed to the established Delft-FLS software?*
5. *What are the effects of fixed weirs and local waterways on the distribution of water and flood simulation results in D-HYDRO?*

The breach discharge characterises the dike breach flow in a fluvial flood model. The breach discharge is highly dependent on the width of the breach. Both **breach discharge** and **breach growth** are therefore variables of interest for analysing the dike breach flow. As stated in the state of the art, the output of flood simulations must be placed in the context of their goal. The guideline for flood simulations distinguishes three possible goals of flood simulations: safety assessment, crisis management, and spatial planning (De Bruin, 2018). Schematisation choices can have a significant local impact, while the global implications in light of the simulation goal are small. Therefore, the effects of schematisations in the distribution of water are analysed, both locally and globally. The global variables that are hereafter combined called "flood simulation results" are: **maximum inundation depth**, **maximum flow velocity**, **maximum rising rate**, and **arrival time**.

The schematisation possibilities that will be analysed in this research are based on the advice given in the guideline for flood modelling (De Bruin, 2018) and experts from Royal HaskoningDHV and Water Board Rivierenland. The guideline divides the Netherlands into seven areas with comparable characteristics important for flood modelling (De Bruin, 2018). This research focuses on one of these seven areas, the "upper river area" (Bovenrivierengebied), shown in Appendix A. It is characterised by high discharges and insignificant tidal influences. A case study area called *Betuwe Tieler en Culemborgerwaarden*, also known as dike ring 43 is used.

1.5 Case study: Betuwe Tieler en Culemborgerwaarden

The study area is one of the former dike rings in the Netherlands, Betuwe Tieler en Culemborgerwaard. This research refers to it by its dike ring number 43. It is part of the work field of Water Board Rivierenland, named after the large rivers that cross the Dutch Delta. This Waterboard is located in Gelderland and Zuid-Holland. The area is enclosed by the *Nederrijn* and the *Lek* in the North, the *Pannerdesh channel* in the East, and the *Waal* and the *Boven Merwede* in the South. In the west, the area is enclosed by the *Diefdijk*. The rivers enclosing the area flow from east to west. The area is part of the so-called "Bovenrivierengebied". This is a part of the Dutch River system where the sea does not influence hydraulic conditions (De Bruin, 2018). Smaller and larger cities in this area are Arnhem-South, Geldermalsen, Culemborg, Heteren, Bemmel, Tiel, and Elst. Highways such as the A2, A15, and A50 cross the area. A large railway crosses from west to the east, called the betuwelijn.

FIGURE 1.2: Location of Dike ring 43 in the Netherlands [Red: Dike ring 43, black: Dutch border]

Two important waters are present. Crossing the entire area from East to West is the river the Linge. Crossing from North at Rijswijk to South at Tiel is the Amsterdam-Rijn Kanaal. The Linge can be divided into two parts: the Boven Linge, which is the part from its source at Doorneburg until the Amsterdam-Rijn Kanaal, and the Beneden Linge, which is the part from the Amsterdam-Rijn Kanaal until the spillway in the Diefdijk. The BovenLinge is an artificial river with a canal-like characteristic. Its inflow is controlled by a weir at higher discharges and a pumping station, which pumps water from the Pannerdesh canal to the Linge at lower discharges. The discharge in the Linge generally lies between 4 and 10 m^3/s (Linge Streek, 2024). The Linge crosses under the Amsterdam-Rijn Kanaal via a siphon. After this, the river starts to behave as a natural river, becoming one after Geldermalsen. Here, the river is meandering and enclosed by floodplains and levees. The Linge ends at a pumping station, pumping the water into the Beneden-Merwede. The capacity of this pumping station is 60 m^3/s (Nederlandse Gemalen Stichting, 2024). The Amsterdam-Rijn kanaal is also enclosed by levees and has a compartmentalising capacity because of that.

FIGURE 1.3: General location of the Linge (not to scale) (Linge Streek, 2024)

The elevation map in figure 1.4 shows a decreasing elevation from east to west. In the east of the area, elevations are approximately 10 m+NAP. In the west, elevations lie around mean sea level (NAP) or are even below NAP. The lowest region is the region around Gorichem and the South of Culemborg. At the downstream point at Gorichem, a construction has been made called the “Dalemse overlaten”. The purpose of these structures is to let water from inside the dike ring flow out. When a dike breach should happen upstream, the water flows into the area. Inside the dike ring, the water flows to the lowest point, accumulating at very high water levels. When the water levels inside the dike ring are higher than outside, the dike can be decommissioned at the *Dalemse Overlaten* to discharge the water to the outside system. Although the idea seems logical and practical, it has never been used or tested. In addition, although the plan was to limit construction around the site, much construction has been done in the last 20 years. Whether these constructions can be used in the case of floods remains the question. Therefore, the *Dalemase Overlaten* are assumed to be non-functional in flood risk calculations.

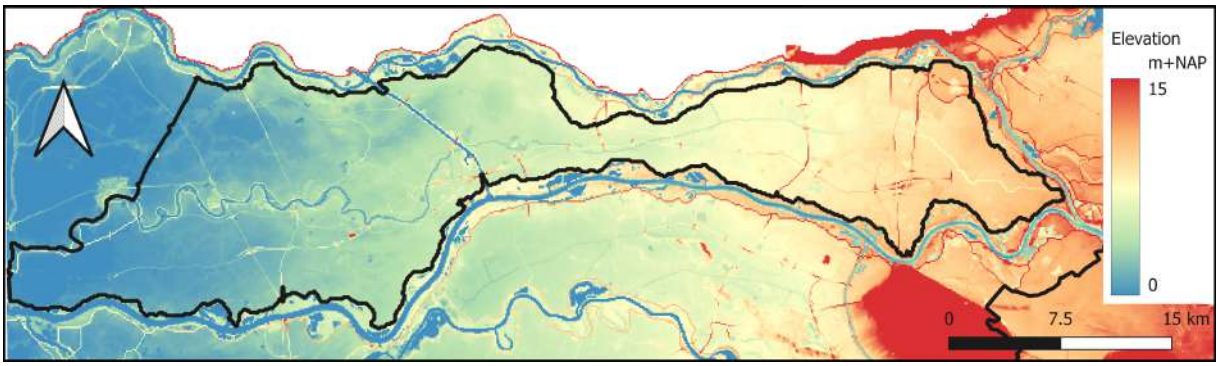

FIGURE 1.4: Elevation map of dike ring 43

The consequences of potential dike breaches in Dike Ring 43 depend highly on the location because of the dike ring's size and its elevation pattern. A dike breach in the east will affect the entire region as water flows westwards. A dike breach at a more westward location will have very low or no impact on the eastern part of the area. A typical discharge on the Waal lies between 850-3000 m^3/s, while a normal discharge on the Neder-Rijn lies between 10 and 720 m^3/s (Rijkswaterstaat, 2024). A dike breach on a location near the Waal will have a more significant impact on the region. For this research, three potential breach locations representing different impact cases are chosen. These potential breaches are located near Bemmel (Waal), Tiel (Waal), and Heteren (Neder-Rijn). These locations and other vital aspects of dike ring 43 are shown in Figure 1.5.

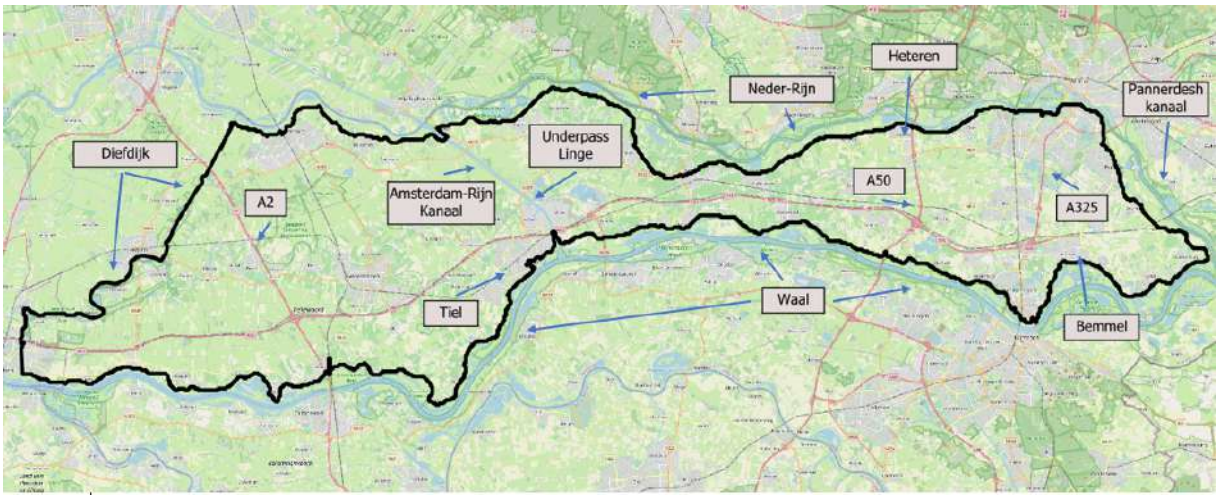

FIGURE 1.5: Indication of important elements of dike ring 43

Water Board Rivierenland has provided two models of the area. One model is made with the modelling software Delft-FLS, and the other with the software D-HYDRO. The Delft-FLS model was made during the VNK1 project, and most of the runs were done in 2006. The D-HYDRO model was created in 2019, with one of the earliest versions of D-HYDRO. Next to that, two D-HYDRO river models are used in this research. One 1D river model of all the Rhine branches, taken from a Water Board Rijn & IJssel model and a 2D river model of the Rhine and Waal made by Deltares.

TABLE 1.2: Overview of models provided for this research

Model name	**Software**	**Provider**
Delft_D43_1998	Delft-FLS	Water Board Rivierenland
HYDRO_D43_2019	D-HYDRO	Water Board Rivierenland
HYDRO_River_1D	D-HYDRO	Water Board Rijn & IJssel
HYDRO_River_2D	D-HYDRO	Deltares

2 Methodology

2.1 General outline

A structured methodology is followed to execute this research and unveil the implications of schematisation choices in D-HYDRO. This research compares basic schematisations with models in which specific other schematisation choices are made. This comparative analysis serves as a tool for unveiling the implications of schematisation choices that may otherwise remain hidden within D-HYDRO. This results in a better understanding of the model's behaviour. Following the guidelines on flood modelling, this research is divided into two aspects of fluvial flood models. These two separated aspects are dike breach flow and the distribution of water, as shown in Figure 1.1. A general overview of the steps taken in this research is depicted in Figure 2.1.

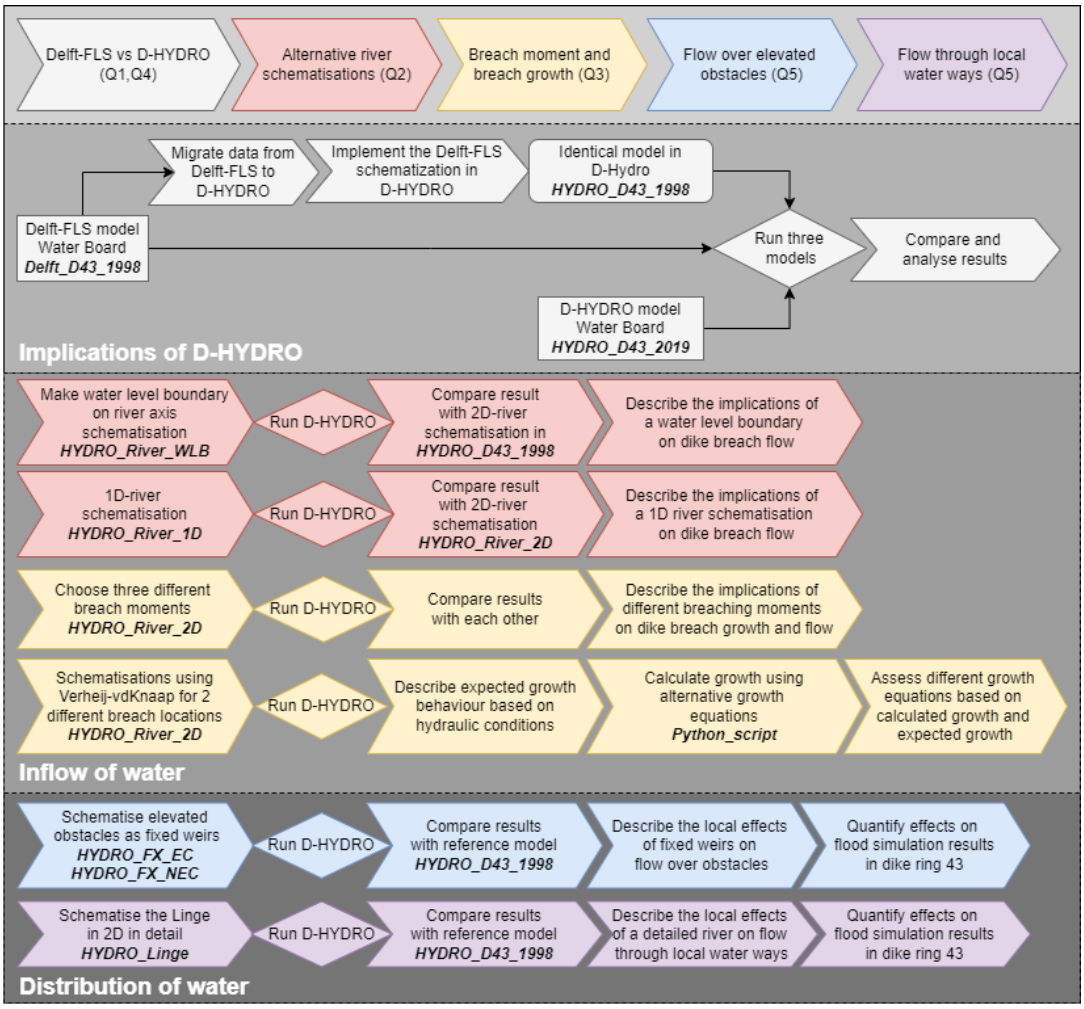

FIGURE 2.1: General overview of the methodology

First, the implications of using the D-HYDRO software for dike breach flow computation (research question 1) and water distribution (research question 4) are analysed. This is done by rebuilding the *Delft_D43_1998* model in the D-HYDRO software. This creates a new model in D-HYDRO with exactly the same schematisation. This new model is called *HYDRO_D43_1998*. The results of these models are compared. Next, the results of the *HYDRO_D43_1998* model are compared to the *HYDRO_D43_2019* model. With the first comparison, differences caused by the calculation cores of Delft-FLS and D-HYDRO can be found. With the second comparison, differences caused by newer schematisation possibilities in D-HYDRO can be found.

Next, different schematisation choices that can be used in the D-HYDRO software are analysed. For research question two, two alternative river schematisations are compared to a full 2D river schematisation. A schematisation that includes only a water level boundary at the river axis near the breach (*HYDRO_River_WLB*) is compared to the 2D river schematisation in *HYDRO_D43_1998*. A 1D-river schematisation (*HYDRO_River_1D*) is compared to a detailed full 2D river model of Deltares (*HYDRO_River_2D*). Results of *HYDRO_River_2D* are also used to compare breach moments and breach growth equations for research question 3.

For research question 5, a schematisation is made that includes fixed weirs with a changed grid cell elevation (*HYDRO_FX_EC*), one that includes fixed weirs without changed grid cell elevation (*HYDRO_FX_NEC*) and a schematisation is made that includes a detailed grid around the Linge (*HYDRO_Linge*). These are altered schematisations based on the *HYDRO_D43_1998* schematisation and are compared to this model.

2.2 The implications of D-HYDRO

To analyse the implications of the D-HYDRO software on dike breach flow and water distribution, first, the Delft-FLS schematisation is rebuilt in D-HYDRO. The model in Delft-FLS is a straight-forward rectangular grid-based model. All higher elements like highways, dikes, and railways are schematised using elevated grid cells. Waterways like the Linge and the Amsterdam Rijn Kanaal are schematised the same way, only with decreased bed levels. Other building blocks are river boundary conditions, several culverts, and dike breaches.

The rectangular grid is translated directly and implemented in D-HYDRO. The bed level and roughness values are interpolated on this grid. This creates the same digital elevation model in D-HYDRO, with higher elements and waterways incorporated into the bed level, as in Delft-FLS. Breaches of the regional dikes along the Amsterdam Rijn Kanaal and the Dalemse overlaten were schematised in the Delft-FLS model. However, all regional dikes are currently considered reliable, which means that they will not fail under the water pressure of the flood wave (M. van de Waart, personal communication, 16 February 2024). Next to that, the Gorichem overlaten is deemed non-functional, as explained in section 1.5. Therefore, breaches of regional dikes and the Dalemse Overlaten were not translated to the D-HYDRO model and were deleted from the Delft-FLS model.

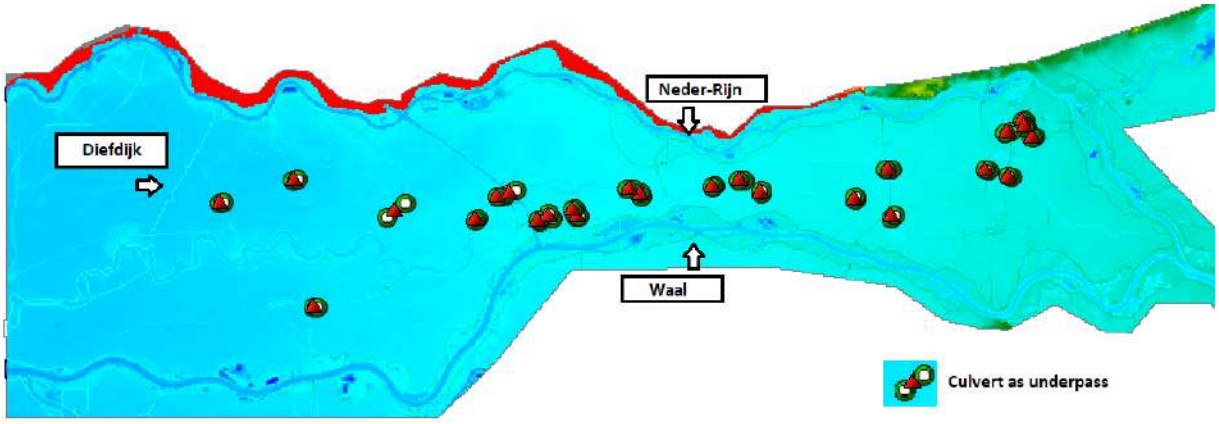

FIGURE 2.2: Screenshot of the D-HYDRO model in the GUI

Culverts are present in the Delft-FLS model. These represent culverts in the Linge, culverts as boundary conditions and underpasses. The culverts used as boundary conditions are a schematisation choice in Delft-FLS. Because boundary conditions can only be placed at the edge of the grid, the culverts are the source of the Linge upstream at Doorneburg and after the Amsterdam Rijn Kanaal. The discharge through the culverts from the Delft-FLS model run is taken and placed as a point source on the D-HYDRO grid to create the same inflow. The inflow discharge is set at 10 $[m^3/s]$, representing roughly the same inflow as in the Delft-FLS model. The computation of flow through a culvert in Delft-FLS is best recreated in D-HYDRO by introducing a 1D channel in the model that includes a weir. This way, the discharge computation is calculated using the simple weir equation explained in section 1.2.2.

A schematisation of the rivers is needed to model a dike breach using the dam break option in D-HYDRO. The Delft-FLS model uses a simple schematisation using the same square grid cells as the dike ring area. This is copied into the D-HYDRO model. Some minor differences are found, which are shown in Figure 2.3. These differences can be attributed to the open boundary conditions in both models. These could not be transferred to the same location in D-HYDRO. The river model in Delft-FLS has not been validated. The shape of the graph and the peak value are of importance. The shape of the water level graph and the peak water level of D-HYDRO are equivalent to that of Delft-FLS. After rebuilding the Delft-FLS

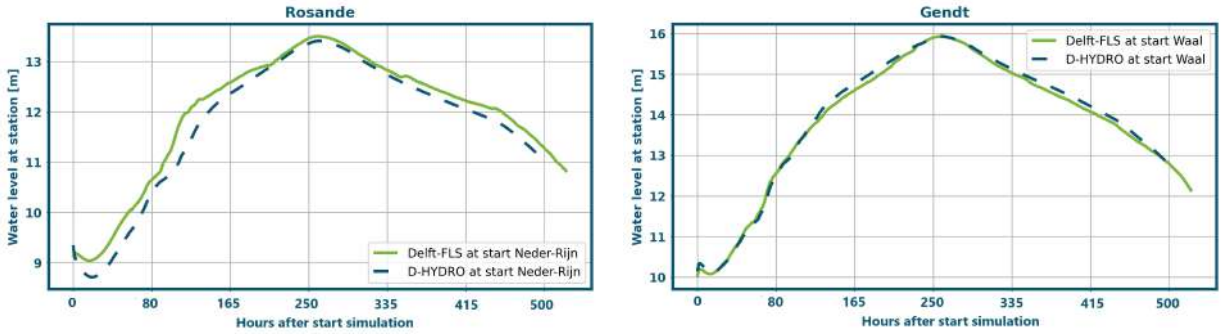

(A) Water level in the Neder-Rijn

(B) Water level in the Waal

FIGURE 2.3: Water levels in the Waal and the Neder-Rijn

schematisation in D-HYDRO, a dike breach simulation is run for three different breach locations. The locations are at Bemmel, Tiel and Heteren [1]. Simulations using the same breach inflow are done using the new model of Water Board Rivierenland as well. The results of both D-HYDRO schematisations and the Deflt-FLS simulations are compared.

2.3 Dike breach flow schematisation choices in D-HYDRO

In D-HYDRO, the inflow through the dike breach is calculated using the weir flow theory. A sub-grid numerical scheme is used, which is explained in section 6.7.1 of the technical reference manual (Deltares, 2023b) and in Appendix B.2. This makes the computation of breach flow in D-HYDRO dependent on the calculation of upstream hydraulic conditions. It is calculated from the upstream and downstream water levels, the geometry of the breach, and upstream flow velocities.

The upstream hydraulic conditions can be computed using a full 2D river model, a 1D river model or a water level boundary close to the breach location. This last option only schematises a part of the river. A full 2D river model is deemed the most accurate, although this is not always preferable. It results in the need for validation runs, high runtimes and a large amount of needed data. In the analyses in this research, a validated 2D-river model of Deltares is used as a reference model (HYDRO_River_2D). The chosen schematisation largely influences the computation of breach discharge and breach growth. The growth of the breach can be set as a predetermined times series, or the Verheij-vdKnaap equation can be used. Other growth equations might be more accurate. Next to implementations of the Verheij-vdKnaap equation, the Van Damme equation will be analysed in this research (Van Damme, 2020) a. The moment of breach initiation influences the amount of flow through the breach. A breach initiation before reaching a peak water level will result in more significant breach discharges. This research will analyse the schematisation options above and the possible synergies between them. The following sections will explain the method of implementing the schematisation choices in Table 2.1.

[1] See Figure 1.5

TABLE 2.1: Schematisation choices for dike breach flow

	Schematisation choice			Used models
Upstream hydraulic conditions	Full 2D river model	Water level boundary	Full 1D river model	Delft_D43_1998 HYDRO_D43_1998 HYDRO_River_2D HYDRO_River_WLB HYDRO_River_1D
Breach initiation moment	Before high water peak	At high water peak (current standard)	After high water peak	HYDRO_River_2D
Breach growth	Verheij-vdKnaap (current standard)	Verheij-vdKnaap alternatives	Van Damme	HYDRO_River_2D

2.3.1 Water level boundary on river axis

Because no validated river model was available, Water Board Rivierenland decided to simplify the dike breach schematisation in their new model of dike ring 43 (HKV and Waterschap Rivierenland, 2020). In this model, the Rijn, Neder-Rijn and Waal are not completely schematised in 2D. On the location of the dike breach, the mesh is extended to the river axis. On the river axis, a water level boundary is placed. This approach might overestimate the breach discharge as water levels are largely independent of the influences of the breach. In this research, this approach is analysed and compared to the simple weir flow implementation of Delft-FLS and a full 2D-river schematisation. This research tries to quantify the possible overestimation of breach discharge due to this approach and tries to find the root causes of this overestimation.

In the simulations done for this research, the water levels are based on the same discharge wave as computed by the river model in Delft_D43_1998. The water levels on the river are, therefore, the same until the moment of breaching. Simulations are done for three breach locations near Bemmel, Tiel and Heteren [1]. An example of the grid for the breach location at Bemmel is shown in Figure 2.4. Synergies between breach growth and breach discharge are included by doing a simulation with predetermined growth and one using the Verheij-vdKnaap equation for every breach location. They are making a total of 12 simulations.

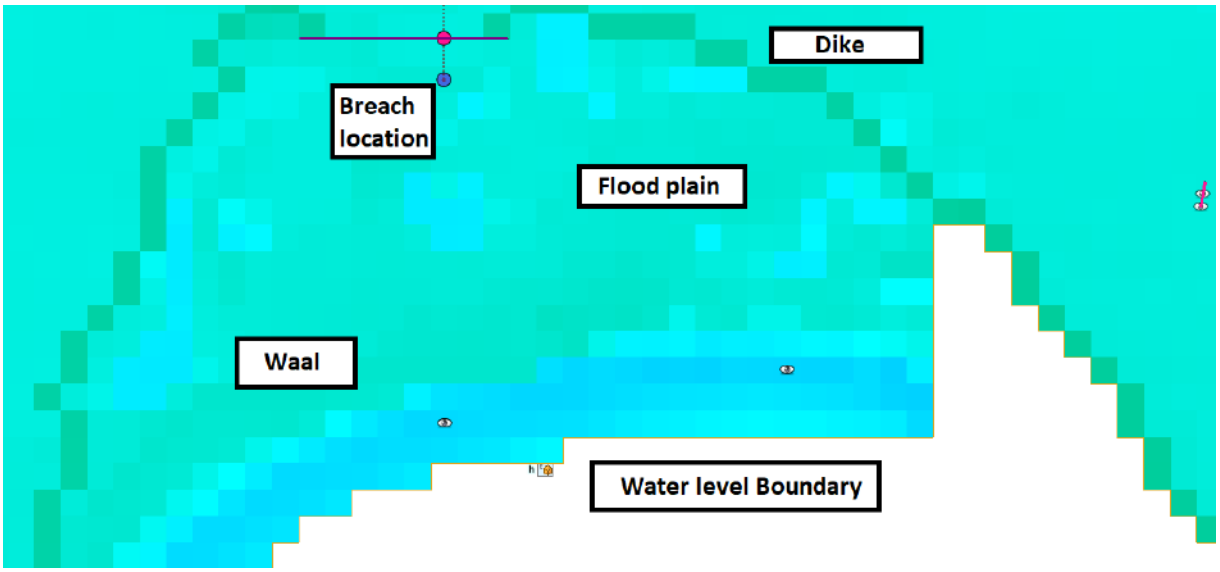

FIGURE 2.4: Water level boundary grid, screenshot of D-HYDRO GUI (not to scale)

[1] See Figure 1.5

2.3.2 1D-river schematisation

The second alternative to a full 2D river schematisation is a 1D river schematisation. This requires much lower calculation times. A river model of the Rhine and Waal is used for this research (HYDRO_River_1D). It is coupled with the 2D grid of HYDRO_D43_1998. In the coupling, Deltares' advice is followed to create one coupling per grid cell and computational 1D point (Deltares, 2023b). The computational points in the 1D branches have the same spatial resolution as the 2D grid. In this research, several schematisations are made for two breach locations, one near Bemmel and one near Tiel[1]. These schematisations are compared to the detailed 2D-river schematisation of HYDRO_River_2D. This research tries to quantify possible differences in breach discharge and tries to find the root causes of these differences. Figure 2.5 shows a schematisation for the two breach locations.

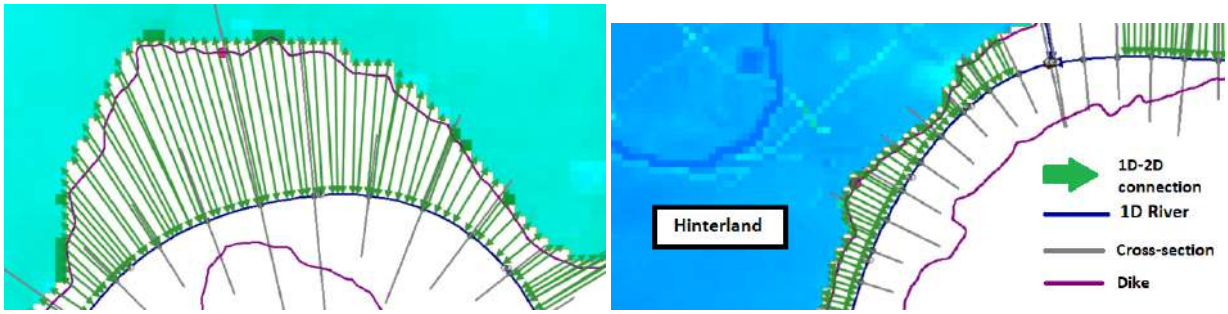

(A) 1D2D breach grid at Bemmel (not to scale) (B) 1D2D breach grid at Tiel (not to scale)

FIGURE 2.5: Coupled 1D river with 2D hinterland screenshots of D-HYDRO GUI

2.3.3 Breach initiation moment

In this research, using the detailed 2D-river model HYDRO_River_2D, the influence of breach moment on the breach discharge is analysed. The exact moment a breach initiates is highly uncertain. Breaches that initiate before a water level peak is reached on the river will result in a more significant breach flow because driving forces increase after breach initiation. In theory, this can also affect breach growth, as flow velocities and water levels in the breach drive this process. A breach initiated before peak water level experiences larger flow velocities for a more extended period and should thus result in a faster-growing breach. This research analyses the effects of breach initiation moment on the breach discharge and width in D-HYDRO.

The breach hydrographs and breach widths are compared for three simulations with different initiation moments. The three moments are chosen to be one day before, at, and after peak water level.

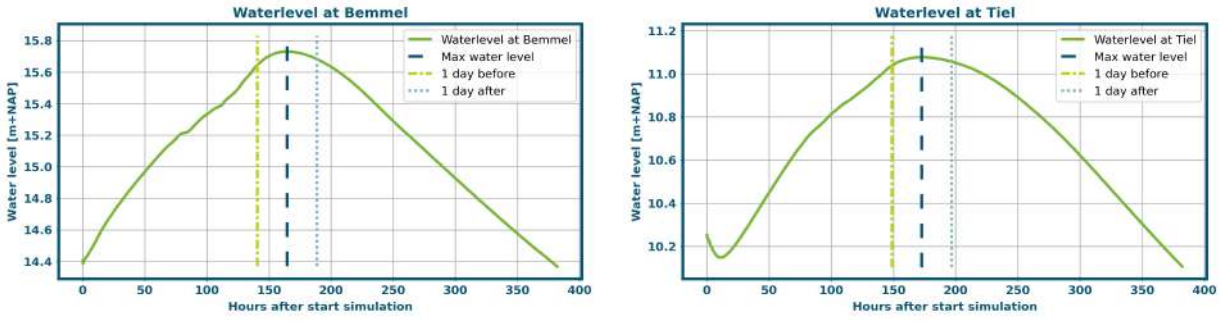

(A) Water level at Bemmel (B) Water level at Tiel

FIGURE 2.6: Water levels from the HYDRO_River_2D model

2.3.4 Computation of breach growth

In the Delft_D43_1998 schematisation, the breach width was determined by a predefined time series. In D-HYDRO, the Verheij-vdKnaap equation can be used to calculate breach width. In Delft-FLS and D-HYDRO, there is no option to adjust the shape of the breach. The depth must be determined in advance, and only the width can be varied. In dike breaches, it is commonly assumed that the dike will erode until the bed level of the area behind it or until less erodible material like rock or concrete is reached. Therefore, in this research, it is assumed that the depth of the breach develops as defined in the original Delft_D43_1998 model, and the shape is always rectangular.

For this research, a comparison is made between different implementations of known breach growth formulations. First, simulations are done using a predetermined breach growth as used in the Delft_D43_1998 model. Next, simulations are done using the standard version of the Verheij-vdKnaap equation for breach growth. From these simulations, the upstream and downstream water levels, flow velocity inside the breach and flow height inside the breach are extracted. With this data, an alternative breach growth is calculated using alternative growth formulations. The alternative growth formulations are versions of a formulation by Van Damme (2020) and versions proposed by Verheij (2003). These breach growth equations cannot be incorporated into the model itself and are calculated in a Python script. Simulations are done for a breach location at Bemmel and Tiel and are therefore only done for the Waal River.

Verheij (2003) derives two coefficients for his logarithmic equation. These are based on functional relationships which transfer flow velocity into water level difference. Two new functions are derived by transferring this back to a relationship, including flow velocity. These functions are here called Verheij_a1 and Verheij_a2. The original and alternative equations are given in equation 2.1, 2.2 and 2.3 respectively.

$$\frac{dB}{dt}_{i+1} = \frac{(g(h_{up} - h_{down}))^{1.5}}{u_c^2} \frac{f_1 f_2}{ln(10)} \frac{1}{1 + \frac{f_2 g}{u_c}(t_{i+1} - t_1)} \tag{2.1}$$

$$\frac{dB}{dt}_{i+1} = f_1 \frac{Ru}{u_c} \frac{f_2 g}{ln(10) u_c} \frac{1}{1 + \frac{f_2 g}{u_c}(t_{i+1} - t_1)} \tag{2.2}$$

$$\frac{dB}{dt}_{i+1} = f_1 \frac{u^2}{u_c^2} \frac{f_2 g}{ln(10) u_c} \frac{1}{1 + \frac{f_2 g}{u_c}(t_{i+1} - t_1)} \tag{2.3}$$

Here, R is the hydraulic radius in the breach approximated by the flow height $[m]$. h_{up} is the upstream water level $[m + NAP]$, h_{down} is the downstream water level $[m + NAP]$, u_c is the critical flow velocity $[m/s]$, u is the flow velocity $[m/s]$, $f2$ and $f3$ are coefficients.

In the paper by van Damme, the displacement equation is derived from a deterministic shear stress relation and a Manning wall shear stress equation. Van Damme derives a growth model by including an expression for the average flow velocity based on weir flow equations. This derivation is unnecessary as the flow velocity can be taken from the model. The displacement equation Van Damme gave is, therefore, rewritten to include average velocity as a parameter. This makes the equation suitable to use in combination with the D-HYDRO software. The displacement relation is given by equation 2.4. Combined with wall shear stress and Manning's equation (equation 2.5), this becomes equation 2.6 for the displacement rate.

$$C = 2m\tau^{0.5} + c_1 \tag{2.4}$$

$$\tau = \rho_w g \frac{u^2 n^2}{R^{\frac{1}{3}}} \tag{2.5}$$

$$\frac{dB}{dt} = 2m\sqrt{\rho_w g} \frac{un}{(R)^{1/6}} + 2c_1 \tag{2.6}$$

Here ρ_w is the density of water $[kg/m^3]$ and n is the Manning roughness coefficient $[S/m^{1/3}]$. The coefficients m and c_1 are deterministic soil parameters. For cases with less knowledge of dike material, Van Damme (2020) argues a value of 0.0002253 $[m^2s/kg]$ for m and a value of 0.008 $[m/s]$ for c_1. These seem very high values. Therefore, a second fit is made based on the displacement-stress relationship found in the ASR experiments (Hunt et al., 2005). The resulting coefficients are m = 0.0000238 $[m^2s/kg]$ and c_1 = -0.0000177 $[m/s]$.

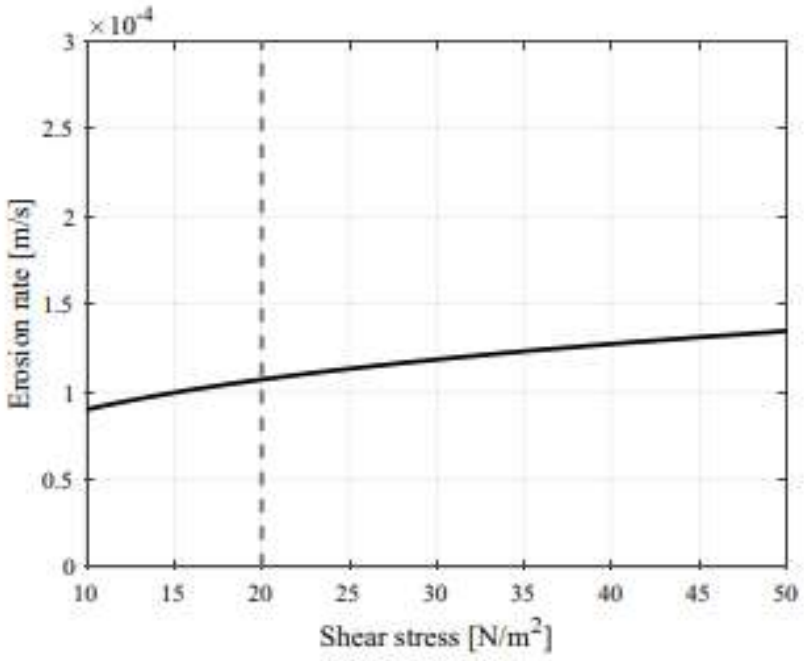

FIGURE 2.7: Erosion rates as a function of the shear stress (Hunt et al., 2005)

2.4 Water distribution schematisation choices in D-HYDRO

The digital elevation model largely determines where water flows. However, several schematisation choices might have a large influence, too. Elevated lines like highways or railways tend to compartmentalise the area and block water. The way these are schematised is, therefore, an important choice. In D-HYDRO, this can be done by elevated grid cells, like in Delft-FLS or by introducing fixed weirs on the grid. Waterways might have a large influence on the through flow of water. The level of detail in the schematisation of waterways can, therefore, influence the distribution of water. The next sections will explain the method of implementing the schematisation choices in Table 2.2.

TABLE 2.2: Schematisation choices for water distribution

	Schematisation choices		**Models used**
Elevated elements	Elevated grid cells	Fixed weirs	HYDRO_D43_1998 HYDRO_FX_EC HYDRO_FX_NEC
Waterways	In coarse grid	Detailed grid	HYDRO_D43_1998 HYDRO_Linge

2.4.1 Elevated obstacles as fixed weirs

Railways, elevated highways, and dikes are schematised as lines of artificially elevated grid cells in Delft_D43_1998. These can be seen in the elevation map shown in Figure 1.4. In D-HYDRO, sudden elevation changes can be schematised as fixed weirs. This analysis aims to unveil the effect of fixed weirs in a study area. Fixed weirs in D-HYDRO replace the elevated grid cells from Delft-FLS. To identify elevated grid cells, an algorithm selects all cells at least 0.5 meters higher than their neighbours. This results in the map shown in Figure 2.8a. Endpoints of elevated lines and intersections of lines are excluded to prevent leakages. This creates an extensive transformation in which all essential elevated elements are schematised as a fixed weir in D-HYDRO. The result is shown in Figure 2.8b. In this figure, all purple lines are fixed weirs. The fixed weirs have the same elevation as the original grid cell. Elements that are now schematised as fixed weir include the Amsterdam Rijnkanaal dikes, Linge dikes, parts of the A2, A15, A50, A325, and the railway Culemborg - Geldermalsen[1]. Mainly the Amsterdam Rijnkanaal dikes and the A50 compartmentalise the study area and might significantly impact through flow. Differences between the elevated grid cell and fixed weir implementation will be best seen around these lines.

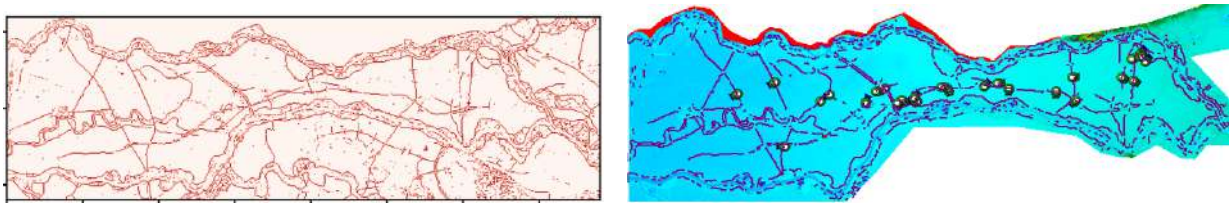

(A) Identified elevated elements in red

(B) Schematised fixed weirs in purple

FIGURE 2.8: Screenshots of dike ring 43 in algorithm (left) and D-HYDRO GUI (right)

Because the original height data and the process to establish the elevation grid are unavailable, the underlying grid cells cannot be transferred to their original height. To see the effect of implementing a universal fixed weir on this grid, the cells are lowered to the highest neighbouring cell, which does not underlie a fixed weir. This creates the first fixed weir schematisation HYDRO_FX_EC. Although changing the bed level of underlying grid cells might better represent the actual situation, it does create more storage potential. The changed grid cells represent 22.91 km^2 of surface area where water can be stored. Therefore, another schematisation is made in which the grid cells are kept to their given bed level in Delft_D43_1998. This second model is called HYDRO_FX_NEC.

Both configurations are compared to the reference model HYDRO_D43_1998[2] on flow characteristics around the elevated line elements. This includes discharge over the elements, water levels, and flow velocities. Next, the impact of differences herein on flood simulation results in the dike ring 43 area is determined.

2.4.2 Flow through local waterways

In dike ring 43, the Linge plays an important role. This local river flows through the entire study area from east to west. A river like this can play a significant role in the propagation of a flood wave. The river can discharge more substantial amounts of water than a plain field. This results in less water on land, dampening the extent of inundation. However, when the flood wave is larger than the river can discharge, the flood wave can spread faster. The river then serves as a sort of highway for the water, inundating areas far in front of the actual flood wave.

In Delft_D43_1998, the Linge is schematised as a line of grid cells with reduced elevation and reduced roughness. This approach essentially schematises the Linge as a river 100 meters wide. In reality, the Linge is, on average, 20 meters wide. This approach can, therefore, majorly overestimate its discharge capacity. However, in D-HYDRO, a flexible mesh can be used. This allows the modeller to incorporate a curvilinear grid of the Linge into the coarser grid, leading to a significant improvement in the accuracy of the model.

[1] See Figure 1.5

[2] Old Delft-FLS schematisation in D-HYDRO

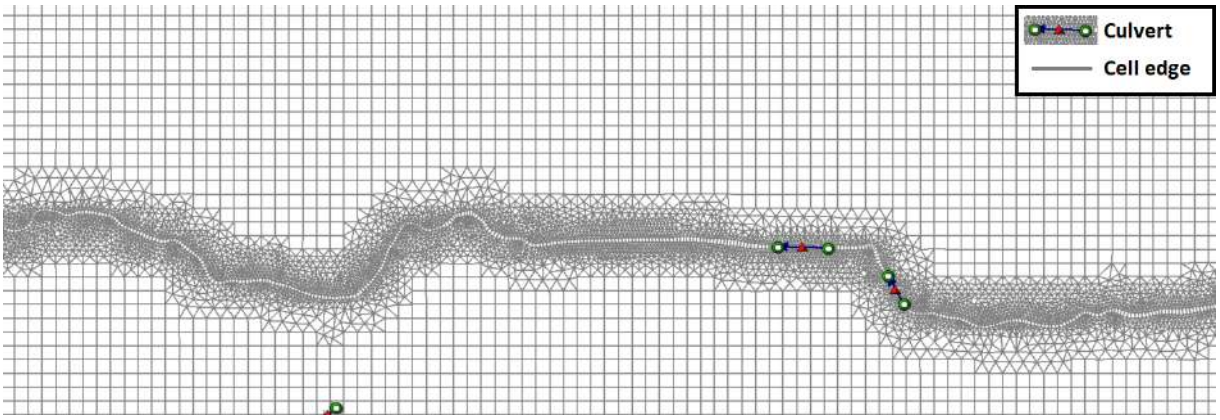

FIGURE 2.9: Cut-out of the refined grid around the Linge

For this research, the grid cells size around the Linge is reduced. This does not create a validated river model, but it vastly improves the accuracy of the discharge capacity of the river. The area around the Linge is cut out from the original grid. Then, from the Legger of the Water Board, a 2D grid of the Linge is made that follows the actual flow direction of the Linge. The river grid and the original grid are coupled using a triangular grid. The grid cells marked as "Linge" will receive the original bed level of the Linge grid cells from the original Delft_D43_1998 model. The grid cells marked as floodplains will receive the bed level of the original grid cells adjacent to the Linge, depending on their position. This creates a model in which the width of the Linge is schematised with higher accuracy (HYDRO_Linge).

The configuration is compared with reference model HYDRO_D43_1998 on flow characteristics around the Linge. This includes flow velocities and water levels. The capacity of the Linge to inundate areas far in front of the actual flood wave will be evaluated. Next, the impact of differences herein on flood simulation results in the dike ring 43 area is determined.

3 Results - Dike breach flow

The computation of dike breach flow determines how much water flows into an area. It is determined by upstream hydraulic conditions on the river, breach growth, breaching moment and area characteristics around the breach. Flood simulations are done for three different locations using the configuration made and described in section 2.2. A location near Bemmel, Tiel and Heteren[1]. With these simulations, the implications of the D-HYDRO software as opposed to the Delft-FLS software and the effect of a water level boundary on the river axis could be determined. Next, simulations are done using a detailed 2D river model of the Rhine/Waal and a 1D river model of the Rhine branches for the locations near Bemmel and Tiel. With these simulations, the effect of different river schematisations, breach growth equations and breach initiation moments are determined.

3.1 The implications of D-HYDRO

Breach flow in Delft-FLS is calculated using a simple weir formula. This calculation is only dependent on the upstream and downstream water levels. The implementation of D-HYDRO is more complex and includes many influencing factors. This section compares the Delft_D43_1998 model and the HYDRO_D43_1998 model. In Delft-FLS and D-HYDRO, the breach growth is set as a predetermined time series. The breach happens around three days before the peak of the discharge wave reaches the breach locations. The only difference between the Delft-FLS and the D-HYDRO model is the computation of dike breach flow. The resulting breach flow hydrograph of three different breach locations is shown in Figure 3.1.

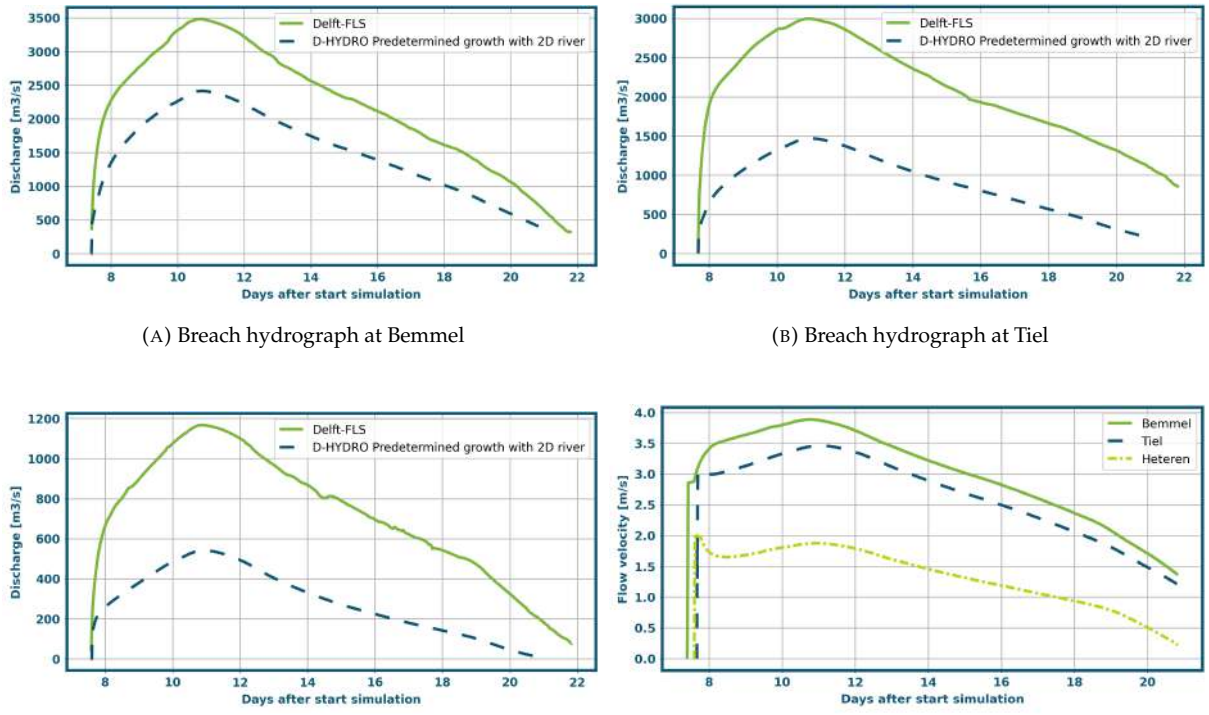

(A) Breach hydrograph at Bemmel

(B) Breach hydrograph at Tiel

(C) Breach hydrograph at Heteren

(D) Flow velocity in D-HYDRO for three breach locations

FIGURE 3.1: Delft-FLS vs D-HYDRO

Three flow stages can be distinguished when looking at the flow velocity data, combined with the geometry of the breach and water levels. The first stage is when the crest level decreases, flow velocity increases rapidly, water levels downstream increase quickly, and water levels upstream decrease. The

[1]See Figure 1.5

second stage is when the breach grows only in width. Here, the flow velocities decrease because of the decreased upstream water levels and the increased downstream water levels. In the third phase, the system stabilises, and the flow velocity and breach discharge become governed by the upstream hydraulic conditions. Figure 3.1 shows that the resulting breach flow in D-HYDRO is much smaller than the breach flow in Delft-FLS. Although the graph follows the same shape, the volumes are much smaller in the D-HYDRO model. From the data, it can be concluded that there is no single cause. Several aspects contribute in some way to the discrepancy between the results of Delft-FLS and D-HYDRO. The first slight difference lies in the computation of upstream and downstream water levels. In Delft-FLS, this is done by averaging over more cells than in D-HYDRO. The cells in Delft-FLS are also placed further from the breach location.

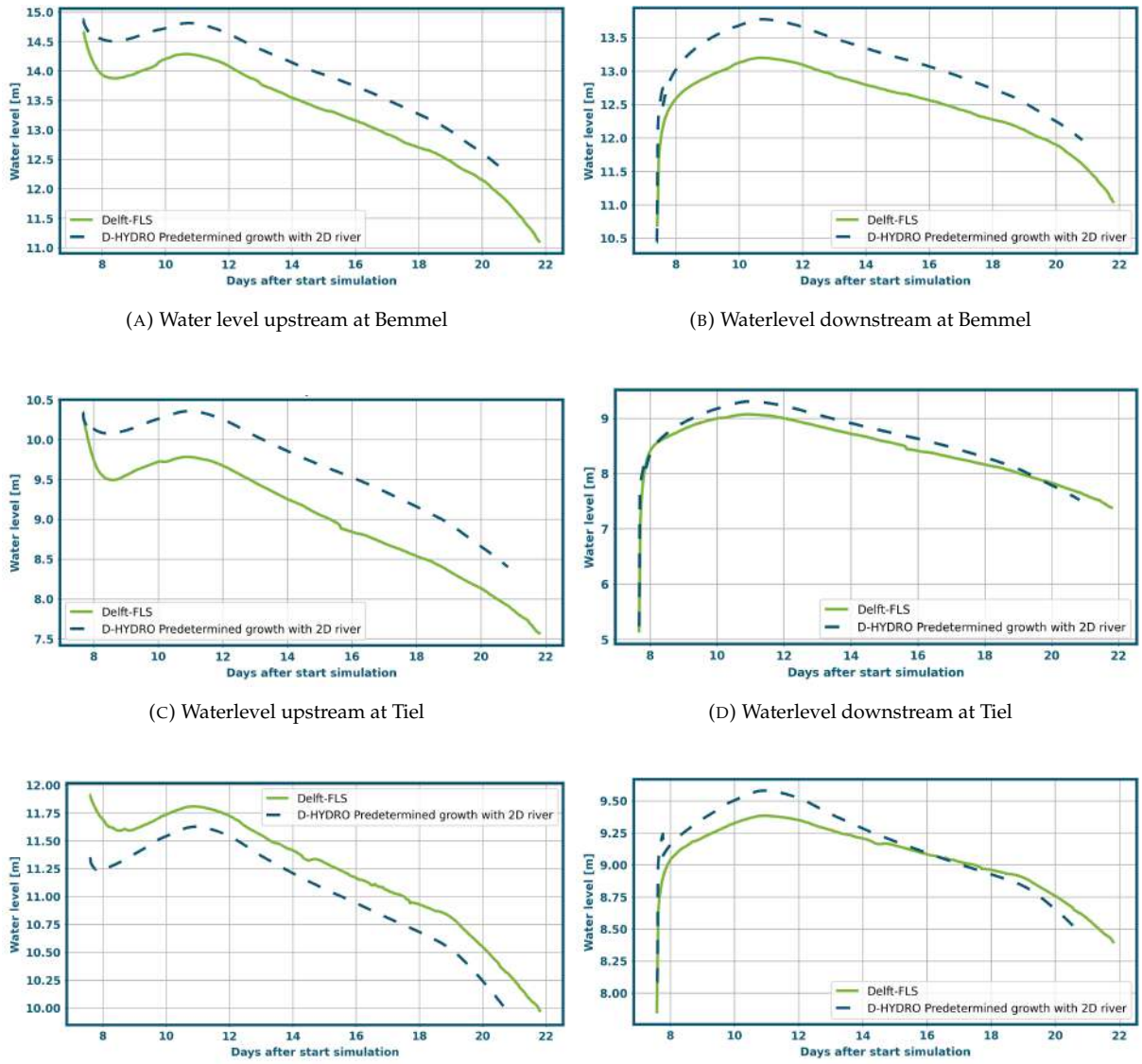

(A) Water level upstream at Bemmel

(B) Waterlevel downstream at Bemmel

(C) Waterlevel upstream at Tiel

(D) Waterlevel downstream at Tiel

(E) Waterlevel upstream at Heteren

(F) Water level downstream at Heteren

FIGURE 3.2: Water levels in the Waal and the Neder-Rijn

The difference in breach discharge cannot only be attributed to the different upstream and downstream water levels. As Figure 3.2 shows, the upstream and downstream water levels and the differences between the models herein are inconsistent. More significant differences lie in the computation of flow through the breach. In Delft-FLS, discharge is calculated directly from upstream and downstream water levels. In D-HYDRO, the discharge through the breach is not calculated using a stage-discharge relationship. Instead, using a sub-grid numerical method, the velocities, flow area and, thus, discharges are computed using the 2D-shallow water equations with a special discretisation of the advection terms in the momentum equation. This makes the flow through a breach in D-HYDRO dependent on the difference

between upstream and downstream water levels and the energy conservation upstream of the breach. This accounts for friction around the breach, velocity gradients and streamlines on the river. The higher water levels and larger absolute differences at Bemmel and Tiel, which do not result in a larger discharge through the breach, show the substantial influence of kinetic energy in the simulations. Dike breach flow in D-HYDRO is thus dependent on upstream and downstream water levels and on the accurate computation of upstream flow direction and flow velocities.

When the main direction of flow on the river is not normal to the breach (as would be in the initial stages of a dike breach along a river), the far-field velocity vector, from which the flow velocity in the breach is calculated, can be substantially lower than the potential velocity in the breach. This velocity vector depends on the breach's orientation to the dominant flow direction in the river. The orientation of the grid cells on the river and the orientation of the snapped dike breach polyline might have a significant influence on this. At the breach location in Tiel, the flow rate near the breach is high, as the breach is close to the main channel of the Waal. This would result in higher flow velocities through the breach. However, the breach is snapped on the square grid in such a way that the orientation of half of the breach width is in the opposite direction of the dominant flow in the river. The discharges through the second flow link crossed by the breach polyline are considerably lower because of this, dampening the discharge through the breach.

Accurate computation of flow velocities towards the breach depends on grid cell size. To show the implications of this in a D-HYDRO model, another configuration is made at the breach location near Bemmel with a grid refinement around the breach location. Here, the grid is refined from 100m by 100m to a 50m by 50m grid. The resulting discharge, flow velocities and water levels are computed and shown in Figure 3.3. It can be seen that the discharges and the flow velocities are considerably higher when using a 50m

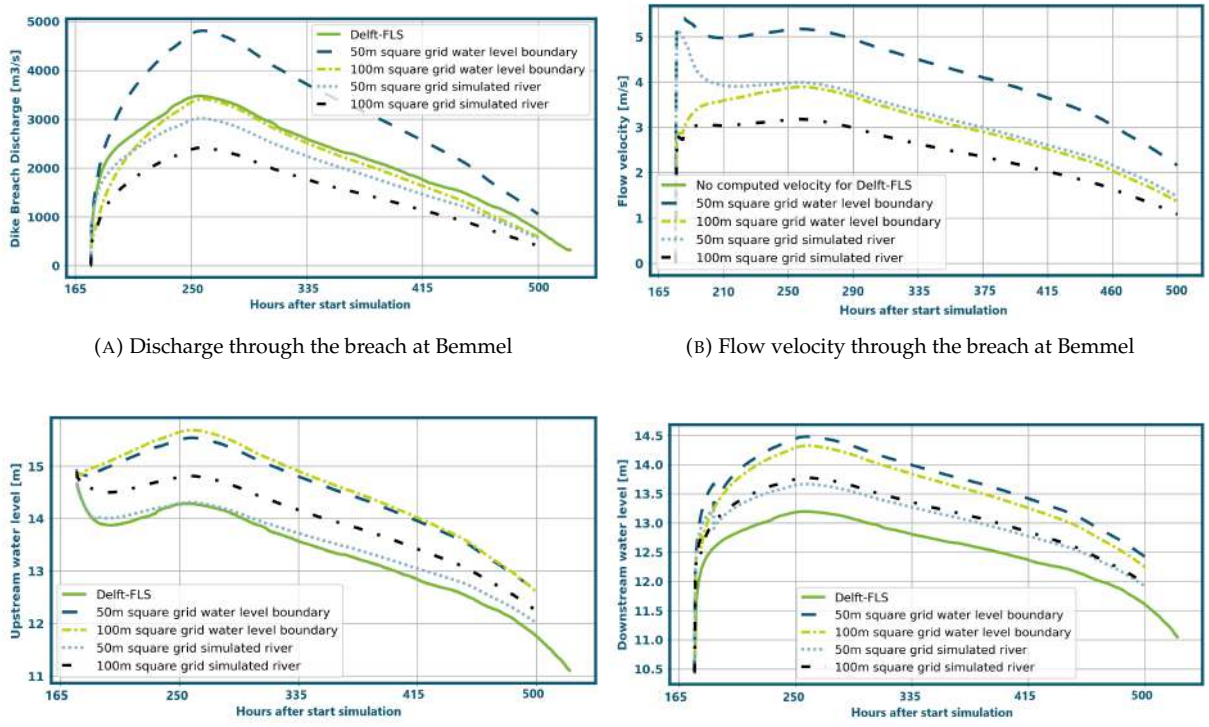

(A) Discharge through the breach at Bemmel

(B) Flow velocity through the breach at Bemmel

(C) Upstream water level through the breach at Bemmel

(D) Downstream water level through the breach at Bemmel

FIGURE 3.3: Breach flow comparison between 50m grid and 100m grid

grid than when using a 100m grid. For the simulation using a water level boundary, upstream water levels decrease slightly and downstream water levels increase compared to a 100m grid. For the simulation where the entire river is schematised, the decrease in the upstream water level is far larger. Again, the downstream water levels increase. This decrease in absolute water level difference and, therefore, gravitational potential does not result in lower flow velocities for both configurations. Flow velocities and discharges increase for the 50m grid.

The literature shows that upstream water levels are expected to decrease rapidly just after a dike breach event (Sun et al., 2017). Upstream flow velocities increase and the flow direction of the river changes partly. Although water levels will rise slightly after the first stage (with or without an increasing discharge wave), the effects are noticeable throughout the simulation. D-HYDRO can capture all these effects. This, however, makes the computation dike breach flow in D-HYDRO dependent on the accurate computation of water levels, flow velocities upstream, flow direction on the river and breach location and orientation. It also makes the computation of dike breach flow sensitive to grid cell size.

3.2 Alternative river schematisations in D-HYDRO

3.2.1 Water level boundary on river axis

For this analysis, four different schematisations are made per dike breach location. Two schematisations use a full 2D river model (HYDRO_D43_1998), of which one with the Verheij-vdKnaap equation as breach growth. Two other schematisations use a water level boundary on the river axis (HYDRO_River_WLB), of which one with the Verheij-vdKnaap equation as breach growth. Figure 3.4 shows the resulting breach discharge and upstream water levels.

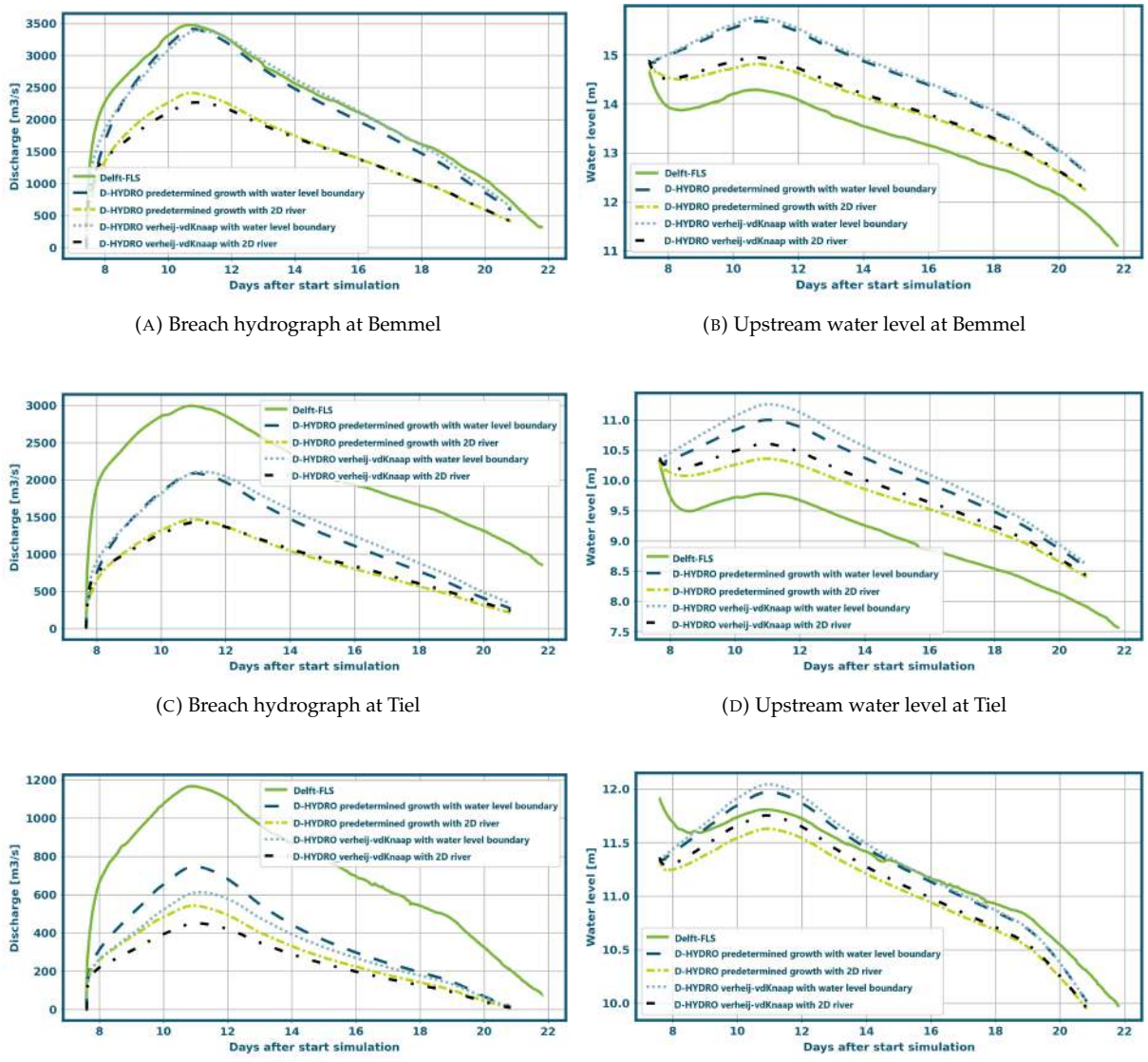

(A) Breach hydrograph at Bemmel

(B) Upstream water level at Bemmel

(C) Breach hydrograph at Tiel

(D) Upstream water level at Tiel

(E) Breach hydrograph at Heteren

(F) Upstream water level at Heteren

FIGURE 3.4: Breach flow comparison between water level boundary and simulated river

Figure 3.4 shows that the breach discharge in the D-HYDRO models, which only schematise a part of the river, is considerably lower than in the Delft-FLS models. This can be attributed to the difference in breach flow computation. However, a higher discharge is observed when the breach discharge is compared to the D-HYDRO models, which include a full 2D river schematisation. The discharge through the breach increases faster and decreases faster. This results in an equal initial and final breach discharge. However, the peak discharge and the cumulative discharge are much larger. This is partly caused by a higher upstream water level and partly caused by an unrealistic flow direction towards the breach.

A dike breach can largely influence water levels and flow velocities on the river upstream of the breach. Water levels decrease, and flow velocities increase. This was, for instance, shown in a flume using an oblique dike breach (Sun et al., 2017). In further simulations done in this research, the water level effects of a breach near Tiel reached up to 15 kilometres upstream. Only schematising a part of the river fails to capture this large-scale effect. By controlling the water level close to the breach, water levels are highly overestimated. In the simulations performed in this research, upstream water levels were up to 1 meter higher when using a water level boundary on the river axis instead of a full 2D river model. In fluvial dike breaches, the breach is often located parallel to the main flow direction of the river. The direction of the main channel flow influences the flow in other directions, such as towards the dike breach. When a breach happens, some flow and momentum are directed towards the breach. The flow through the breach influences streamlines on the river up to a certain distance from the breach location and causes a water level draw-down (Kamrath et al., 2006). The part of the river flow that is influenced by the breach depends on the specific characteristics of the breach. Because there is no main channel flow in the simulations using a water level boundary, all the flow is directed at the breach. This leads to overestimating the velocity gradient and momentum towards the breach.

The simulations show that the use of a water level boundary can lead to an overestimation of the peak dike breach discharge of 1000 m^3/s (43%) at Bemmel, 500 m^3/s (33%) at Tiel and 200 m^3/s (36%) at Heteren compared to a simulation with main channel flow.

3.2.2 1D-river schematisation

Several 1D river schematisations are made for a breach location near Bemmel and Tiel to analyse the impacts of a 1D river schematisation on the breach discharge. The results of these 1D river schematisations (HYDRO_River_2D) are compared to those of a detailed 2D river schematisation (HYDRO_River_2D). All simulations have the same predetermined breach growth.

The most significant differences between the 2D and 1D schematisation are apparent in the bathymetry, roughness and local flow computation representation. In the 2D model, because it has a small grid size, the bathymetry of the river and the floodplains is included in detail. This means floodplains on both sides of the river can have different sizes and 2D shapes, sheltered areas can be present and local low or high elevation points can be schematised. In the 1D model, the bathymetry is simplified to a ZW cross-section. At a location on the river branch, values are given for the river's height (z) and width (w). This creates cross-sections, from which the bathymetry of the river is determined. This approach cannot schematise the local details of floodplains. The computation of the dike breach flow is also different. In the 2D schematisation, upstream flow velocities and water levels are taken from the upstream grid cells close to the dike breach line. These local values can vastly differ from the main channel's hydraulic conditions. In the 1D schematisation, upstream velocities and water levels are taken from a single computational point. In this computational point, the flow velocity and water level are a result of a weighted average over the entire cross-section of the river.

Figure 3.5 compares a simulation with a 1D river schematisation and a simulation with a detailed 2D river schematisation. Confirming the effects shown by Sun et al. (2017), both the 2D simulations and 1D simulations show a drop in water level and an increase in flow velocity on the river after the initiation of the breach. However, the breach discharge is substantially higher in the 1D model for both locations. The peak discharge at Tiel is 1150 m^3/s (62%) higher, and the peak discharge at Bemmel is 400 m^3/s (20%) higher. At Tiel, the main difference lies in the computation of the flow height in the breach, which is considerably higher in the 1D simulation. At Bemmel, it can be seen that both flow velocity and flow height are overall higher in the 1D simulation.

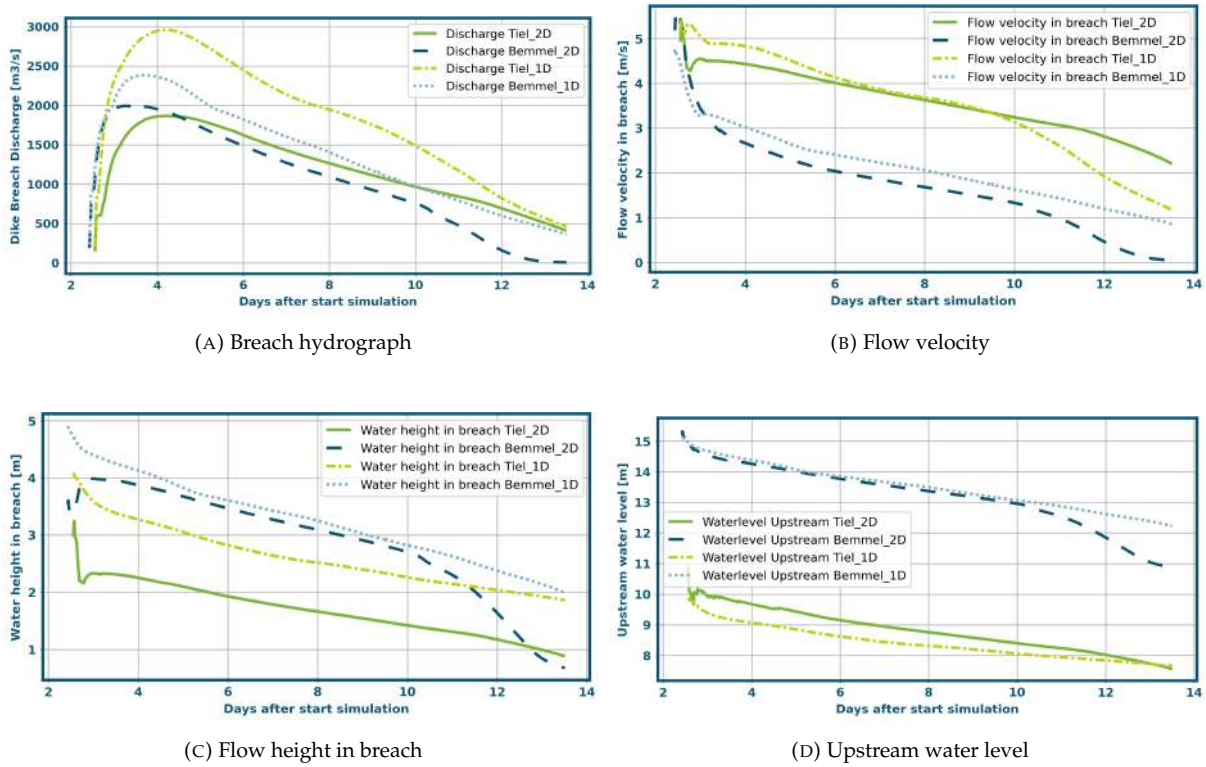

(A) Breach hydrograph

(B) Flow velocity

(C) Flow height in breach

(D) Upstream water level

FIGURE 3.5: Breach flow comparison between 1D river and 2D river schematisation

The first cause of differences can be found in the computation of upstream water levels close to the breach. The 2D simulations show an extra local decrease in water level around the breach on top of the water level decrease apparent in a larger part of the river. At Bemmel, this is roughly 15 centimetres; at Tiel, this is 25 centimetres. This extra local decrease in water level is not computed by the 1D simulation as there is no spatially varying water level in a 1D cross-section. This local water level reduction decreases the potential water level and flow velocity in the breach.

The breach location at Bemmel is covered behind a ridge, which makes it essentially a large extra storage area without significant flow. This flood plain characteristic is accurately schematised in the 2D model. Flow velocities around the breach are low, and flow is directed towards the breach. The influence of the main channel flow is insignificant. In the 1D schematisation, this sheltered area cannot accurately be schematised as hydraulic conditions are averaged over the entire river width. This means that the main channel flow does have a significant influence. By including this part of the river, flow velocities are higher and water levels are higher. This results in a higher upstream momentum, higher flow height in the breach, higher flow velocities in the breach and thus breach discharge.

At Tiel, the breach location lies close to the main channel of the Waal, in a small floodplain. Here, near the breach location, flow velocities are low, but a little further in the main channel, flow velocities are high. There is a clear main flow direction parallel to the breach. Theoretically, this would result in lower velocity gradients towards the breach (Kamrath et al., 2006). The 2D model seems to capture this, as the water level difference between upstream and downstream is higher at Tiel than at Bemmel, but peak discharge is roughly the same. The 1D model does not capture this local effect. The 1D model of D-HYDRO computes a single flow velocity value and water level value per computational point. The averaged flow velocity value is much larger than the local values computed by the 2D model. This is amplified by the effect that a breach has on flow velocities in the main channel of a river. Velocity in computational points of the 1D schematisation increases from 1.10 m/s to 1.85 m/s, while the 2D simulation only computes a local increase from 0.4 m/s to 0.65 m/s. Because of this, an even larger momentum towards the breach is computed in the 1D simulation.

Quantifying the individual contributions of the abovementioned effects on breach discharge is impossible. There is a clear synergy of elements that lead to the observed differences. However, the simulations show that the simplifications in the computation of flow and in bathymetry and area characteristics around the breach of a 1D river schematisation can lead to a significant overestimation of breach discharge. In this study, overestimations of peak discharge of 1150 m^3/s (62%) and 400 m^3/s (20%) are found. The effects of local flow velocities, water levels and local friction on the breach discharge are substantial. The averaged values of a 1D simulation cannot capture these local effects. The performed simulations always resulted in higher breach discharge for a 1D schematisation. This is not limited to a specific location but is found in two places with vastly different flow conditions.

3.3 Breach initiation moment and breach growth

3.3.1 Breach initiation moment

To analyse the impacts of different breach initiation moments on the breach discharge and breach width, several schematisations are made for a breach location near Bemmel. In Figure 3.6 a comparison is made between simulations with a breach initiation a day before peak water level, at peak water level and one day after peak water level. The Verheij-vdKnaap equation is used to calculate breach growth.

Figure 3.6a shows a similar pattern in discharge distribution for all breach initiation moments. This observation can be made because, in all simulations, the breach reaches a final width of around 90 meters (Figure 3.6b). The bell-shaped water level distribution on the river causes roughly the same hydraulic conditions before peak water level as after peak water level. By simulating a breach initiation before the peak, the increase of discharge right after the breach, the maximum dike breach discharge and the decrease in breach discharge can be found. All other simulations will follow the same curve from a different initiation point.

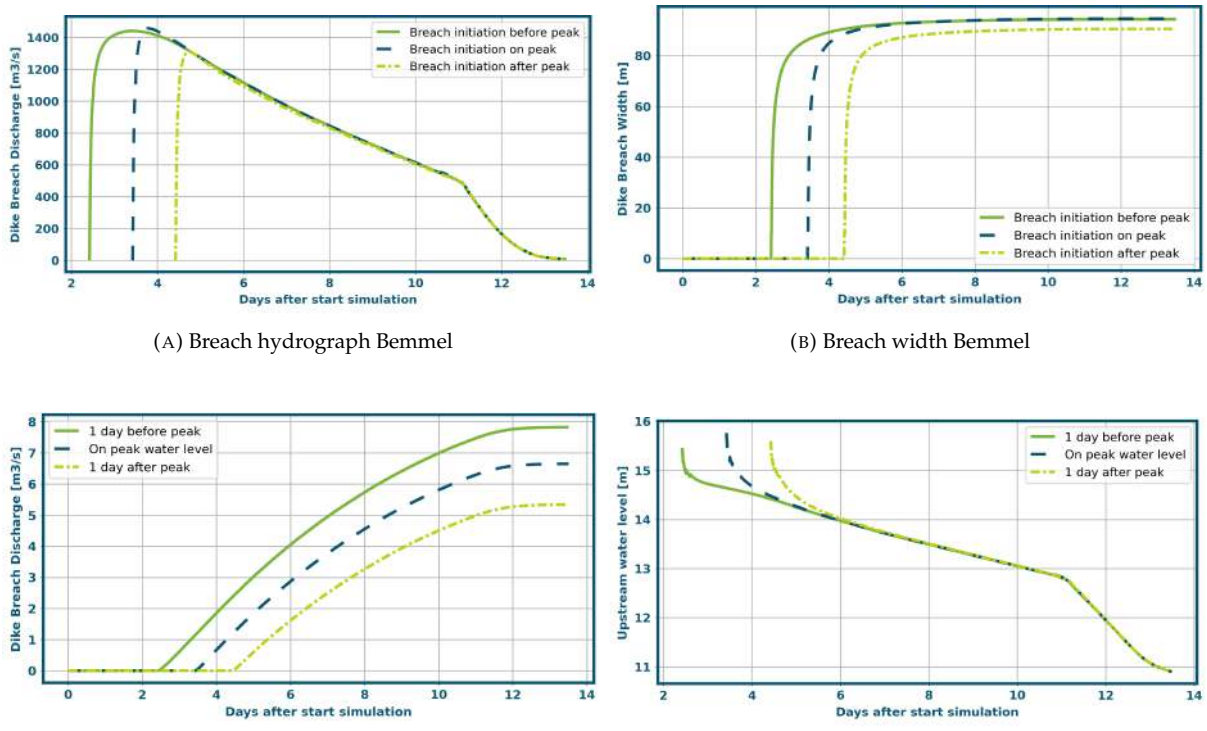

(A) Breach hydrograph Bemmel

(B) Breach width Bemmel

(C) Cumulative discharge

(D) Upstream water level

FIGURE 3.6: Breach flow comparison for three moments of breach initiation

Three phases can be distinguished:

1. Because of the use of the Verheij-vdKnaap equation, the breach grows more than 90% of its final width in the first 14 hours. The increase in breach discharge is governed by the increase in breach width in this phase. This results in equal discharges for all simulations.
2. Breach growth slows down, and breach discharge increase gradually becomes governed by upstream hydraulic conditions. Because the breach width has an upper limit, the breach discharge has a maximum at the highest upstream water level. At Bemmel, the maximum breach discharge is 1440 m^3/s.
3. The breach width is not significantly changing anymore. Upstream hydraulic conditions fully govern the decrease in breach discharge. This results in equal discharges for all simulations because there are no significant differences in breach width.

The guideline for flood simulations advises initiating the breach at the water level peak (De Bruin, 2018). This choice was made due to its unambiguity and the great uncertainty regarding the moment of breakthrough. Simulations depicted in section 4.1 have shown that inundation depths are highly dependent on cumulative discharge. Flow velocities and rise rates are more correlated with peak discharges. The difference in cumulative discharge between 1 day **before** peak water level and on peak water level (1.18E8 m^3) is smaller than between 1 day **after** peak water level and peak water level (1.31E8 m^3). The same maximum discharge is reached when initiating the breach before or at peak water level. Based on cumulative discharge and peak discharge, breach initiation at peak water level is the logical average choice. However, this only holds when breach width is not significantly different between simulations. The validity of the reasoning above is thus dependent on using the Verheij-vdKnaap equation for breach growth or a predetermined time series. When another breach growth formulation is used, a different choice can be made based on the effects of the chosen moment on the breach growth and breach discharge.

From Figure 3.6b, it can be seen that the breach growth calculated with the Verheij-vdKnaap equation is almost independent of the breach initiation moment. A breach that happens a day after the peak water level does result in a slightly lower breach width, but the growth pattern is the same. A lower initial water level difference causes this slightly lower breach width. The final width can, therefore, not be reached before the water level difference over the breach becomes too small. In all simulations, breach width quickly approaches an upper limit. However, according to Verheij (2003), it is highly questionable if a breach width has an upper limit. Flow velocity is at a high level for much longer when the breaching process starts before the water level peaks. In theory, this should generate a faster-growing breach and larger breach width as opposed to breaches that initiate later. For breach discharge, this would result in a faster increase and a higher peak discharge. Without an upper limit to breach width, breach discharge would decline slower, too. This all would result in an exponential upward trend in cumulative breach discharge towards earlier breaching moments.

3.3.2 Computation of breach growth

To analyse the impact of the chosen breach growth model, simulations are done using HYDRO_River_2D for the breach location at Tiel and Bemmel. Simulations are done using the Verheij-vdKnaap equation as a breach growth model. The growth calculated by the model is analysed. Next, alternative breach growths are calculated based on data from the simulations using the equations described in section 2.3.4. A comparison is made between all growth models, and their validity is assessed.

Figure 3.7 shows a final breach width of around 100 meters for Bemmel and 175 meters for Tiel. As shown in the previous section, more than 90% of the final breach width is reached in the first 14 hours. The Verheij-vdKnaap equation includes a term that relates the current time to the breach initiation time. Because this is included in the logarithmic equation, breach width always has an upper limit. This upper limit is reached at eight days for Bemmel and at 12 days for Tiel. In the first 24 hours, flow velocity and flow height in the breach are lower at Tiel than at Bemmel. Yet, in this period, the breach at Tiel grows 50 meters larger than the breach at Bemmel. This shows that by using the Verheij-vdKnaap equation, hydraulic conditions in the breach are not reflected in the growth of the breach.

In D-HYDRO, using the Verheij-vdKnaap equation, the growth in a certain timestep is calculated from the difference between upstream and downstream water levels and the current time. The actual flow velocity or height in the breach is not considered. This means that although the upstream flow conditions

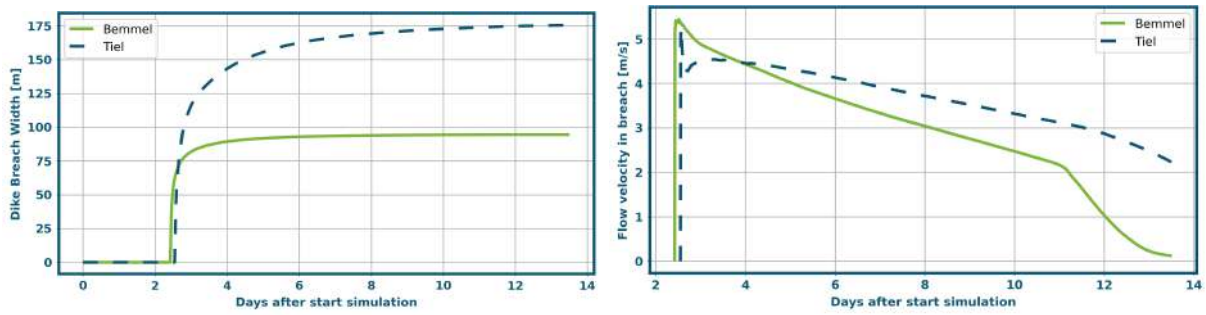

(A) Breach width

(B) Flow velocity inside breach

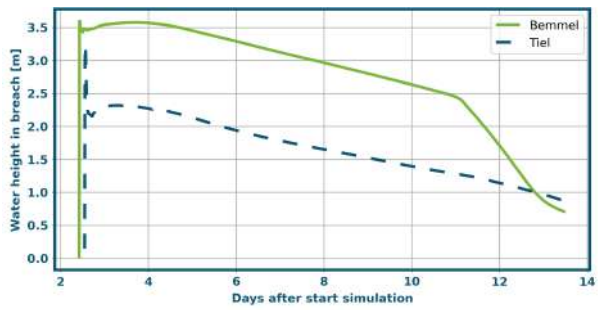

(C) Flow height inside breach

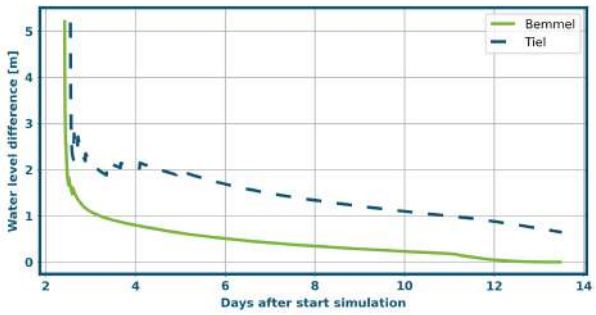

(D) Water level difference

FIGURE 3.7: Breach according to the Verheij-vdKnaap equation

can limit the breach discharge, the breach growth is not. The water level difference between upstream and downstream of the breach is more significant at Tiel, which causes a faster breach growth than at Bemmel.

This dependence on water level differences can cause accuracy problems when flow through the breach is governed by upstream water level (supercritical flow) or in cases where flow through the breach is limited by available energy and flow direction on the river. This would be the case at Tiel. The dependence on breach time can also cause accuracy problems when sub-critical flow is reached very late. At Bemmel, for instance, sub-critical flow is reached at around 11 days. Here, flow velocities decrease rapidly, and breach discharge becomes insignificant. It is expected that the breach will stop growing at this point. However, the Verheij-vdKnaap equation predicts a stop in growth three days earlier. Based on the simulation's flow velocity and flow height data, the calculated breach growth pattern seems unrealistic. It is, therefore, highly questionable if the calculated final width is accurate.

Because of the lack of causality between hydraulic conditions in the breach and breach growth calculated by the Verheij-vdKnaap equation, it seems logical to search for better relationships. In this research, four alternatives are analysed. Two are based on Verheij (2003), and two are based on Van Damme (2020). Figure 3.8 shows a comparison.

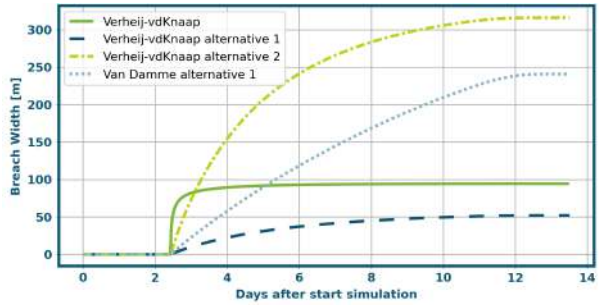

(A) Breach width at Bemmel

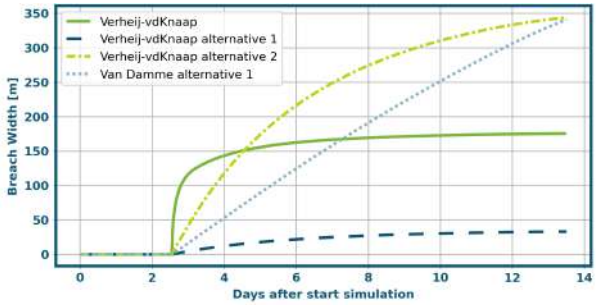

(B) Breach width at Tiel

FIGURE 3.8: Breach width comparison for four different growth equations

Verheij-vdKnaap_a1 is based on hydraulic radius and water level difference. The predicted breach width is low, 52 meters for Bemmel and 43 meters for Tiel. The curve is smooth, increasing faster in the first 12 hours for Bemmel than for Tiel. The growth appears to reach an upper limit at around 12 days for Bemmel and around 13.5 days for Tiel. Verheij-vdKnaap_a2 is based on flow velocity. The predicted breach width is larger. The breach reaches 320 m for Bemmel and 345 m for Tiel. The curve shows the same characteristics as Verheij-vdKnaap_a1, although the difference in growth between Bemmel and Tiel in the first 12 hours is larger. No upper limit in the breach width is reached at Tiel; at Bemmel, the upper limit is reached at 12 days. Van Damme alternative one is based on flow velocity and hydraulic radius. It shows a breach width of 245 meters for Bemmel and 345 meters for Tiel. The curve is much more linear than the Verheij-vdKnaap-based equations. The breach at Tiel shows no upper limit, while the breach at Bemmel does. At Bemmel, reaching the upper limit is initiated simultaneously as flow velocities and flow height decrease rapidly. Van Damme alternative two has predicted breach widths of 16 km for Bemmel and 17.7 km for Tiel. Large coefficient values cause this; it is deemed unrealistic and is therefore not shown here.

In theory, based on the flow velocity and flow height data, several aspects can be expected from the breach growth.

1. The larger velocity and flow height at Bemmel in the first 24 hours should result in a faster breach growth at Bemmel in this stage.
2. As the breach near Bemmel decreases rapidly in discharge after 11.5 days, the growth rate should also decrease rapidly from this point.
3. The decrease in flow height is roughly the same for Tiel and Bemmel, but the flow velocity decreases faster at Bemmel. This should result in a faster decrease in the growth rate at Bemmel.
4. The lower flow velocity overall and the sudden fast decrease in flow velocity and flow height after 11.5 days at Bemmel should result in a lower breach width at Bemmel.
5. As flow velocities stay high at Tiel, breach growth should continue here until the end of the simulation
6. There should be visible differences in breach growth between breaches with different initiation times

A comparison between simulations with different breach initiation moments is given in Figure 3.9.

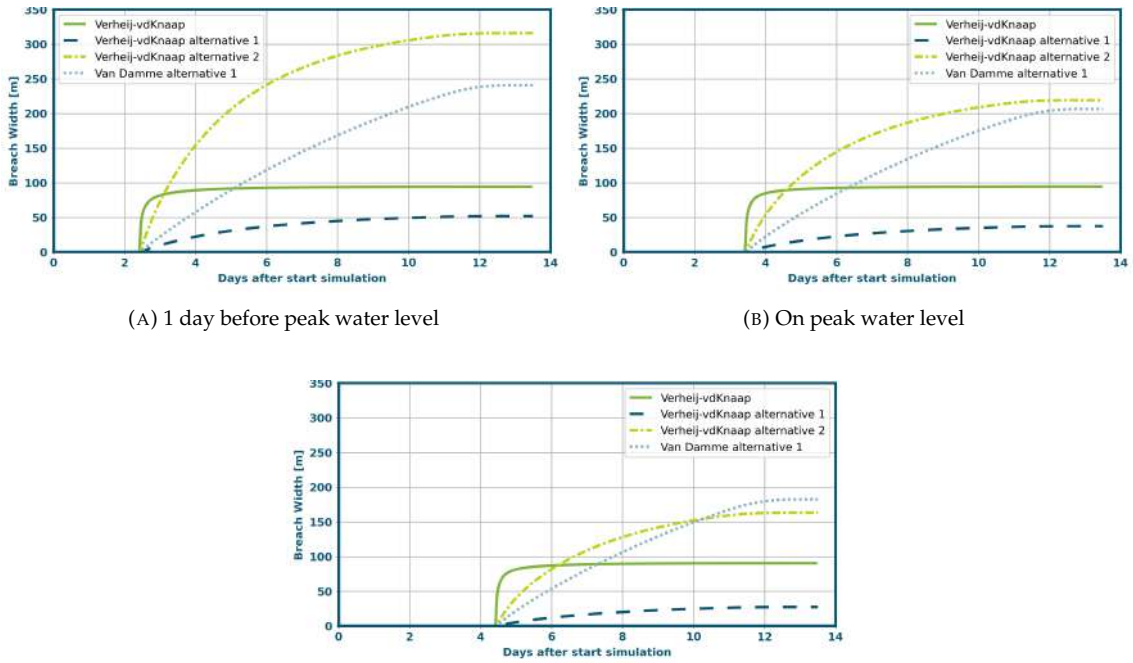

(A) 1 day before peak water level

(B) On peak water level

(C) 1 day after peak water level

FIGURE 3.9: Breach growth at three different initiation moments

Table 3.1 shows an assessment of the four breach growth models based on the above six expectations.

TABLE 3.1: Assessment of growth equation according to expectations based on observed hydraulic conditions [expectation reflected (+)] [expectation not reflected (-)]

Expectation	Verheij-vdKnaap	Verheij-vdKnaap a1	Verheij-vdKnaap a2	Van Damme
1	-	+	+	+
2	-	-	+	+
3	+	+	+	+
4	+	-	+	+
5	-	-	+	+
6	-	+	+	+

Erosion and shear stress are highly dependent on the soil and geometric characteristics of the breach. This research has used values based on a single experiment for the Van Damme equation and the recommended values for the Verheij-vdKnaap equations. It is, therefore, impossible to prove the accuracy of the predicted breach widths. A faster-growing breach would result in lower flow height and flow velocities. This would then result in lower breach growth. Because there is no option to include different breach growth equations in D-HYDRO, this codependency could not be reflected in the analyses done in this research. However, it can be concluded that the Verheij-vdKnaap equation, as implemented in the D-HYDRO software, is unable to predict breach growth based on the hydraulic conditions in the breach. There is no causality between flow height and flow velocity in the breach and breach growth. Equations based on flow velocity and flow height, as shown in this research, are much more consistent with observed hydraulic conditions. Based on the simulations carried out in this research, Verheij-vdKnaap_a2 and the Van Damme equation seem to produce more realistic results than the Verheij-vdKnaap equation that is implemented in D-HYDRO.

4 Results - Distribution of water

The digital elevation model and characteristics of the area largely determine water distribution. Elevated elements like highways, waterways, and underpasses are essential characteristics of the region. How these elements are schematised can greatly influence inundation patterns, depths and flow velocities. Flood simulations are done for three different locations using the configuration made and described in section 2.1, a location near Bemmel, Tiel and Heteren.

4.1 The implications of D-HYDRO

The computational cores of Delft-FLS and D-HYDRO are based on the same principles. However, the two software packages are not entirely the same. By rebuilding a Delft-FLS schematisation in D-HYDRO, two similar schematisations are created in two different software packages. Because the schematisations are the same, differences in flood simulation results, result from differences in the calculation cores. In this section, first, the Delft_D43_1998 model and the HYDRO_D43_1998 model are compared. Next, simulations are done using a newer detailed D-HYDRO model of Water Board Rivierenland (HYDRO_D43_2019). By comparing results from Delft-FLS simulations and both D-HYDRO models, the implications of the D-HYDRO software as opposed to the Delft-FLS software are determined. Figure 4.1 shows a map of the maximum inundation depth for the breach location at Bemmel[1] for Delft_D43_1998 and HYDRO_D43_1998.

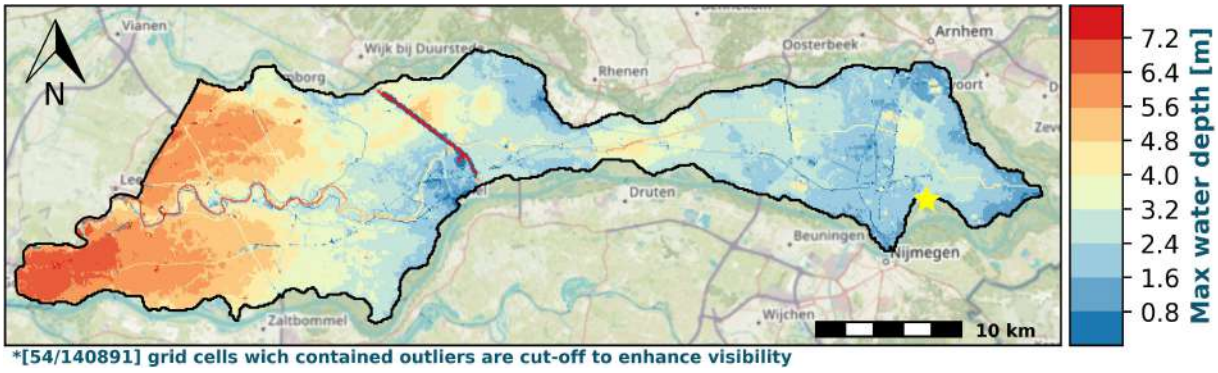

(A) HYDRO_D43_1998

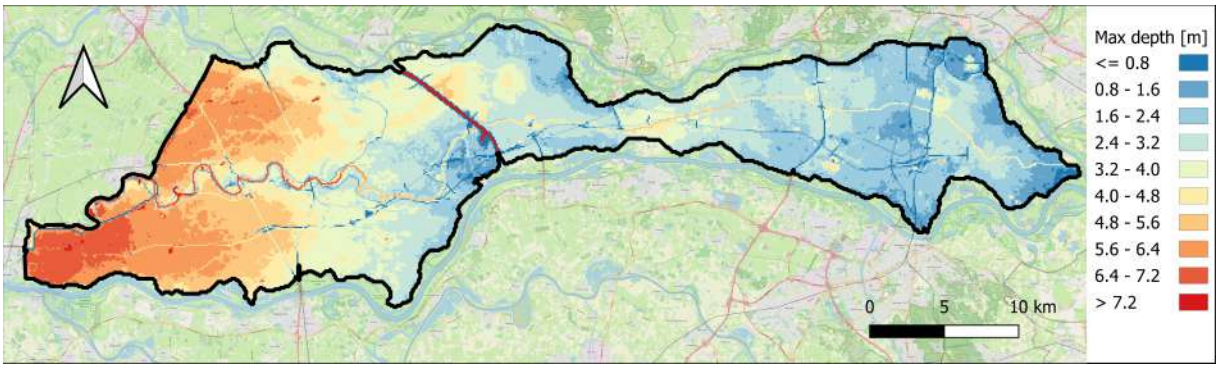

(B) Delft_D43_1998

FIGURE 4.1: Maximum inundation depth at Bemmel [Yellow star = Breach location]

[1]See Figure 1.5

The inundation extent is equal for both models. From the breach location in the eastern part of the dike ring, water flows westwards and accumulates in the lowest areas. Both models have almost no areas with a lower water depth than 0.8 meters. Close to the breach location, west of the A325[1], Delft-FLS (Figure 4.1b) computes lower water depths at some locations. These differences arise at the end of the simulation. At the end of the simulation, Delft-FLS computes flow over the Diefdijk[1] in the western part of the dike ring. In the D-HYDRO model (Figure 4.1a), there is no flow over the Diefdijk simply because this area is not included in the model domain. The maximum water depth at the western side of the Diefdijk only reaches up to 0.2 centimetres, which leads to more storage space in the western part of the area. Because of that, water depths at locations with a higher elevation reach a lower maximum. Locally, it causes lower water depths in the Delft-FLS model of around 10 centimetres. Maximum flow velocities, rise rates and arrival times are all relatively equal for both models. This leads to the conclusion that differences in maximum inundation depth are not caused by differences in flow computation but by the extended storage space west of the Diefdijk.

Although slight differences were found between Delft-FLS and D-HYDRO, these can all be explained. They can mainly be attributed to the difference in the model domain. These differences are insignificant for the flood simulation output variables this study aims at (maximum inundation depth, maximum flow velocity, maximum rise rate and arrival time).

In Figure 4.2 the results HYDRO_D43_2019[2] are shown. This model has a largely different and much more detailed schematisation than the other two models. HYDRO_D43_2019 has a detailed unstructured grid, includes fixed weirs and more than 2638 underpasses and divers. If significant differences are observed between HYDRO_D43_1998[3] and HYDRO_D43_2019. In that case, they can be attributed to the differences in schematisation. In the simulations of HYDRO_D43_2019, the inflow of water is the same as that of HYDRO_D43_1998.

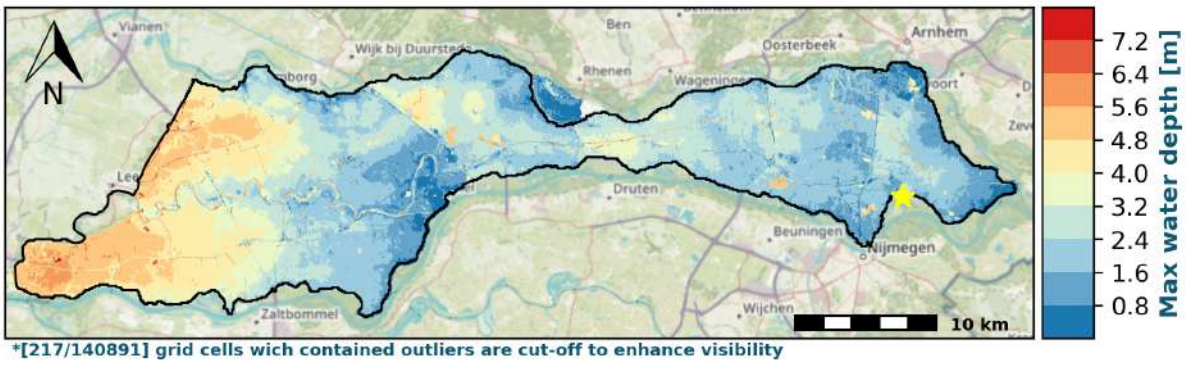

FIGURE 4.2: Maximum inundation depth Bemmel [HYDRO_D43_2019]

HYDRO_D43_2019 clearly shows lower inundation depths across the entire area. A large part of this difference can be attributed to the more detailed grid and elevation model. The detailed grid has an average grid cell size of 1600 m^2, while the Delft-FLS grid has a square grid cell size of 10000 m^2 (100mx100m). Because the grid of HYDRO_D43_2019 is a flexible mesh, it can follow the contours of the landscape better. Many smaller waterways have been included in the digital elevation model. Because there are divers included in a floodplain in the centre of the area, even more, extra storage volume can be used. This all creates a more significant potential storage volume in HYDRO_D43_2019. In HYDRO_D43_1998, elevated elements like highways are included as 100mx100m grid cells. However, the area's highways are mostly not more than 60 meters wide. In HYDRO_D43_2019, these elements are accurately sized. Schematising these elements in more detail creates even more potential storage volume than in HYDRO_D43_1998.

By multiplying the surface area of every grid cell with a potential storage height (based on bed elevation and a reference height) an estimate of the difference in storage volume can be made. HYDRO_D43_2019 has 107.3E6m^3, more storage volume, which is about 4% of the total water volume flowing into the area. This is calculated excluding the extra floodplain that is inundated south of Rhenen[1].

[2]New detailed D-HYDRO schematisation
[3]Delft-FLS schematisation rebuild in D-HYDRO
[1]See Figure 1.5

In Figure 4.3, a map of the maximum flow velocity is shown for HYDRO_D43_1998 and HYDRO_D43_2019.

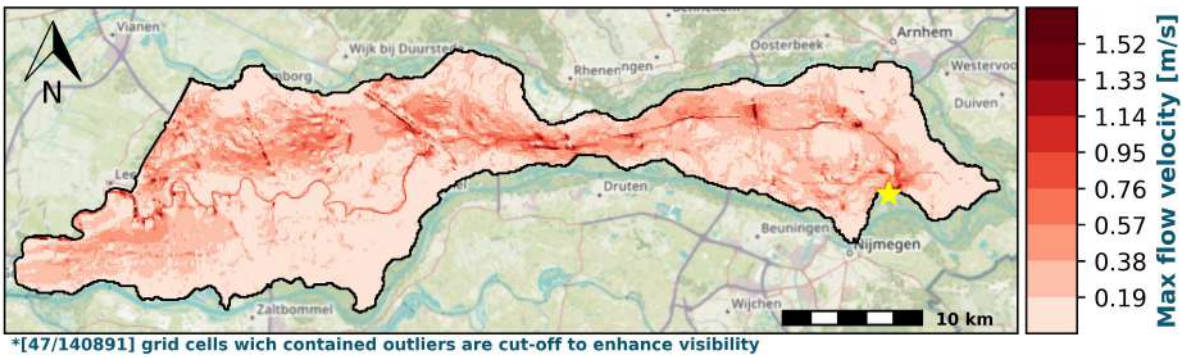

(A) HYDRO_D43_1998

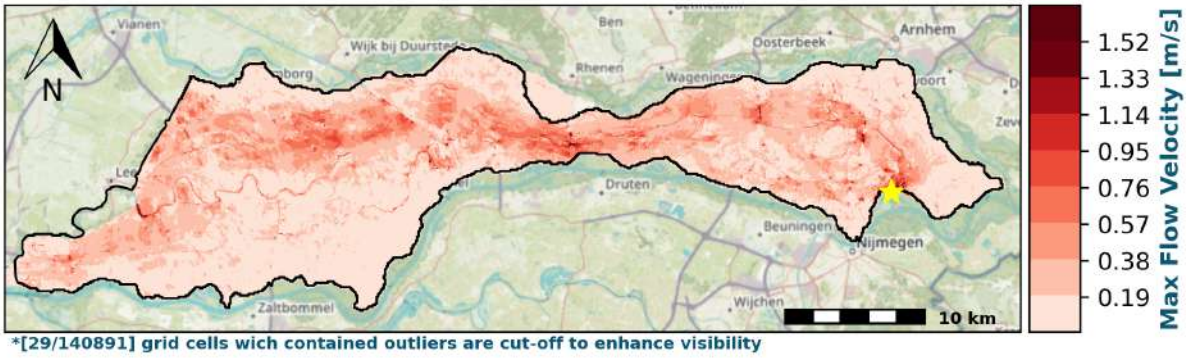

(B) HYDRO_D43_2019

FIGURE 4.3: Maximum flow velocity at Bemmel [Yellow star = Breach location]

The comparison shows that flow velocities are fairly similar for both schematisations. Flow velocities higher than 2 m/s are only found at elevated and compartmentalising elements and in the Linge. The main flood wave travels the same path. First, to the north in the direction of the Linge and west underneath the A325 south of the A15[1]. The bulk of the flood wave passes the A50[1] at the same point, creating high flow velocities. Over this highway, flow velocities reach 2 m/s in HYDRO_D43_1998 (Figure 4.3a)[2] and 1.45 m/s in HYDRO_D43_2019 (Figure 4.3b)[3]. From this point, the main flood wave largely follows the Linge until the Amsterdam-Rijn Kanaal[1] (ARK). High flow velocities are found in both models for the narrow part in the centre of the dike ring. Some differences are found west of the ARK. The high flow velocities in HYDRO_D43_1998 are concentrated at higher elements in the area. In HYDRO_D43_2019, these hotspots are also found, but the flow velocity overall is higher.

In HYDRO_D43_1998, many high-velocity hotpots are found, while the flood wave in HYDRO_D43_2019 is more spread out. The more detailed grid and the many underpasses of HYDRO_D43_2019 can play a large part in this. A significant cause of the differences west of the ARK can be attributed to a siphon of the Linge under the ARK. This underpass is present in HYDRO_D43_1998 but not in HYDRO_D43_2019. This has two significant consequences. Firstly, flow velocities- in the Linge are higher in HYDRO_D43_1998, and extensive inundation is found close to the Diefdijk[1]. Secondly, it causes a larger concentrated flood wave over the ARK dikes in HYDRO_D43_2019. Locally, this results in higher flow velocities between the ARK dikes and the A2[1].

[1]See Figure 1.5
[2]Delft-FLS schematisation rebuild in D-HYDRO
[3]New detailed D-HYDRO schematisation

Figure 4.4 shows a map of the maximum rise rate for for HYDRO_D43_1998 and HYDRO_D43_2019.

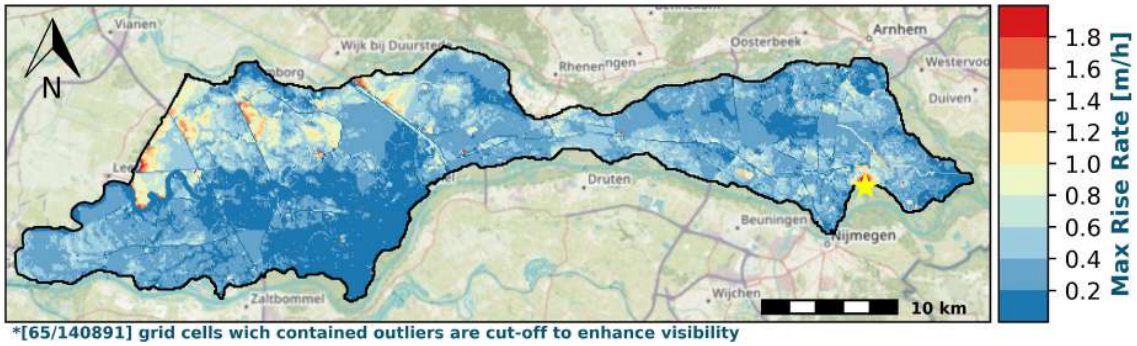

(A) HYDRO_D43_1998

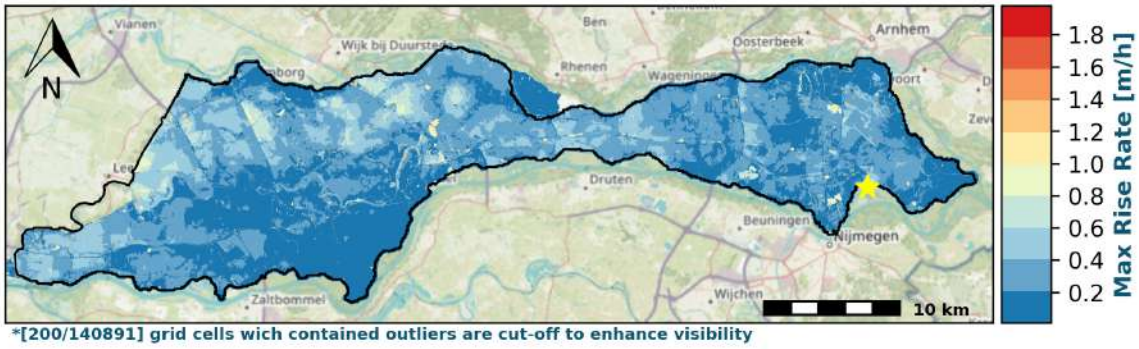

(B) HYDRO_D43_2019

FIGURE 4.4: Maximum rise rate at Bemmel [Yellow start = breach location]

The comparison of HYDRO_D43_1998 (Figure 4.4a)[1] and HYDRO_D43_2019 (Figure 4.4b)[2] shows significant differences in rise rates. Rise rates in HYDRO_D43_2019 are lower in the entire area. HYDRO_D43_1998 shows an average rise rate of 0.64 m/h, while HYDRO_D43_2019 shows an average of 0.41 m/h. In both models, the area south of the Linge and west of the Amsterdam-Rijn Kanaal show low rise rates smaller than 0.2 m/h. However, this area of low-rise rates is larger and more uniform in HYDRO_D43_2019. Some hotspots in model 1 show rise rates higher than 2 m/h. These can primarily be found near the ARK dikes, A2 and the Diefdijk[3]. Close to the breach location, these same high-rise rates are calculated. In HYDRO_D43_2019, peak rise rates are found at the same elevated elements. However, peak rise rates in this simulation are much lower. Only at the A2, ARK and close to the breach location are rise rates between 1 m/h and 1.2 m/h found. In HYDRO_D43_1998, these rise rates values are found all over the area. Differences in rise rates can be attributed to two differences in schematisation.

Firstly, the differences in grid size and digital elevation model. The coarse grid of HYDRO_D43_1998 includes larger elevation jumps between cells and areas than the finer grid of HYDRO_D43_2019. Elevation differences between cells can be as large as 0.4 meters. While water rises in a grid cell, the flooded area expands slower in this grid. Water accumulates in the low grid cells to higher depths before flowing over to other cells. In the finer grid, the flooded area increases faster with increasing water depth, resulting in lower rise rates. In HYDRO_D43_1998, the highest rise rates are found in the first 0.5 meters of water depth. Areas with relatively lower elevations show significant rise rates. This creates large local differences in rise rates, as shown in Figure 4.4a by the spotty pattern all over the area. This pattern in rise rate values is far smoother in HYDRO_D43_2019.

[1] Delft-FLS, schematisation rebuild in D-HYDRO
[2] New detailed D-HYDRO schematisation
[3] See Figure 1.5

Secondly, significant differences in rise rates close to elevated elements can be attributed to the many underpasses in HYDRO_D43_2019. With many underpasses, water will rise slower against these elements as some water can flow through. Rise rate differences close to the breach location show that the detailed elevation grid and the underpasses of HYDRO_D43_2019 allow for faster water flow. The faster flow and more spread-out flood wave cause lower rise rates in the recent D-HYDRO schematisation.

Figure 4.5 shows a map of the arrival time for HYDRO_D43_1998 and HYDRO_D43_2019.

(A) HYDRO_D43_1998

(B) HYDRO_D43_2019

FIGURE 4.5: Arrival time at Bemmel [Yellow star = breach location]

Arrival times on a 24-hour scale are not significantly different between both schematisations. This is caused by the major compartmentalising elements like the A50 and the ARK dikes[1]. It can, for instance, be seen that in both models, everything east of the A50 floods within a day. However, two major differences can be seen. First, the arrival times in HYDRO_D43_2019 (Figure 4.4b)[2] propagate more uniformly from east to west. This is caused by the many underpasses in the model, ensuring water can pass a high element at many places. In HYDRO_D43_1998 (Figure 4.5a)[3], the number of these initial underflow locations is small. Secondly, the Linge has a significant influence in HYDRO_D43_1998. The land west of the ARK dikes was inundated earlier because there is a diver for the Linge underneath the ARK in this model, which is not present in HYDRO_D43_2019.

These results show that the impact of the D-HYDRO software on water distribution is not a characteristic of the software itself but is instead a result of the various added modelling choices that the software provides. All flood simulation result variables show significant differences between the old and new schematisation. Differences in flood simulation results computed by the D-HYDRO model as opposed to the Delft-FLS model are caused by a more detailed grid and DEM, schematisation of the Linge and its tributaries, more and detailed elevated elements, inclusion of fixed weirs and the inclusion of underpasses and divers. This research does not include the calculation of Dutch safety norms as Schippers (2023) did. However, the simulations presented above, combined with the results from Schippers, show largely different flood simulation results if flood simulations for dike ring 43 were performed with D-HYDRO as opposed to those done with Delft-FLS.

[1] See Figure 1.5
[2] New detailed D-HYDRO schematisation
[3] Delft-FLS schematisation rebuild in D-HYDRO

4.2 Fixed weirs and local waterways in D-HYDRO

4.2.1 Elevated obstacles as fixed weirs

In Delft-FLS, elevated obstacles, such as highways and regional dikes, are schematised by artificially increasing elevation levels of grid cells. This results in a line of elevated grid cells. In D-HYDRO, it is possible to schematise such objects as fixed weirs on the 2D grid. This gives more freedom and accuracy in the location of these elements and should be better in computing flow over sudden elevation changes. This is because of the discontinuous nature of flow over an obstacle. Two schematisations are made for the breach location at Bemmel[1]. In the first schematisation, fixed weirs are introduced on the grid without changing the elevation of the underlying grid cells (HYDRO_FX_NEC). In the second schematisation, grid cells artificially elevated in the reference model (HYDRO_D43_1998) are reduced in height before implementing the fixed weirs (HYDRO_FX_EC). Changing the elevation of the grid cells increases the area where water can potentially be stored by 22.9 km^2, which can, therefore, have effects unrelated to the fixed weirs themselves.

This section compares the implementation of fixed weirs in a model with HYDRO_D43_1998. First, it quantifies the local effects of universal fixed weirs on flow over obstacles in a D-HYDRO model. Next, it explains the impact on flood simulation results.

Local effects of fixed weirs

Simulations of the first schematisation HYDRO_FX_NEC (without elevation change) show that elevated elements like the A325, A50 and ARK dikes[1] have a significant compartmentalising effect. Flow over these elements primarily concentrates at a specific lower location of this element. A comparison of flow at these locations between the HYDRO_D43_1998 reference model and a simulation including fixed weirs is shown in Figure 4.6.

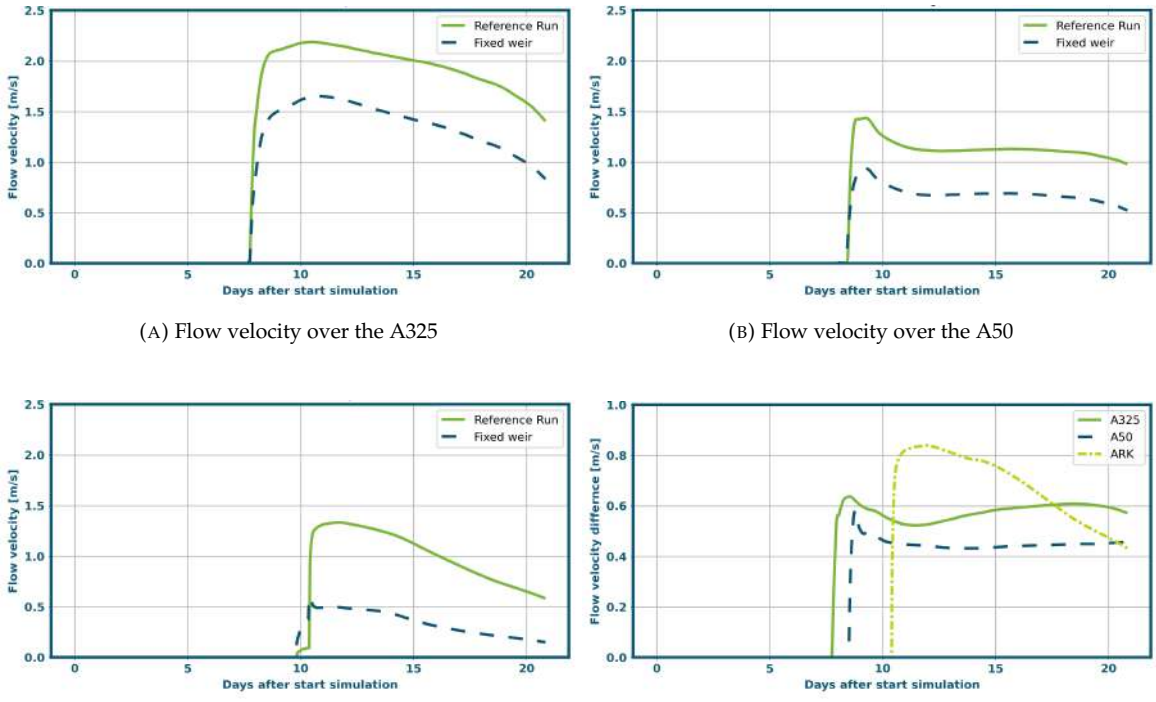

(A) Flow velocity over the A325

(B) Flow velocity over the A50

(C) Flow velocity over the ARK dikes

(D) Difference elevated grid cells and fixed weirs

FIGURE 4.6: Flow velocity over elevated lines

The highways and dikes in Figure 4.6 block the flow from east to west. The water level increases upstream of the elevated line until it can flow over the line at its lowest point. Implementing a fixed weir significantly reduces the flow velocity and total through flow over a line element. The figure shows that

[1]See Figure 1.5

flow velocities at the chosen locations are much lower when a fixed weir is implemented. At the most upstream location (A325)[1], the difference in flow velocity reaches 0.6 m/s. The flow velocities are the highest at this location as it is closest to the breach location. The difference in flow velocity is the largest at the Amsterdam-Rijn kanaal[1]. Here, two dikes (thus two fixed weirs close behind each other) decrease the velocity of the water. The shown reduction in flow velocities by fixed weirs at these compartmentalising elements is mainly a local effect. Downstream of the weir, the effect is mostly gone in 500 meters, and no differences are found between HYDRO_D43_1998 and the model, including fixed weirs. Flow velocity differences are present on the flood wave's main flow route. This is, however, not significant as the difference never reaches higher values than 0.05 m/s. The influence of other fixed weirs, which do not have a compartmentalising effect, is negligible. This is because the flood wave travels around it or the water depth has increased to a level far above the weir's crest.

A lower flow velocity at the though-flow location would suggest an increased water level upstream of the elevated element. In the second simulation, where the underlying grid cells of fixed weirs are not decreased in height, fixed weirs indeed cause an increase in upstream water level. This is shown in Figure 4.7.

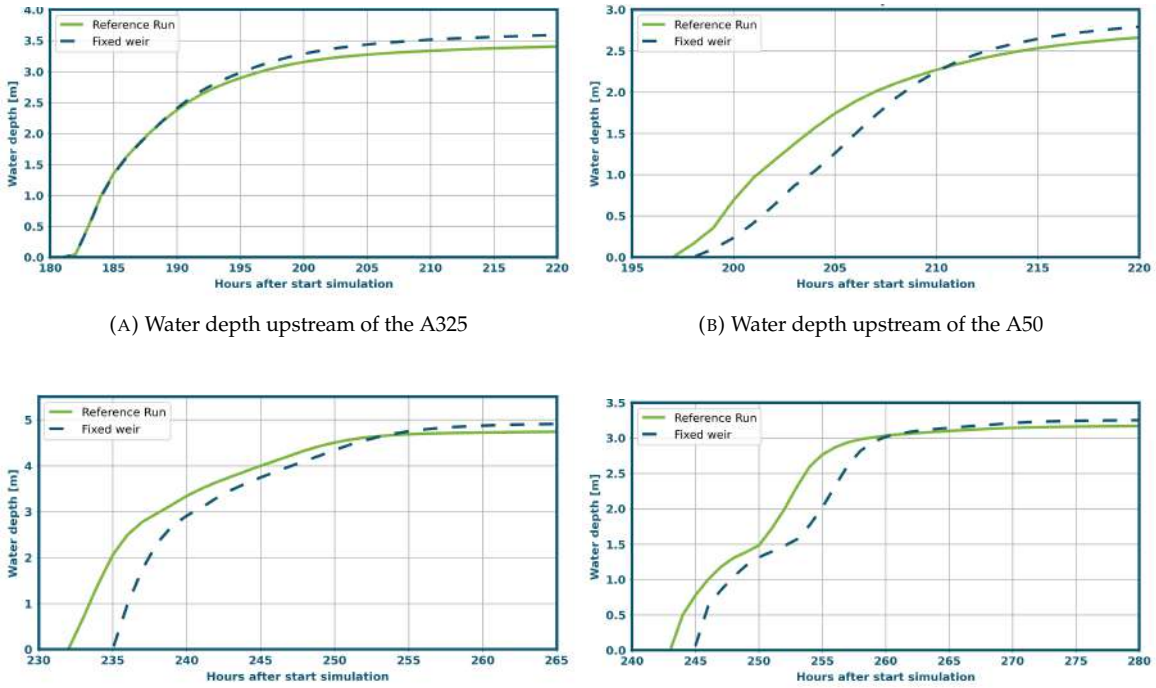

(A) Water depth upstream of the A325

(B) Water depth upstream of the A50

(C) Water depth upstream of the ARK dikes

(D) Water depth downstream of the ARK dikes

FIGURE 4.7: Water depth at four locations without elevation change

The most significant differences are found upstream, east of the A325 and the A50[1]. At the A325, for a simulation including fixed weirs, the water depth is 0.15 meters higher than that of the reference simulation. At the A50, this is 0.19 meters. In the downstream area west of the Amsterdam-Rijn kanaal, this difference has decreased to 0.05 meters. The flood wave is delayed when fixed weirs are used. East of the A325, there is no delay. After this first compartmentalising element, the front of the flood wave is delayed one hour. East of the Amsterdam-Rijn kanaal, this has increased to 3.5 hours. After the Amsterdam-Rijn kanaal[1], the delay has decreased to 2 hours. This is because the Linge inundates the area before the ARK dikes overflow. Although delayed, the rise rates are practically equal in both simulations.

In the dike breach simulations of section 2.3, a large grid cell size influence was found on the flow velocity over fixed weirs. As flow velocities are much lower and the horizontal scale at which water flows to the lowest point on the weir is much larger than in a river, the directional change in flow lines is of less influence. However, the computation of the velocity gradient towards the weir might still be inaccurate, using grid cells of 100 meters. The simulations are therefore performed again, but now with a grid cell

[1]See Figure 1.5

size of 50 meters around all implemented fixed weirs. The resulting flow velocities over the main elevated elements are shown in Figure 4.8.

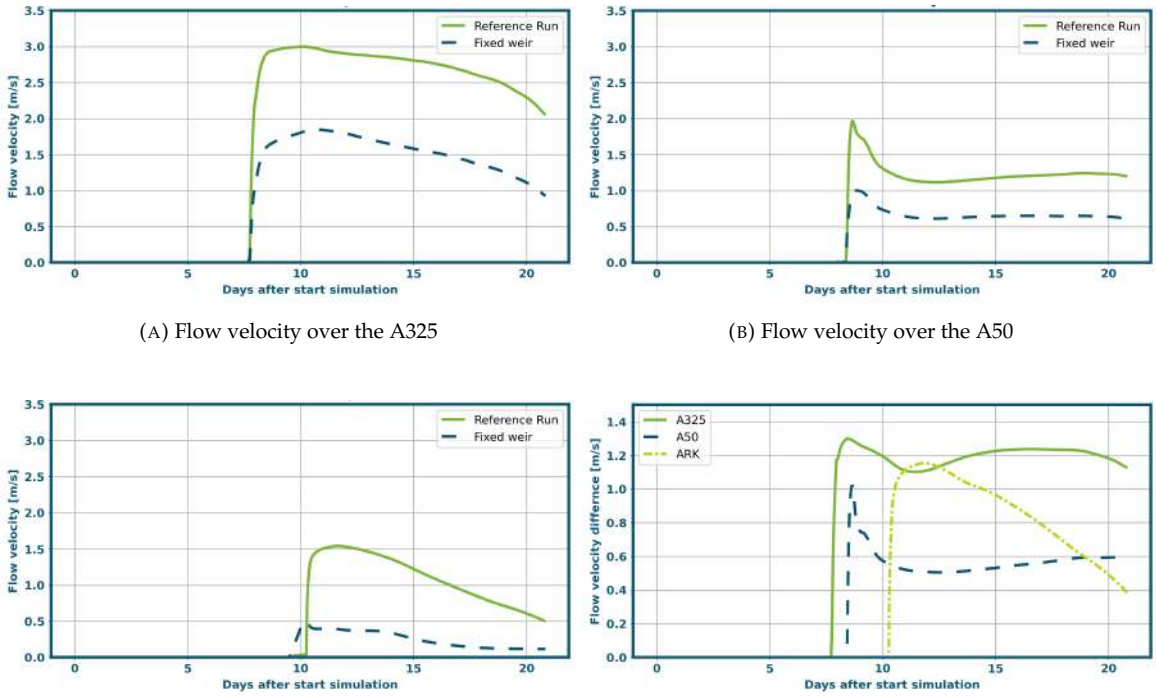

(A) Flow velocity over the A325

(B) Flow velocity over the A50

(C) Flow velocity over the Amsterdam-Rijn kanaal dikes

(D) Difference elevated grid cells and fixed weirss

FIGURE 4.8: Flow velocity over elevated lines with reduced grid cell size

It can be seen that reducing the grid cell size increases the flow velocity over the elevated element when no fixed weir is implemented. The reduced grid cell size of 50m can compute larger velocity gradients over the same distance as a 100m grid cell. Implementing the fixed weir ensures that significant velocity increases in the mesh are not computed. It reduces the computed flow velocities over the elevated obstacle up to 1.3 m/s at the A325, 1 m/s at the A50 and 1.15 m/s at the ARK dikes[1]. When the simulation with a 100m grid and the simulation with a 50m grid (both including fixed weirs) are compared, practically no differences in flow velocities are found. This shows that the computed velocity at the fixed weir crest is largely independent of grid cell size.

Although it seems to conflict with several conclusions drawn in section 3.1, it does not necessarily. Flow over the fixed weirs implemented in the study area is primarily normal to the orientation of the weir and flow velocities are low. The kinetic energy of the water upstream of the fixed weir is much less significant than on the river. This makes flow velocity at the fixed weir primarily governed by differences in water level upstream and downstream of the weir. The water level upstream of the weir is mainly influenced by the weir flow itself, without prominent influences of upstream hydraulic conditions. This vastly reduces the influence of grid cell size compared to the dike breach flow calculation.

Effects of fixed weirs on flood simulation results

The simulations show that implementing fixed weirs on elevated elements can substantially influence the through flow of water in the area. Flow velocities over the elevated lines that compartmentalise the area are significantly reduced. Effects on flood simulation output variables of interest are found in the maximum inundation, maximum rise rate and arrival time. Significant maximum flow velocity differences are only found directly around the elevated elements.

Here, the output of two simulations for a breach near Bemmel is compared with the HYDRO_D43_1998 reference model. One simulation with fixed weirs and changed elevation, HYDRO_FX_EC and one simulation with fixed weirs without changed elevation, HYDRO_FX_NEC. Figure 4.9 shows the maximum inundation depths.

[1]See Figure 1.5

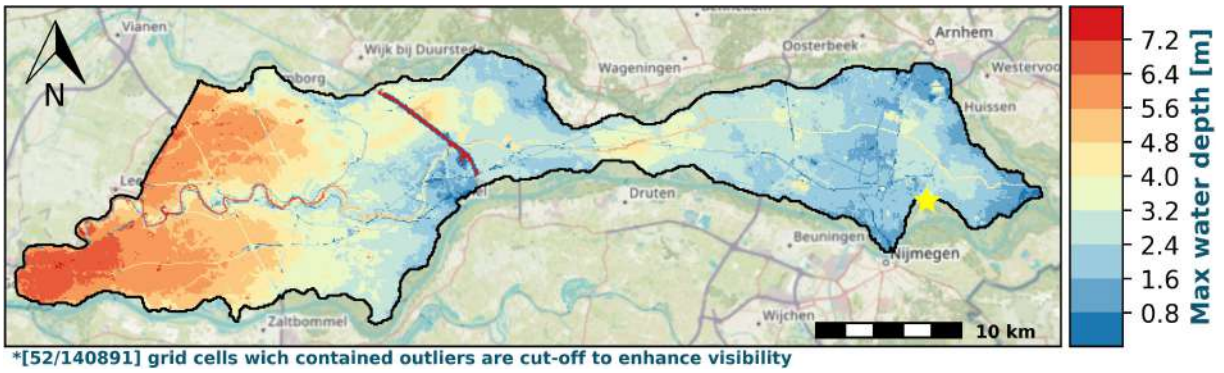

(A) HYDRO_D43_1998

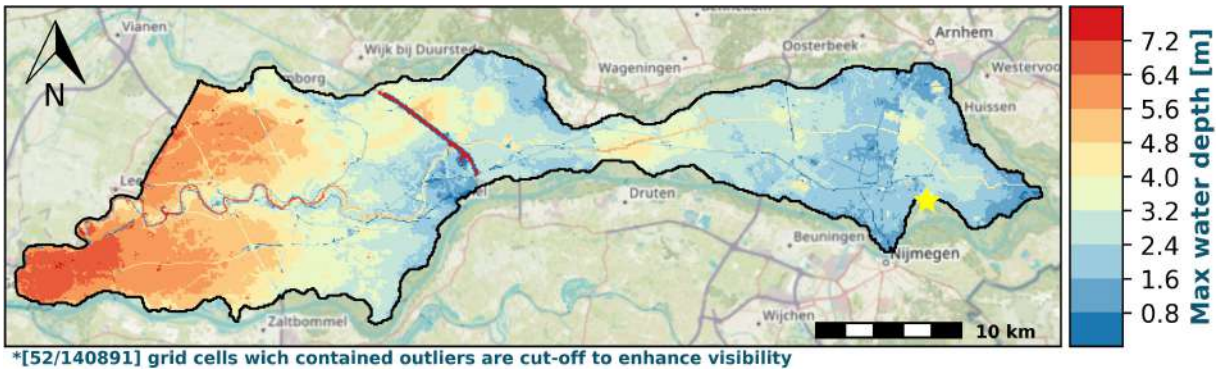

(B) Fixed weir schematisation **without** changed elevation

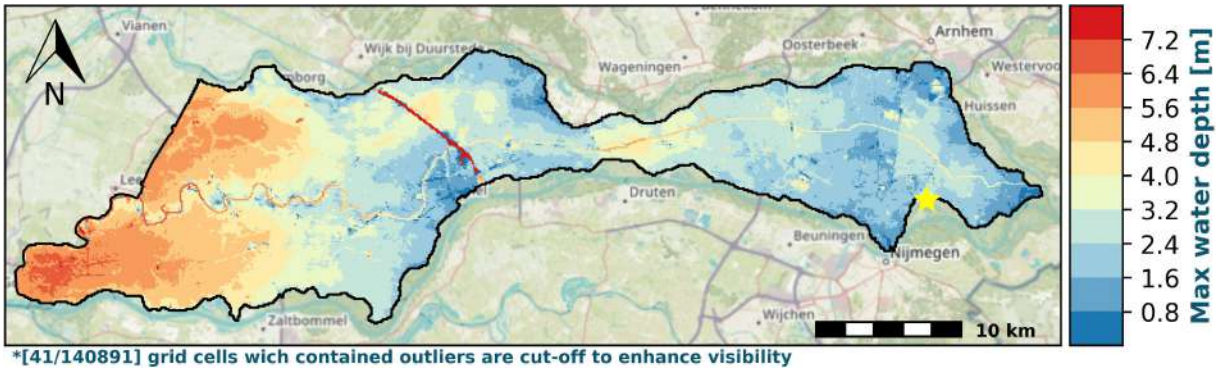

(C) Fixed weir schematisation **with** changed elevation

FIGURE 4.9: Maximum inundation depth [Yellow star = breach location]]

In the first simulation (Figure 4.9b) where the bed level of grid cells behind fixed weirs has not been reduced, almost no significant differences in maximum inundation depth were found. The only significant differences that are found are locally around the fixed weirs. Here, the water depths are higher for the simulation with fixed weirs. This can be seen locally at the ARK dikes and the A325[1]. The differences are never over 20 centimetres, and the affected area is minimal. This shows that although fixed weirs significantly affect the flow computation over the elevated element, with a large flood wave, the effects on maximum inundation in the area are negligible.

In the second simulation (Figure 4.9c), where the bed level of grid cells has been reduced, the effect is much more significant. When the results of this simulation are compared with the HYDRO_D43_1998 reference simulation, considerable differences are found throughout the entire area. West of the A325, local water depth decreased up to 0.8 meters. The area with a water depth over 1.5 meters decreases with 6.1 km^2. The most significant differences are found at the extreme water depths in the western part of

[1]See Figure 1.5

the study area. The area with a water depth larger than 5.6 meters decreased with 22 km^2. This same effect is seen for the maximum rise rates in the area. The differences between the simulation with and without fixed weirs (with the same elevation) are negligible. Differences in rise rate classes are at most 1.3 km^2. A more significant effect is seen when the elevation downstream of the fixed weirs is changed. In this simulation, the area with a rise rate larger than 0.5 m/h is decreased by 22.78 km^2 compared to the reference simulation.

From Figure 4.7, it could be concluded that implementing fixed weirs has the potential to delay the flood wave. For maximum inundation and rise rates, the largest effect was seen in the simulation with elevation change. However, the largest effects for arrival times are found for the simulation without elevation change. This shows the impact of fixed weirs on the grid. The inundation extent after the first 30 hours is shown in Figure 4.10

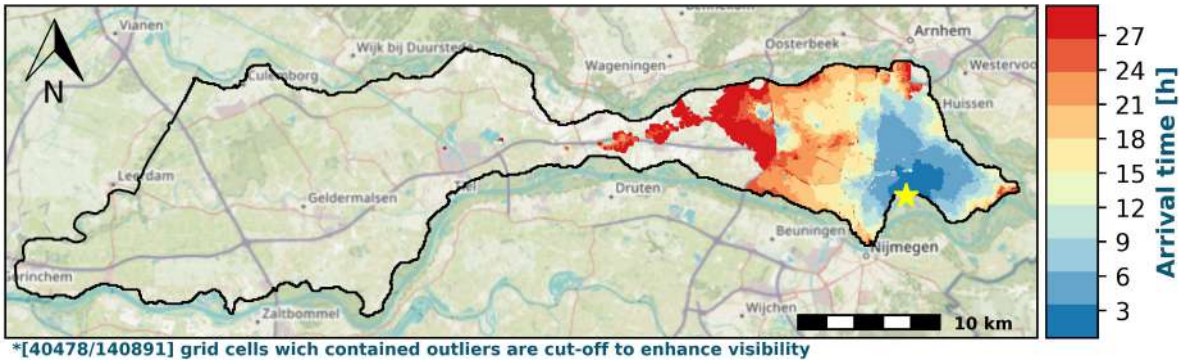

(A) HYDRO_D43_1998

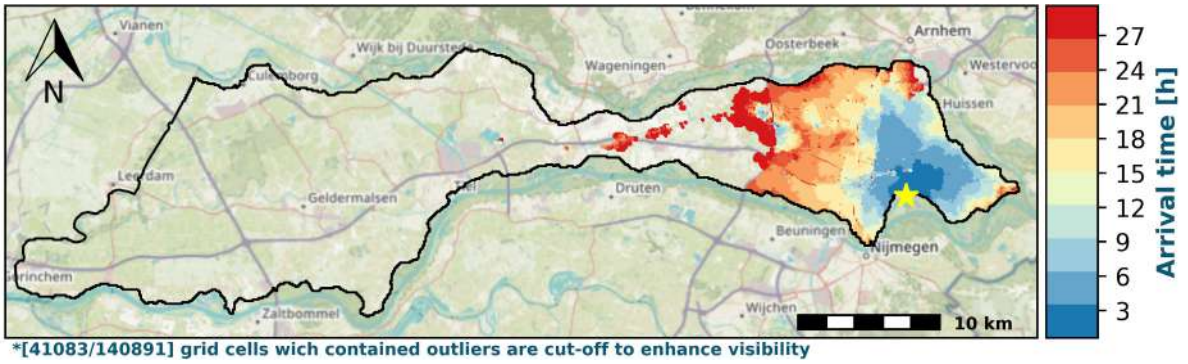

(B) Fixed weir schematisation **without** changed elevation

FIGURE 4.10: Arrival time at Bemmel [Yellow start = breach location]

Here, it can be seen that the implementation of fixed weirs delays the flood wave mainly North of the Linge[1]. The area that is inundated within 30 hours decreases with 8.9 km^2. For large areas between the A325 and the A50[2], the flood wave is delayed 1-3 hours. The difference in the inundated area within 50 hours is still about 9 km^2 between the two simulations. The delay of the flood wave can increase up to 10 hours in the western part of the dike ring. This is 10 hours on a total arrival time larger than 72 hours.

Although the difference in flow computation between elevated elements as fixed weirs and elevated elements as elevated grid cells is significant, the differences in flood simulation results are minimal. The results show that accurate schematisation of the storage capacity of the area between compartmentalising elements has significantly more influence on maximum inundation and rise rate than the accurate computation of energy losses at sudden elevation changes (fixed weirs). Arrival times can be influenced largely by fixed weir implementation. However, this is only seen when the underlying grid cell height is unchanged. This suggests that the downstream area of the fixed weir is of larger influence than the upstream area. An accurate representation of the crest of the elevated element is then essential.

[1]See Figure 1.3
[2]See Figure 1.5

4.2.2 Flow through local waterways

Waterways can have a significant influence on the through flow of water. To analyse the impact of a waterway on the propagation of the flood wave, two schematisations are made that include the Linge[1]. The first schematisation is the HYDRO_D43_1998 reference model in which the Linge is schematised as a line of grid cells with a uniform size of 100m by 100 m. This is the approach of Delft-FLS and makes the river effectively 100 meters wide. In reality, it is only 30 meters wide on average. A second, more detailed schematisation is made with the actual dimensions of the Linge, HYDRO_Linge.

First, the local effects of waterways are analysed by comparing the two schematisations. Next, the effects of waterways on flood simulation results in dike ring 43 are quantified.

Local effects of a waterway

The Linge influences the direction of the flood wave and the inundation pattern. When discharge through the Linge increases, areas prone to flooding will flood. This can happen more than 15 kilometres in front of the actual flood wave. Figure 4.11 shows the water levels of two locations near the Linge. One location is near the Bovenlinge (east of the Amsterdam-Rijn kanaal)[1] and one location is near the Benedenlinge (west of the Amsterdam-Rijn kanaal)[1]. Both locations inundate before the actual flood wave arrives because the Linge overflows.

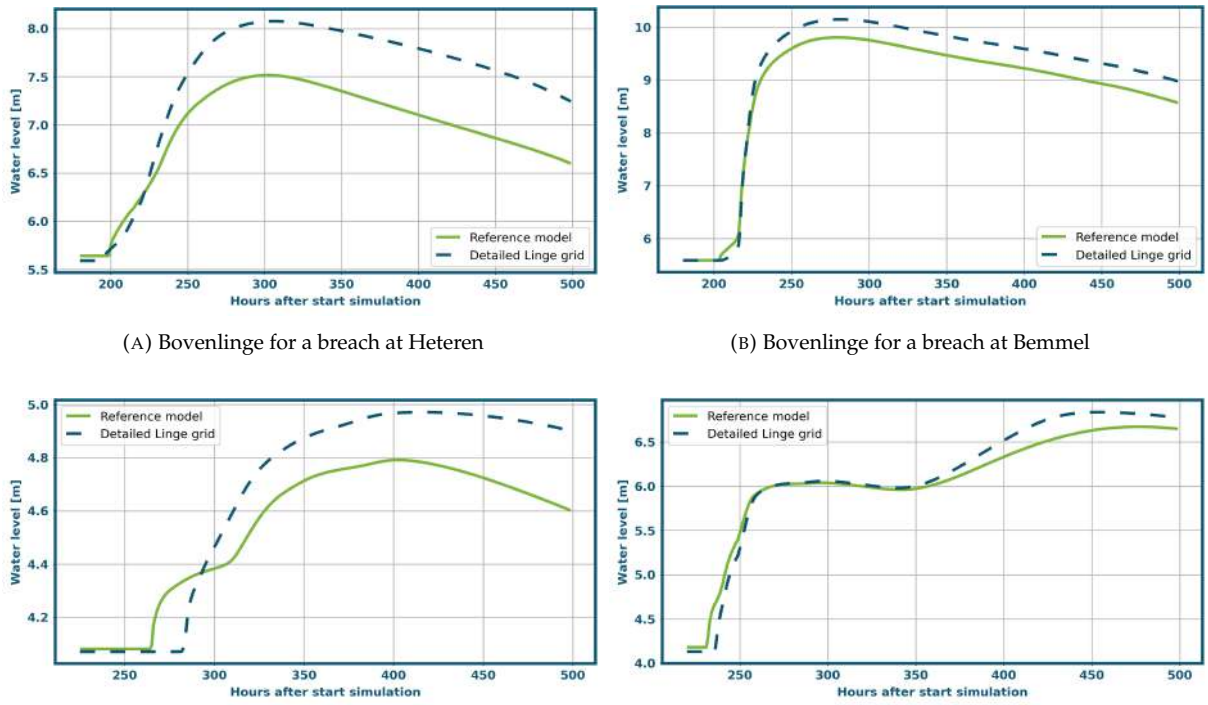

(A) Bovenlinge for a breach at Heteren

(B) Bovenlinge for a breach at Bemmel

(C) Benedenlinge for a breach at Heteren

(D) Benedenlinge for a breach at Bemmel

FIGURE 4.11: Water levels at two locations near the Linge

For the HYDRO_D43_1998 reference run, the influence of the Linge is undeniable. For a breach at Heteren, near the Bovenlinge, the land inundates at 200 hours while the actual flood wave over land arrives almost a day later. Although the delay of the overland flow is smaller for a breach at Bemmel, the same effect is seen. At the location near the Benedenlinge, this effect is emphasised because the ARK dikes block the overland flow. Because of the Linge, the land inundates here more than two days before the larger wave arrives. The inundation that can be attributed to the Linge largely depends on its schematisation. When the Linge is schematised in more detail, the inundation magnitude caused by overflowing of the Linge decreases. In Figure 4.11a for instance, inundation only attributed to overflowing of the Linge in HYDRO_D43_1998 is 0.55m and for the HYDRO_Linge run 0.35m.

[1]See Figure 1.3

Closer to the flood wave, the Linge has a guiding effect. Flow velocities are higher around the Linge, which causes more water to be discharged around it. When the flood wave hits a compartmentalising element like the A50[1], water can only flow further through the Linge. The elevated element blocks the most significant amount of water, while the Linge discharges water further into the hinterland. Flow velocities through the river are the same in both simulations.

The influence of a waterway on the propagation and inundation of a flood wave is highly correlated with its size. A comparison between the HYDRO_D43_1998 model and the HYDRO_Linge model shows the significant influence of the discharge capacity of the river. Maximum water levels close to the Bovenlinge are higher when the Linge is schematised in detail. For a breach at Heteren, this can amount to more than 0.5m higher than in the HYDRO_D43_1998 model. The relative influence of a detailed schematisation of the Linge decreases when the flood wave magnitude increases. The differences between the schematisations are smaller for a breach at Bemmel than for a breach at Heteren. At the location near the Benedenlinge, the lower discharge capacity of the detailed Linge causes inundation to start 17 hours later than in the HYDRO_D43_1998 reference simulation. With the larger flood wave from Bemmel, this difference in arrival time is 4 hours.

The relative influence and the effect of a waterway such as the Linge is thus dependent on the area's characteristics, the waterway's size and the flood wave's magnitude. The relative influence of a waterway decreases with a larger flood wave and increases with waterway size. This leads to the conclusion that a waterway must be sufficiently large, relative to the magnitude of the flood wave and the potential flooded area, to have a significant impact.

Effects of a waterway on flood simulation results

The detailed schematisation of the Linge causes differences in arrival time, water depth and rise rates along the Linge as opposed to the HYDRO_D43_1998 model. Inundation levels are higher when the discharge capacity of the Linge is decreased. The relative influence of the Linge decreases when the flood wave magnitude increases. The output of the detailed Linge schematisation is compared with the HYDRO_D43_1998 for a breach at Bemmel and a breach at Heteren. Figure 4.12 and Figure 4.13 show the maximum inundation depths.

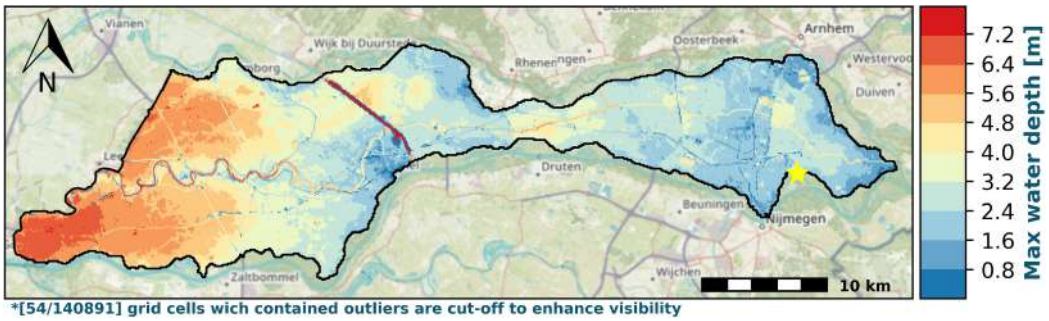

(A) HYDRO_D43_1998

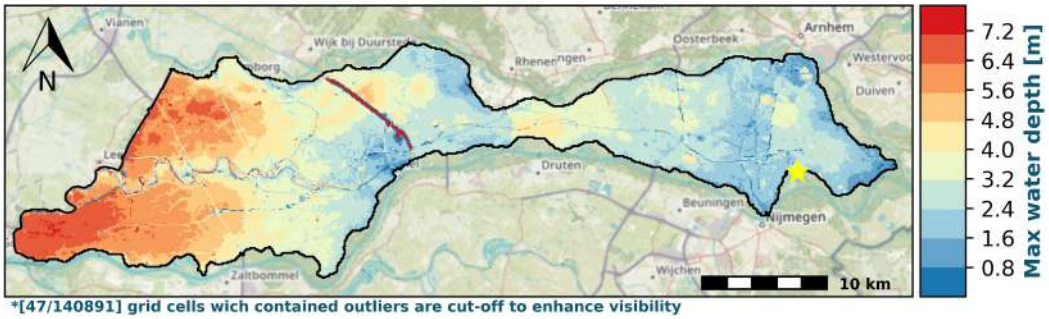

(B) HYDRO_Linge

FIGURE 4.12: Maximum inundation dike breach at Bemmel [Yellow star = breach location]

[1]See Figure 1.5

The influence of the Linge can be seen by comparing both models in Figure 4.12. Overall, water depths are higher in the HYDRO_Linge model. The most significant differences can be found in the centre of the dike ring, between the A50 and the ARK[1]. At the narrow part of the dike ring, water depths are up to 1 meter higher when the Linge is schematised in more detail. The waterway increases the discharge capacity and the storage capacity in the area. The Linge's storage and discharge capacity is larger in the HYDRO_D43_1998 reference model. No fundamental differences are found in the upstream part, close to the breach location. Here, the influence of the inflow at the breach on the propagation of the flood wave and the water depth is more significant than the influence of the Linge.

Figure 4.13 shows the maximum inundation depths for a breach at Heteren. The breach at Heteren has a much lower breach discharge. The maximum breach discharge for this breach is 1200 m^3/s, while the maximum breach discharge at Bemmel is 3500 m^3/s. This second comparison is made to analyse the influence of the Linge for a flood wave with a smaller magnitude.

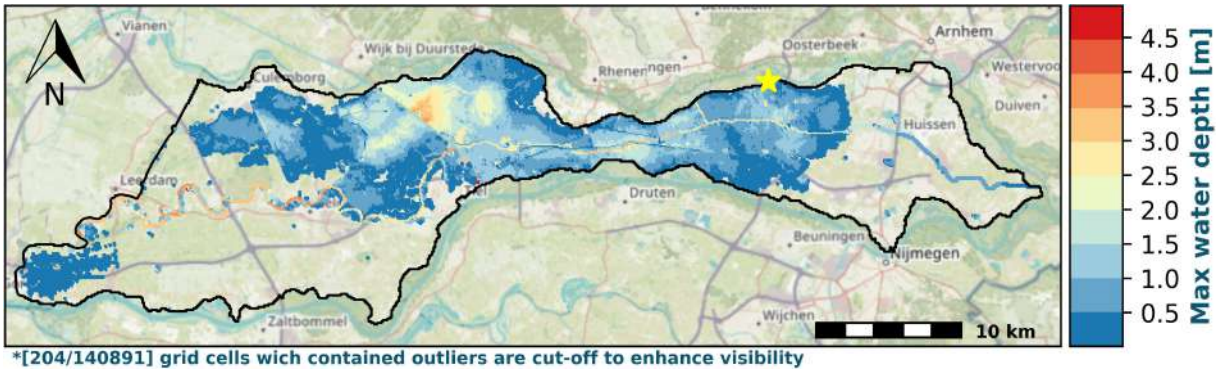

(A) HYDRO_D43_1998

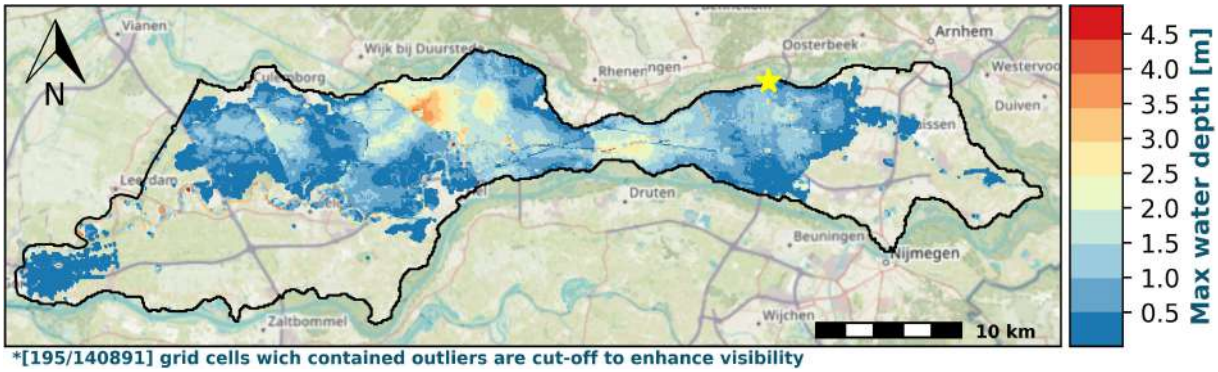

(B) HYDRO_Linge

FIGURE 4.13: Maximum inundation dike breach at Heteren [Yellow star = breach location]

The differences in inundation depth between HYDRO_D43_1998 and HYDRO_Linge are larger when the magnitude of the flood wave is smaller. For a breach at Heteren, differences in maximum inundation depth are found close to the breach location, while this was not the case for a breach at Bemmel. Water depths are up to 0.5 meters lower in the HYDRO_D43_1998 reference model, close to the breach location. It can be seen that the inundation extent is larger when the Linge is schematised in detail. The flood wave has spread to the A2[1] and even past it. In the east, water has spread further towards the A325[1]. In HYDRO_D43_1998, no inundation is found near the Linge in this part. The most significant differences in maximum inundation depth are again found in the centre of the dike ring, at the narrow part. Here, HYDRO_Linge computes water depths up to 1 meter higher than HYDRO_D43_1998.

[1]See Figure 1.5

A higher discharge capacity around a waterway can reduce rise rates in the area. A comparison of rise rates between the HYDRO_D43_1998 reference model and HYDRO_Linge for a breach at Bemmel is shown in Figure 4.14.

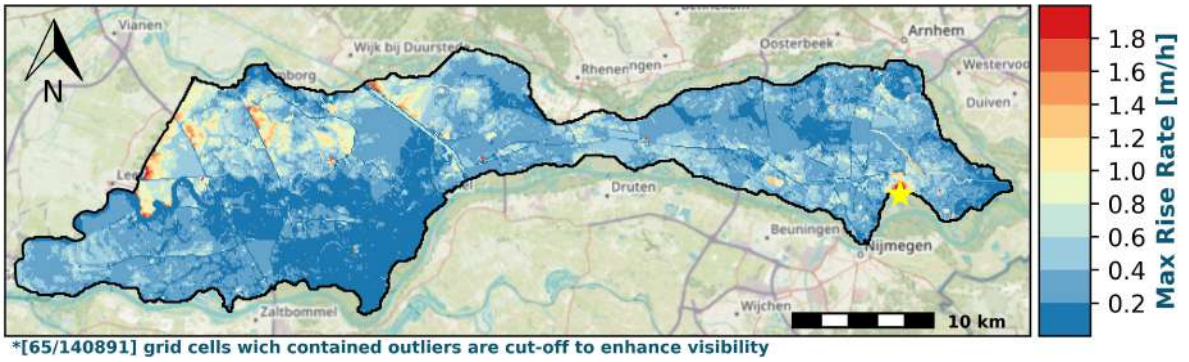

(A) HYDRO_D43_1998

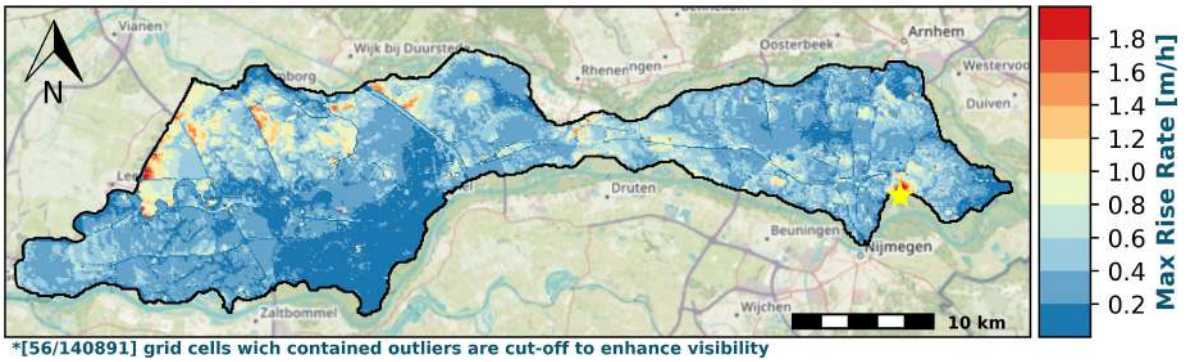

(B) HYDRO_Linge

FIGURE 4.14: Maximum rise rate dike breach at Bemmel [Yellow star = breach location]

Regarding rise rates, the most significant differences are found in the large flood wave of Bemmel. With the detailed Linge grid of HYDRO_Linge, rise rates are higher than for the reference run. This difference can increase up to 0.6 m/h. In the upstream region of the dike ring, differences in rise rates are more significant than in the downstream region of the dike ring. This difference can be explained by looking at the specific role the Linge plays here. Upstream, the water rises fast, mainly because of the flood wave over land, pushed by the large inflow at the dike breach. The Linge discharges water from the region, decreasing rise rates. In the HYDRO_D43_1998 reference run, the Linge has a much larger discharge capacity, causing lower rise rates compared to the detailed Linge model. Further downstream, the influence of the dike breach becomes less and the influence of the Linge on flood wave propagation increases. Especially west of the Amsterdam-Rijn kanaal. Here, land is inundated because the Linge overflows two days before the ARK dikes overflow. Rise rates following from inundation from the Linge are much lower than those from the over-land flood wave. Therefore, rise rates are lower here and differences between the reference simulation and the detailed Linge simulation are far less significant.

Figure 4.11 showed the influence of the Linge on arrival times close to the waterway. Figure 4.15 compares the HYDRO_D43_1998 reference model and the HYDRO_Linge detailed Linge model on arrival times in the first 100 hours after the breach at Heteren.

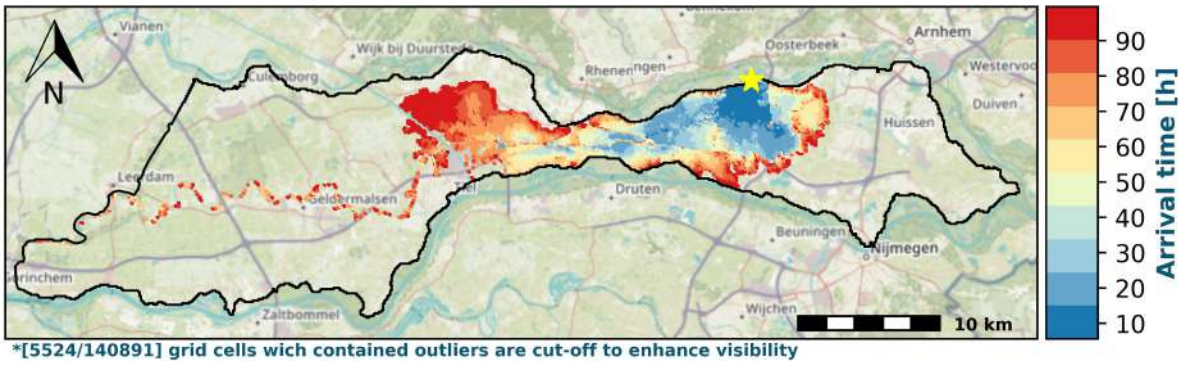

(A) HYDRO_D43_1998

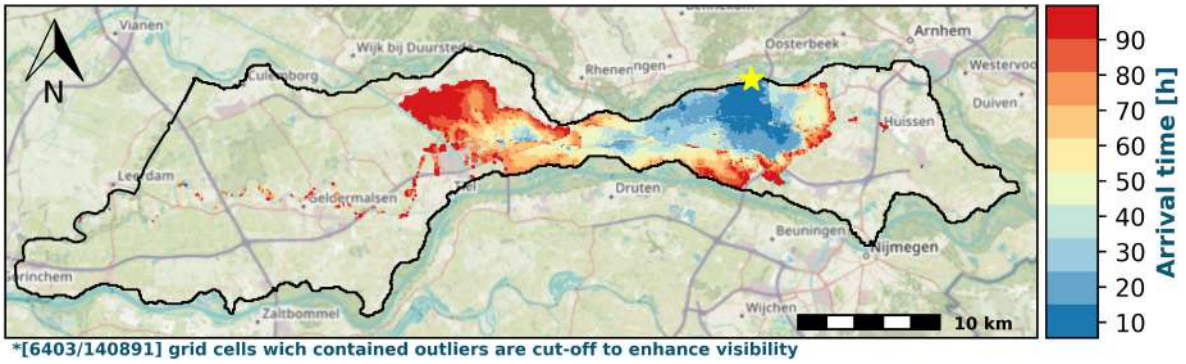

(B) HYDRO_Linge

FIGURE 4.15: Arrival time dike breach at Heteren [Yellow star = breach location]

This comparison shows the significant influence the Linge can have on arrival times. In the HYDRO_D43_1998 reference run, in the first 10 hours, the flood wave flows to the Linge. Here, the water gets discharged downstream, effectively blocking water from flowing further South. In the HYDRO_Linge simulation, the effect is far less, causing water to flow further south in the first 10 hours. The map of the reference run shows large areas around the Linge that inundate before the flood wave over land arrives. This is less for HYDRO_Linge. Here, the map patterns show a much more gradual inundation pattern from the breach towards downstream areas. In specific places around Linge, the difference in arrival time can amount to up to 20 hours.

The differences in flood simulation results between the Linge in a coarse grid and a refined grid are significant. Rise rates and water depths increase when the Linge is schematised in more detail. This shows that accurate schematisation of the storage and discharge capacity of such a waterway as the Linge is vital in simulations of large-scale floods. In the Delft-FLS model runs, the storage capacity of the Linge was largely overestimated. This has resulted in an underestimation of water depths and rise rates. The exact impact largely depends on the study area's location and the magnitude of the flood wave. The most significant differences between the HYDRO_D43_1998 model and the HYDRO_Linge model were found in the centre of the dike ring. Here, the dike ring is only 3.5 km wide. This shows that the relative influence of a waterway is also dependent on the available storage space around it. The results show that a waterway's influence on flood simulation results decreases when the waterway decreases in size.

5 Discussion

5.1 Research potential

When Schippers (2023) showed significant differences between the D-HYDRO and Delft-FLS software, several conclusions were drawn. She concluded that differences could be attributed to different breach growth, elevated elements, and more underpasses included in the D-HYDRO model. This research supports these findings. However, rebuilding a Delft-FLS model of dike ring 43 in D-HYDRO revealed more differences between both software packages. This allowed for a deep understanding of complexities and sensitivities in the D-HYDRO software itself.

Direction and guidance in fluvial flood model schematisation

By comparing a schematisation built in Delft-FLS and a schematisation built in D-HYDRO, the impact of schematisations or calculations inherent in the D-HYDRO software could be isolated and quantified. For instance, it has been shown that the numerical scheme used in D-HYDRO to calculate breach flow is an improvement over the simple weir flow equations used in Delft-FLS while at the same time showing that this makes D-HYDRO sensitive to an accurate computation of upstream flow velocities, water levels and floodplain characteristics. By identifying the most critical aspects of a fluvial flood model (breach flow, DEM, elevated elements, underpasses and waterways) and placing their impact and importance in the context of different flood simulation goals, this research can serve as a future guide to build fluvial flood models. This also gives focus and direction to modellers or researchers in improving different aspects of fluvial flood model schematisations in D-HYDRO and fluvial flood models in general.

A different look at dike breaches

Many researchers have recognized the importance of dike breach flow and growth in fluvial flood models. It has been a variable in sensitivity analyses and uncertainty analyses in this field. However, less research has been conducted into factors influencing breach flow and breach growth in 2D flood models. This research contributes to filling this gap. It provides insights into the computation of dike breach flow and growth in D-HYDRO and evaluates different schematisation techniques. It also sheds light on the implications of alternative river schematisations and demonstrates which river and floodplain characteristics can significantly influence dike breach flow. By comparing simulations of different breach locations, breaching moments, and different breach growth formulations, the hidden implications of the widely used Verheij-vdKnaap equation were identified. This equation, a standard in fluvial flood modelling, was found to have significant implications that could alter the field's consensus. This research can, therefore, provide incentives to update and improve breach growth formulations in fluvial flood models.

Flood risk assessment

In addition to the assessment of primary flood defences, measures can be designed within the area that achieves the same safety requirements as strengthening dikes by looking at the impact of a flood. This research not only provides extra insights into aspects of fluvial flood simulations used for different policy goals but also shows ample chances for actualising current flood models and flood simulation results used in flood risk management. Therefore, the results of this research can pre-eminently be used in designing new guidelines for fluvial flood models used in an integral area assessment, flood risk assessments, crisis management or the actualisation of flood safety norms for primary flood defences in the Netherlands.

Looking at flood impact assessment, if an area should prepare for a flood, the assumption should be that the dikes will hold until their designed water level. Flood events will then only occur before the design water level, in case of unforeseen events and at the design water level. In both cases, the probability that this happens while water levels on the river are still rising is much larger than the probability of occurrence exactly at peak water level. This research shows an exponentially increasing breach discharge towards earlier breaching moments when the Verheij-vdKnaap equation is not used. This more significant impact and higher probability cause a greater risk for breaches initiated before peak water level. From a risk perspective, combining the results of this research and the ever-increasing impact of floods caused

by increasing hydraulic conditions on the river that dikes can withstand, an incentive could be provided to re-evaluate choices regarding breach growth formulation and breach initiation moment.

5.2 Limitations

Area characteristics

As stated in the research scope, this research is primarily based on the Upper River area in the Netherlands. As area characteristics play a significant role in the distribution of water, isolating variables for this research was a difficult task. Using simple models with coarse grids, it has been tried to isolate the effects of added fixed weirs and detailed schematisation of waterways. Significant differences in flood simulation results were found which can be attributed to these elements, although the influence of specific area characteristics cannot be excluded. The same applies to the computation of breach discharge, largely dependent on specific local floodplain and river characteristics. By comparing different breach locations, breach moments, and breach growth, this research has tried to exclude the influence of area characteristics on conclusions. However, only one discharge wave was used, and only three breach locations could be investigated. This might not be enough to exclude all influencing area characteristics. It has already been identified that river slope or tidal influences could be factors causing different quantitative results. Based on this study, general quantitative conclusions about the effect of specific schematisations are hard to draw. However, reasonable assumptions can be made using the effects studied here. For instance, a 1D model with xyz-cross sections instead of zw-cross sections would better represent specific local floodplain characteristics. The difference in breach discharge between such a 1D model and a 2D model would probably be smaller than calculated in this research, which used zw-cross sections.

Model limitations

In this research, a schematisation in Delft-FLS was rebuilt in D-HYDRO. This has highlighted the hidden differences in flow computation between the two models. By increasing the complexity and detail in the model step-by-step, hidden sensitivity is unveiled, and essential aspects of a D-HYDRO schematisation are identified. However, rebuilding a Delft-FLS schematisation limits the exact quantification of differences. The grid in Delft-FLS is a coarse square grid, and the schematisation of the river is built with the same grid cell size of 100m. The validity of the river model is, therefore, questionable. Simulations with a smaller grid cell size have shown that square grid cells with a size of 100m can compute unrealistic flow velocities around dike breaches. However, simulations done with the detailed 2D river schematisation of Deltares support the conclusions drawn using the Delft-FLS schematisation.

Using the D-HYDRO software package can lead to specific conclusions about D-HYDRO flow computation. First, the fixed weirs are a particular option of D-HYDRO and are not available in other software packages. Although these software packages have their own schematisation options to compute flow over sudden elevation changes, the effects could differ. Secondly, the breach flow computation of D-HYDRO is specific to this software package. Although it shows an excellent capability for computing expected breach flow and effects on river flow, it might have sensitivities that have not been found in this research. Thirdly, the D-HYDRO software does not allow for breach flow computations that are different from the Verheij-vdKnaap equation. The alternative breach growths had to be calculated using simulation results using the Verheij-vdKnaap growth. From these simulations, flow velocity and flow height were taken. From this, breach growth was calculated outside D-HYDRO and without simulation feedback. It has been acknowledged that a larger breach width would decrease the breach's flow velocity and height. This would then slow down breach growth. As this feedback is not present in the calculation, the actual width values following from the alternative breach growth equations could be lower than calculated in this research.

5.3 Generalisation

This study uses flooding of the large area of dike ring 43 as a case study. This area and the rivers from which a flood occurs are characterised as "Upper river area". As explained in the scope of this research, the Upper River area has specific characteristics that are not directly transferable to other locations worldwide. This discussion also touched upon the fact that quantitative observations are primarily dependent on the particular area characteristics. However, most conclusions of this research are applicable in other areas or at least give insight into possible model behaviour in different locations worldwide.

Breach flow

Significant differences were found between Delft-FLS and D-HYDRO in the computation of breach flow. Based on the findings of this research and several other studies, it can be concluded that the D-HYDRO computation is more accurate. In Delft-FLS, breach flow only depends on upstream and downstream water levels. In D-HYDRO, the breach flow computation depends on upstream and downstream water levels, flow direction and flow velocity on the river. A breach influences flow velocities and water levels on the river (Sun et al., 2017). It also influences streamlines and flow direction (Kamrath et al., 2006). The stage-discharge relation in Delft-FLS can only partly influence water levels; its accuracy is highly debatable as large areas of active cells are involved. Because momentum is not conserved, flow velocities inside the breach can be unrealistic. Because of this, the results of the Delft-FLS models are questionable in situations with higher flow velocities and oblique breach orientations. Lindermuth et al. (2021) showed that the discharge coefficient of side weirs (used in breach flow computation) depends on river slope, weir height, width, water depth and main channel width. Primarily, this can be related to the river's pressure head and kinetic energy. Comparable influencing factors for breach flow were found in this research. As all these variables change during a simulation, discharge coefficients change. Simple weir flow equations, like those used in Delft-FLS, using a single value for the discharge coefficient, will therefore not accurately compute dike breach discharge. Because energy loss is computed downstream of the dike breach and energy is conserved until the breach line, it seems that the fixed weir numerical scheme used to compute breach flow in the D-HYDRO software significantly improves this aspect. With the right schematisation, flow velocities and water levels inside the breach could be computed accurately. Although the differences in breach discharge values depend on the specific area characteristics around that breach, all other conclusions regarding the implications of the D-HYDRO dike breach discharge computation can be transferred to other locations worldwide. The findings of this research regarding the root causes of overestimation of breach discharge in case of a water level boundary or a 1D river schematisation can be used to make accurate predictions of differences in most other locations in the world with insignificant tidal influences. All identified influences of river characteristics are applicable for different software packages and models, but the exact effects on breach flow are only valid for D-HYDRO simulations.

Breach growth

This research showed significant flaws in the computation of breach growth using the Verheij-vdKnaap equation. These flaws are inherent to the equation itself, and the performed simulations serve as an example in which the equation is invalid. This research has shown that the water level difference approach does not reflect actual hydraulic conditions in the breach. The same flaws will be present in other situations and models that compute breach flow for more than 14 hours. In all situations where breach flow does not quickly reach a sub-critical state with low flow velocities, the validity of the Verheij-vdKnaap equation can be questioned.

The high dependence on the period that a breach is open stems from the calibration of historical events. The most recent historical events included in this calibration are from 1953, and the most recent tests are from 1998 (Verheij, 2003). With increasing hydraulic conditions and dike height, it seems questionable if these historical events are still representative of current situations. The field experiments are mostly done based on reservoirs in which water levels upstream drop, and water levels downstream rise quickly. There is no dominant flow direction upstream of the breach. This research has shown that breach flow can become steady for long periods of high water levels. As a breakthrough can happen before a water level peak, water levels upstream of the breach might increase after failure. This research advocates for a breach growth equation based on flow velocity, flow height and dike material. A well-calibrated function would better represent the correlation between hydraulic conditions in the breach and breach growth, regardless of the location of the breach or the modeling software.

Water distribution

The effects of different schematisation choices on flood simulation results cannot be seen separately from the goal of the simulation and area characteristics. This research shows that fixed weirs and waterways can greatly influence arrival times in the area. This would be primarily important for crisis management goals. It can be concluded that the influence of fixed weirs is more considerable in larger flooded areas. The influence increases when the height of the fixed weir is more extensive and relevant to the flood wave magnitude. The same goes for waterways. For small polders without significant compartmentalising elements, it is less critical to accurately schematise these elevated elements and waterways.

Although quantitative effects shown in this research are closely related to specific area characteristics, the qualitative effects of fixed weirs are inherent in the flow calculation. Implementing a fixed weir will always compute lower flow velocities over an elevated element than a single line of grid cells would. Flow velocities over compartmentalising elements can largely influence arrival times. Therefore, it is fair to say that including fixed or 2D weirs is very important in every flood simulation in which arrival times are a variable of interest.

6 Conclusions and Recommendations

6.1 Conclusions

1) ***What implications does the use of the D-HYDRO software have for the computation of dike breach flow, as opposed to the established Delft-FLS software?***

Breach flow in Delft-FLS is calculated using a simple weir formula. This approach neglects energy losses, water surface drawdown or momentum conservation and only depends on the upstream and downstream water levels. In D-HYDRO, discharges are computed using the 2D-shallow water equations with a particular discretisation of the advection terms in the momentum equation. This makes the flow through a breach in D-HYDRO dependent on the energy conservation upstream of the breach. It accounts for friction around the breach, velocity gradients and streamlines on the river. In D-HYDRO, significant differences in breach discharge can be found at locations with similar water levels but different flow directions, flow velocities, bottom slope or channel width. This approach captures expected hydraulic conditions better than a simple weir equation approach. It does make modelling a dike breach more complex as modellers have to account for more aspects when making schematisation choices. D-HYDRO will, in general, compute lower breach discharges than Delft-FLS.

2) ***What are the effects of alternative river schematisations on dike breach flow, as opposed to a full 2D river schematisation in a fluvial flood model?***

In general, with fluvial floods, the main flow direction on the river is oblique to the breach orientation, resulting in reduced momentum in the direction of the breach. Using a water level boundary at the river axis causes a main flow direction towards the dike breach because river flow is not computed. It also reduces water level drawdown. This overestimates upstream water levels up to one meter and highly overestimates potential energy towards the breach. This study found that the overestimation of peak breach discharge due to the water level boundary approach can be 33-43% of the peak breach of a full 2D river model. Absolute numbers highly depend on the location of the dike breach and hydraulic conditions on the river. Breaches in large floodplains, far from the main channel, have relatively low flow velocities. Here, the main overestimation will come from the overestimation of the upstream water level, as the influence of the breach on the river cannot be computed. Simulations using a detailed river model have shown that the effect of a breach on the water levels and flow velocity in the Waal can reach up to 20 km upstream.

Simulations using a 1D river schematisation have shown that this approach computes higher breach discharges than a 2D river schematisation. Higher peak discharges of 1150 m^3/s and 400 m^3/s are found, which is respectively 62% and 20% of the peak discharge found with full 2D river models. Breach discharge is highly influenced by a decrease in local water levels around the breach, local flow velocities in flood plains, bed friction, dry areas, or local elevations around the breach. A 2D schematisation can capture all these local influences. On the other hand, the values of a 1D simulation, which are averaged over a cross-section, cannot fully capture this, resulting in significantly higher breach discharges. A breach results in higher flow velocities in the main channel upstream of the breach. In a 1D simulation, this greatly affects flow velocities upstream of the breach, from which breach discharge is calculated. Local flow velocities in a 2D simulation are much less affected. This results in an even higher breach discharge in the 1D schematisation than the 2D schematisation.

3) ***What are the effects of different breach initiation moments and growth equations on breach growth and breach flow in a fluvial flood model?***

With D-HYDRO, a modeller can choose to compute breach growth using the Verheij-vdKnaap equation. Using the Verheij-vdKnaap equation for breach growth in D-HYDRO makes the final breach width insensitive to the moment of breaching. As 90% of the breach widening occurs in the first 14 hours, the final breach width is always reached. As a result, breach discharge has a sharp maximum at peak water level. When water levels decline, breach discharge is the same, regardless of the period that a breach is open. This hides the possible devastating effect that a breakthrough before peak water level can have. Because there is a maximum to the breach width and, thus, a maximum to breach discharge, the cumulative discharge has a declining upward trend toward earlier breach moments. However, at earlier breach

moments, when a breach grows faster and broader because of increasing hydraulic conditions after the breaching moment, the cumulative discharge would have an exponential upward trend towards earlier breaching moments. This research has shown that using a Verheij-vdKnaap equation variant that includes a velocity term and implementing the shear stress equation of Van Damme is sensitive to breach moment.

The Verheij-vdKnaap equation does not consider underlying developments in flow velocities, flow height and upstream energy level. High water levels in the Waal remain on average for two weeks. This is far longer than the expected growth time in the Verheij-vdKnaap equation. Because the breach growth is weakly correlated with flow velocity and highly correlated with the initial water level difference and the current time step, growth predictions always follow the same structure. Here, the most significant growth was found in the first 14 hours, where dike breach flow is not yet fully developed and is governed by considerable water level differences. Because of the similarity in this part, resulting dike breach hydrographs are similar. This research shows that breach growth formulations based on flow velocity and flow height in the breach, rather than upstream and downstream water levels, are increasingly sensitive to computed hydraulic conditions in the breach. Using the Verheij-vdKnaap equation in D-HYDRO essentially limits the computed breach width. When observing the hydraulic conditions of the breach in the simulations performed, it can be concluded that the calculated breach growth can significantly underestimate the actual possible breach width. The alternative breach growth equations shown in this research are proven to better relate breach growth to hydraulic conditions computed by the model.

4) ***What implications does the use of the D-HYDRO software have for the computation of water distribution, as opposed to the established Delft-FLS software?***

In this study, a Delft-FLS model is rebuilt in D-HYDRO using the same schematisation. There have been no significant differences in flood simulation results between the rebuild schematisation in D-HYDRO and Delft-FLS. Differences between Delft-FLS and D-HYDRO result from the advanced schematisation options that D-HYDRO offers. The flexible mesh of D-HYDRO allows for the representation of elevation and waterways in the area more accurately and, with that, storage volume. This generally results in lower inundation depths in D-HYDRO. By implementing fixed weirs and underpasses, elevated lines can be more accurately schematised in D-HYDRO. This results in lower rising rates. The exact differences largely depend on the magnitude of the flood wave and local area characteristics. Significant differences can also be attributed to the choice to exclude an underpass under the Amsterdam Rijn-kanaal from the new schematisation. This shows that modelling choices in the operation of channels or the reliability of regional dikes and elevated lines can greatly influence modelling results. By providing all these options, D-HYDRO will create a more accurate representation of fluvial floods than Delft-FLS. Differences between simulations performed with Delft-FLS and more detailed simulations performed with D-HYDRO are significant.

5) ***What are the effects of fixed weirs and local waterways on the distribution of water and flood simulation results in D-HYDRO?***

A mesh with elevated grid cells computes large flow velocities over elevated elements. By implementing fixed weirs, much lower flow velocities over elevated elements are computed. These lower flow velocities cause higher water depths upstream of the elevated element and a delay in the flood wave. Depth differences of up to 20 centimetres and delays of up to 4 hours are found at fixed weirs. Effects on flood simulation results are seen in maximum inundation depth and arrival time. A small effect in maximum inundation can be attributed to the flow computation, but this is insignificant to the effect of added storage volume. For maximum inundation, it is more critical to schematise the dimensions of the elevated line accurately. Accurate schematisation of this dimension cannot be done using fixed weirs, as these have a universal width and slope. D-HYDRO has another option called 2D-weirs for this. However, the computation of flow over these elements is different from fixed weirs. Arrival times are primarily affected by the implementation of fixed weirs. Simulations have shown that implementing fixed weirs for compartmentalising elevated lines can delay a flood wave by 10 hours in the first 72 hours of the flood. This largely depends on the magnitude of the flood wave and the elevated element's compartmentalising capacity.

Waterways have a significant influence on the propagation of a flood wave and the discharge of water to lower areas. Locations around waterways inundate far before the actual flood wave reaches that location. In simulations done in this research extensive inundation around waterways was found more than a day before the actual flood wave arrived. Smaller waterways have a smaller discharge capacity and, therefore,

a smaller effect on inundation downstream. The relative effect of a waterway decreases with a more significant flood wave and increases with waterway size. This leads to the conclusion that a waterway must be sufficiently large relative to the magnitude of the flood wave and the storage capacity of the surrounding area to have a significant impact. Waterways with enough discharge capacity relative to the flood wave can significantly lower maximum inundation depths and maximum rise rates. With smaller flood waves, waterways can substantially affect the inundated area, as water can spread to locations that might be closed for an over-land flood wave by a compartmentalising element. Therefore, it is essential to understand the possible effects of a local waterway before a decision on its schematisation is made. This decision must always be made in the context of the flood simulation's goal.

"The objective of this research was To unveil the implications of the use of D-HYDRO and its different schematisation possibilities for the computation of dike breach flow and water distribution in fluvial flood models"

This research has unveiled the implications of breach flow computation in D-HYDRO on breach discharge as opposed to Delft-FLS. It has identified prominent influencing factors in breach flow computation, showing that D-HYDRO computes much lower breach discharges than Delft-FLS. Alternative river schematisations are unveiled to have significant effects that can vastly overestimate breach discharge. Next, to breach flow computation, this research has revealed flaws in the Verheij-vdKnaap equation for breach growth. It has shown that this approach can underestimate breach width and does not reflect computed hydraulic conditions. Other breach growth equations show a better representation of hydraulic conditions. When the Verheij-vdKnaap equation is used, breach width mainly depends on the breach moment. This hides the possible devastating effect that a breakthrough before peak water level can have. The proposed alternative growth equations are sensitive to breach moment.

Next to implications for dike breach flow, this study has shown the effects of fixed weirs and local waterways on flood simulation results. It has been revealed that the implementation of fixed weirs can greatly influence arrival time. For maximum inundation depth and rise rates, accurate representation of storage volume is the most critical factor in the schematisation of elevated elements. It has been unveiled that waterways can significantly influence arrival times, rise rates around waterways and maximum inundation depth. The influence of fixed weirs and waterways depends on their size, the flooded area's size and the flood wave's magnitude.

Effects of breach flow computation, breach growth computation, and local effects of fixed weirs and waterways can be translated to other areas in the Netherlands and fluvial flood simulations in general. However, global effects are primarily dependent on area characteristics. River or coastal areas with tidal influences might result in a different quantification of the effects of different breach growth schematisation on dike breach discharge. Assessments of the validity of 1D, water level boundary or Verheij-vdKnaap approaches might differ in these areas. Therefore, this research topic should be extended to an international context, to smaller dike rings in the Netherlands and areas with prominent tidal influences.

6.2 Recommendations

6.2.1 Further research

Uncertainty in modelling aspects and differences between modelling packages partly drove this study. This research has quantified some significant differences and has unveiled the consequences of specific schematisation choices in D-HYDRO. This makes the results of fluvial flood models highly dependent on the specific model made or the specific decisions of the modeller. As policy and flood safety standards are designed based on these flood simulations, every research that contributes to a reduction of uncertainty in flood models, standardisation of modelling approaches or advancement in schematisation of specific parts of a flood model is relevant for fluvial flood modelling and flood risk management in general. Based on the conclusions of this research, some specific recommendations for further research are made.

First, this research showed significant differences in breach discharge between Delft-FLS and D-HYDRO, which could be attributed to a difference in breach flow calculation between the two models. This research has been focused on implementing D-HYDRO, but many established software packages exist for fluvial flood modelling (for instance, 3Di, Hec-Ras, Tyrgron). These all have their way of calculating breach flow. Different implementations of breach flow computations should be compared and assessed. As there has been a lot of research into modelling breach flow and growth, the implementations of established 2D modelling packages should be tested against breach flow modules like BRES and BREACH or extensive experiments like the Lillo experiment. Such a type of assessment would identify flaws and strengths in widely used modelling packages, reduce uncertainty in fluvial flood models and guide modellers in a policy domain to choose the right modelling package for their goals.

Second, inundation depths and patterns are primarily dependent on breach discharge. Some sensitivity analyses have been done into the sensitivity of parameters of fluvial flood models in which breach discharge was seen as a parameter. However, this research has shown that breach discharge is sensitive to many factors. These factors include breach geometry, growth rate, upstream and downstream water levels, flow direction and flow velocities on the river, local friction around the breach and floodplain characteristics. According to the literature, breach discharge could also be affected by other factors such as river slope, crest level, bed elevation behind the breach and grid size around the breach. An extensive sensitivity analysis of the computation of breach flow in 2D flood models, which includes as many of these factors as possible, will largely contribute to reducing uncertainty in breach flow computation. This can then be used in assessments of different implementations of breach flow computation in widely used modelling packages.

Third, the dependence on local river, floodplain and hinterland characteristics shows that breach discharge can be largely different between locations in the same normative dike section in the Netherlands. By understanding river and floodplain characteristics that influence breach flow, locations in dike sections can be identified for which breach discharge would be maximum. A comprehensive research into identifying such critical locations in dike sections can largely contribute to flood safety in the Netherlands.

Fourth, one of the most uncertain elements of breach flow is the development of the breach width. Breach growth can be modelled in many different ways. This research has shown that although correlated to historic dike breaches, the Verheij-vdKnaap equation has some significant flaws. More elaborate breach growth models mostly require specific data or are challenging to implement in a numeric model. A substantial chance of reducing uncertainty in fluvial flood models lies in developing a new breach growth model. This breach growth model should be based on flow height in the breach, flow velocity in the breach and dike material. By combining the large amount of research that has been done on this topic, it should be possible to develop a model which is easy to implement in packages such as D-HYDRO, reflects hydraulic conditions and different growth phases of a breach and can be widely used for different dike types. Validation of this model against expected behaviour, historic dike breaches and experiments could lead to a new standard for fluvial flood modelling, replacing the Verheij-vdKnaap equation formulated in 2003.

Fifth, the recommendation in the last paragraph assumes that all field experiments and research done into breach growth are sufficient to develop a generic growth equation. However, even with the considerable amount of research, some aspects found in this study are largely overlooked. Field experiments are mostly done based on reservoirs in which water levels upstream drop, and water levels downstream rise quickly. There is no dominant flow direction upstream of the breach. This research has shown that breach flow can become steady for long periods of high water levels. As a breakthrough can happen

before a water level peak, water levels upstream of the breach might increase after failure. It has shown a significant influence of a dominant flow direction oblique from the breach orientation. Next to this, the actual width of the breach might significantly influence flow velocities and flow height in the breach, too. Large field experiments that focus on representing actual breach conditions in the upper river area (prolonged periods of high water, increasing water level after breakthrough, significant flow velocity upstream, oblique main flow direction and large breach width) will contribute mainly to an accurate understanding of real-world dike breach conditions. This can then contribute to fluvial flood models of Dutch dike rings, including an accurate breach development and vastly reduced uncertainty in dike breach discharge.

Sixth, this research has used a specific case study area to study the effect of different schematisation choices. Discussions have been made about generalising these results to fluvial flood models in general. Further research on this topic should focus on different areas with other specific characteristics. Although the local effect of schematisation choices can be transferred to other areas, global effects largely depend on area characteristics. An identified factor that could lead to different results is dike ring size. Flow velocities were of minor interest in this research as the area is relatively flat. In an international context, basins with much steeper slopes could increase the importance of flow velocity as flood simulation results. Roughness, fixed weirs, and breach location could be much larger factors influencing flood simulation results here. For breach flow computation, this research has focused on the upper river area, where high water levels remain for longer periods, and there is no tidal influence. However, close to the sea, storms and tidal influence can affect breach growth and flow differently. The topic of this research should, therefore, be extended to an international context, to smaller dike rings in the Netherlands and areas with large tidal influences.

Seventh, this research has shown the influence of waterways and fixed weirs on flood simulation results. However, it was noted that the effect of these elements largely depends on their size, the flooded area's size, and the flood wave's magnitude. This would differ per area and flood scenario. Research that relates the size of elevated elements, waterways and flood waves to their corresponding effects can create focus and standardisation in the schematisation of flood models in the Netherlands. Research that identifies important waterways and elevated elements in each protected area in the Netherlands can largely guide modellers in the policy domain in building their schematisations. It can contribute to a standardised way of including these types of elements in a schematisation and contribute to the guidelines for flood modelling.

A last recommendation can be made on the implementation of complex roughness formulations. This research has not included the influence of roughness in the analyses of water distribution. However, a plan was made to include D-HYDRO's trachytope roughness formulations. Today's standard in Dutch flood modelling is to translate a land use map to a single roughness value per grid cell. This is, for instance, done with look-up tables provided in the guideline for flood modelling. It is, however, known that friction due to vegetation is much more complex than that. River models like WAQUA already use a more complex roughness formulation. Research into implementing more complex roughness formulations for fluvial flood models can contribute to accuracy in flow velocities and water depths, especially in an international context. This research should define different potential roughness formulations and test their applicability. This can be done by creating standardised tables which translate land use into roughness input variables like stem density and vegetation height.

6.2.2 Recommendations for flood simulation guidelines

The possible modelling choices and set-up of the models in this research are primarily based on the guidelines for flood modelling (De Bruin, 2018). The results of this research give a good insight into the impact these choices could have on the intended flood simulation results. This provides an excellent opportunity to make recommendations on improving or expanding these guidelines based on the findings of this research. As D-HYDRO slowly becomes the standard in the Netherlands, the guidelines could include specific advice on implementations in D-HYDRO.

Translating goals to schematisation requirements

The guideline includes a section that advises on specific elements to focus on in a flood model schematisation (section 2.1). This section briefly discusses focus points connected to different flood simulation goals (economic risk, mortality, and crisis management). Based on the results of this research, this small section can be elaborated, serving as an elaborate guide on what to include in a schematisation.

This study has shown significant differences in inundation between a rectangular 100m grid and a detailed, flexible mesh grid. As many elevated elements and waterways can be included, a 100m grid seems too large to advise for reliable inundation maps. To determine economic damage, the focus should be on an accurate computation of dike breach flow. Next to that, storage volume must be schematised as accurately as possible. This means including accurate dimensions of elevated elements, using 2D weirs and including significantly large waterways in the digital elevation model. Using the flexible mesh of D-HYDRO can accurately follow contours in the area's elevation. To include mortality, it is essential to compute rise rates accurately. These are mainly dependent on areas around elevated obstacles. Large elevated obstacles should, therefore, be schematised as 2D weirs with accurate dimensions and include all relative underpasses. It should be noted that waterways can have a large local effect on rise rates. An analysis should be made of the effects of waterways in the area, and decisions should be made on whether to include them. Decisions should not be made based on runtime considerations but on knowledge of specific waterways' effects on the intended flood simulation result. This decision cannot be seen separately from the expected flood wave magnitude.

A more extensive elaboration can be given to requirements of crisis management simulations. This research has shown that many factors can influence arrival times. It is necessary to use a small grid resolution. This grid should be made around elevated lines and waterways. Elevated lines should be incorporated as 2D weirs with accurate dimensions. Waterways should be included in detail, in 2D or 1D. Including underpasses and divers makes sure that rise rates close to elevated lines are more accurate and water spreads everywhere it is supposed to. Also, decisions should be made on the failure of secondary flood defences. For instance, the failure of these high elements can be modelled using real-time coupling in D-HYDRO.

Lastly, it should be noted that compartementalising elements significantly influence all intended flood simulation results. These elements should be identified at the start of the schematisation. Accurate schematisation of underpasses, flow over these elements, and their dimensions is essential. For these elevated elements (and for waterways) in general, influence and significance decrease with decreasing size and with increasing flood wave magnitude.

Location of boundary conditions, breach location and hydraulic river conditions

To compute dike breach flow, it is essential to schematise hydraulic conditions upstream of the breach. The guideline for flood simulations focuses on the accurate computation of upstream water levels. In that light, recommendations are given on the location of boundary conditions in different river schematisations (section 5.2.1). However, this research has shown that flow velocities, flow direction and channel width significantly influence the computed breach discharge. Local friction, dry areas, elevations and decreases in water level around the breach considerably influence breach discharge. Focus in the computation of upstream hydraulic conditions should therefore be broadened to include an accurate computation of local flow velocities, flow direction and water depth. This research has shown that a water level boundary on the river axis or a 1D river schematisation cannot accurately capture these local flow conditions, resulting in much higher breach discharges than a 2D schematisation. It is therefore recommended to:

1. Always schematise the river around the breach location in a detailed 2D grid. As influences on water levels and flow velocities reach far upstream, a boundary condition should be placed at least 20 km upstream from the breach location.
2. Using a water level boundary close to the breach location should be avoided. Using this, overestimates water levels and momentum towards the breach. This can largely overestimate dike breach discharge, even for small dike rings.

The importance of the local river schematisation around the breach shows that the choice of breach location should be made more carefully. In the guideline, it is advised to consider area characteristics like elevated elements or differences in land use inside the dike ring when choosing dike breach locations (section 4.1). Based on the findings of this research, it is recommended to consider local river characteristics in the choice of breach location as well. The orientation of the breach, distance from the main flow direction and river flow width are essential factors that can largely influence breach discharge. This makes it possible that two locations in a normative dike section result in vastly different breach discharges.

Breach moment

In the guideline, one sentence is dedicated to the effect of a dike breach event before the water level peak. It only states that a flood would be larger when a breach initiates before the peak water level. Modellers should be better attended to the devastating effect that a breakthrough before peak water level can have. Because of the use of the Verheij-vdKnaap equation, a maximum width and, thus, maximum breach discharge is quickly reached. Cumulative discharge has, therefore, a declining upward trend toward earlier breach moments. However, when a breach grows faster and wider because of increasing hydraulic conditions after the breaching moment, the cumulative discharge would have an exponential upward trend towards earlier breaching moments. It is plausible that a breach would grow faster and wider when a breakthrough initiates before the peak water level. It might be advisable to re-evaluate the choice to standardise breakthrough at the water level peak.

The Verheij-vdKnaap equation

The guideline advises using the Verheij-vdKnaap equation to calculate breach growth because this formulation considers water level differences over the breach. However, this research has identified major flaws in the Verheij-vdKnaap equation. One of these flaws is that the relationship between water level differences and flow velocity in the Verheij-vdKnaap equation is inaccurate. Because of this, the equation does not reflect computed hydraulic conditions in the breach. The advice on the breach growth model in the guideline must be elaborated. It should at least include information on all shortcomings of the Verheij-vdKnaap equation presented in this study and include example situations in which the equation might not be valid. It should be noted that the Verheij-vdKnaap equation will predict similar breach widths for similar initial water level differences irrespective of the development of breach flow. It would be recommended to include the second alternative Verheij-vdKnaap equation presented in this research and the Van Damme formulation as viable alternatives.

Bibliography

Arcadis, RoyalHaskoning, & Fugro. (2005). *Overstromingsrisico dijkring 36 land van heusden / de maaskant en 36a keent* (tech. rep.). Projectbureau VNK.

de Bruin, K. (2018). *Leidraad voor het maken van overstromingssimulaties* (tech. rep.). Deltares.

Deltares. (2024). *Manual sobek1d2d*. https://content.oss.deltares.nl/sobek2/SOBEK_User_Manual.pdf

Deltares. (2023a). *Delft3d fm suite 2d3d* [Accessed: 14-12-2023]. https://www.deltares.nl/en/software-and-data/products/delft3d-flexible-mesh-suite

Deltares. (n.d.). *Over herman kernkamp* [Accessed: 21-01-24].

Deltares. (2023b). *Technical reference manual d-flow flexible mesh* (tech. rep.). Deltares.

ENW. (2017). *Fundamentals of flood protection* (tech. rep.). Ministry of Infrastructure and the Environment.

Fread, D. (1988). *Breach: An erosion model for earthen dam failures*. https://api.semanticscholar.org/CorpusID:127366624

Havermans, O. (2024). *Waarom hogere dijken ons niet altijd het beste beschermen tegen overstromingen* [Accessed: 23-04-2024]. https://www.trouw.nl/duurzaamheid-economie/waarom-hogere-dijken-ons-niet-altijd-het-beste-beschermen-tegen-overstromingen~b19fa656/?referrer=https://www.bing.com/

HKV & Waterschap Rivierenland. (2020). *Uitgangspunten notitie overstromingsberekeningen met d-hydro voor waterschap rivierenland* [PR4360.10].

Hunt, S., Hanson, G., Cook, K., & Kadavy, K. (2005). Breach widening observations from earthen embankment tests. *Trans ASAE*, *48*. https://doi.org/10.13031/2013.18521

Kamrath, P., Disse, M., Hammer, M., & Köngeter, J. (2006). Assessment of discharge through a dike breach and simulation of flood wave propagation. *Natural Hazards*, *38*, 63–78. https://doi.org/10.1007/s11069-005-8600-x

Kaufmann, M., Doorn-Hoekveld, W. V., Gilissen, H., & Rijswick, H. V. (2015). *Drowning in safety. analysing and evaluating flood risk governance in the netherlands* (tech. rep.). STARFLOOD Consortium.

Linge Streek. (2024). *Rivier de linge* [Accessed: 02-03-2024]. https://lingestreek.nl/rivier-de-linge/

Ministerie van Infrastructuur en Milieu, Interprovinciaal Overleg, & Unie van Waterschappen. (2011). *De methode van vnk2 nader verklaard* (tech. rep.). Projectbureau VNK2.

Nederlandse Gemalen Stichting. (2024). *Mr. dr. g. kolff* [Accessed: 02-03-2024]. https://www.gemalen.nl/gemaal_detail.asp?gem_id=1158

Nelen en Schuurmans. (n.d.). *About us* [Accessed: 21-01-24].

OECD. (2014). *Water governance in the netherlandss: Fit for the future?* https://doi.org/https://doi.org/https://doi.org/10.1787/9789264102637-en

PBL. (2007). *Correction wording flood risks for the netherlands in ipcc report* [Accessed: 14-12-2023]. https://www.pbl.nl/en/correction-wording-flood-risks

Rijkswaterstaat. (2024). *Rijkswaterstaat waterinfo* [Accessed: 23-04-2024]. https://waterinfo.rws.nl/#/publiek/waterafvoer

Schippers, I. (2023). *Evaluating spatial measures with a d-hydro model to reduce flood risk based on the dutch flood safety standards* [Master's thesis, University of Twente] [Master thesis report].

Stelling, G., Kernkamp, H., & M., L. (1998). Delft floodingsystem: A powerful tool for inundation assessment based upon a positive flow simulation [edited by V. Babovic and L. C.Larsen]. *Hydroinformatics*, *98*, 449–456.

Sun, J., Lu, L., Lin, B., & Liu, L. (2017). Processes of dike-break induced flows: A combined experimental and numerical model study. *International Journal of Sediment Research*, *32*(4), 465–471. https://doi.org/https://doi.org/10.1016/j.ijsrc.2017.09.002

Teng, J., Jakeman, A., Vaze, J., Croke, B., Dutta, D., & Kim, S. (2017). Flood inundation modelling: A review of methods, recent advances and uncertainty analysis. *Environmental Modelling Software*, *90*, 201–216. https://doi.org/https://doi.org/10.1016/j.envsoft.2017.01.006

USACE Hydrologic Engineering Center. (2024). *Hec-ras mapper* [Accessed: 14-12-2023]. https://www.hec.usace.army.mil/confluence/rasdocs/rmum/latest

van Damme, M. (2020). An analytical process-based approach to predicting breach width in levees constructed from dilatant soils. *Natural hazards*, *101*, 59–85. https://doi.org/https://doi.org/10.1007/s11069-020-03862-8

Verbeek, B. (2019). *Modelling dike breach formation due to headcut erosion* [Master's thesis, TU Delft] [Doctoral Dissertation Report].

Verheij, H. (2003). *Aanpassen van het bresgroeimodel in his-om* (tech. rep.). Delft hydraulics.

Verschelling, E. (2000). *Manual delft-1d2d* (tech. rep.). delft hydraulics.

Visser, P. (1998). *Breach growth in sand dikes* [Doctoral dissertation, TU Delft].

Wahl, T. (2004). Uncertainty of predictions of embankment dam breach parameters. *Journal of Hydraulic Engineering*, *130*(5). https://doi.org/https://doi.org/10.1061/(ASCE)0733-9429(2004)130:5(389)

Westerhof, S., Booij, M., Berg, M., Huting, R., & Warmink, J. (2023). Uncertainty analysis of risk-based flood safety standards in the netherlands through a scenario-based approach. *International Journal of River Basin Management*, *21*(3), 559–574. https://doi.org/10.1080/15715124.2022.2060243

A Research scope information

This appendix gives some extra information about the scope of this research. It shows the "Boven Rivieren" area and the discharge wave used in this research.

A.1 Upper River Area

FIGURE A.1: Upper River Area

A.2 Discharge wave

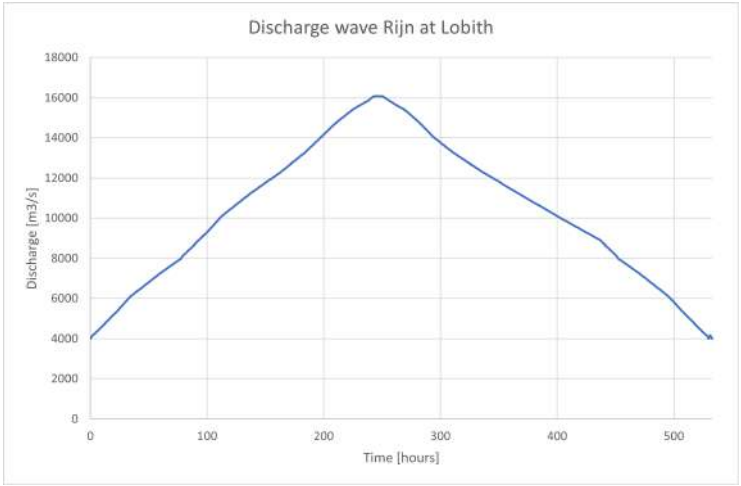

FIGURE A.2: Discharge wave Rijn at Lobith

B Equations and scripts

This appendix shows background information on algorithms, equation derivations and python scripts used in this research

B.1 Derivation alternative Verheij-vdKnaap equations

The basic logarithmic equation from which the Verheij-vdKnaap equation in D-HYDRO is derived is:

$$B = c_1 log(1 + \frac{t}{c_2}) \tag{B.1}$$

In which B is breach width [m] and t is time [s] (Verheij, 2003).

$$c_2 = \frac{u_c}{g c_3} \tag{B.2}$$

$$c_1 = H \frac{u}{u_c} \tag{B.3}$$

The Verheij-vdKnaap equation is derived by substituting $u = g/H$ and $q = g^{0.5} H^{1.5}$ which results in:

$$c_1 = c_4 \frac{g^{0.5} H^{1.5}}{u_c} \tag{B.4}$$

This research uses equation B.3 directly for Verheij-vdKnaap_a1. For Verheij-vdKnaap_a2 an alternative formulation for c_1 is used proposed in Verheij (2003).

$$c_1 = \frac{u^2}{u_c^2} \tag{B.5}$$

Implementing the three descriptions for c_1 Of equation B.3, B.4 and B.5 into equation B.1 gives for the original Verheij-vdKnaap equation:

$$B = c_4 \frac{g^{0.5} H^{1.5}}{u_c} log(1 + \frac{c_3 g}{u_c} t) \tag{B.6}$$

For Verheij-vdKnaap alternative 1:

$$B = c_4 H \frac{u}{u_c} log(1 + \frac{c_3 g}{u_c} t) \tag{B.7}$$

For Verheij-vdKnaap alternative 2:

$$B = c_4 \frac{u^2}{u_c^2} log(1 + \frac{c_3 g}{u_c} t) \tag{B.8}$$

$$\frac{dB}{dt}_{i+1} = \frac{(g(h_{up} - h_{down}))^{1.5}}{u_c^2} \frac{f_1 f_2}{ln(10)} \frac{1}{1 + \frac{f_2 g}{u_c}(t_{i+1} - t_1)} \tag{B.9}$$

$$\frac{dB}{dt}_{i+1} = f_1 \frac{Ru}{u_c} \frac{f_2 g}{ln(10) u_c} \frac{1}{1 + \frac{f_2 g}{u_c}(t_{i+1} - t_1)} \tag{B.10}$$

$$\frac{dB}{dt}_{i+1} = f_1 \frac{u^2}{u_c^2} \frac{f_2 g}{ln(10) u_c} \frac{1}{1 + \frac{f_2 g}{u_c}(t_{i+1} - t_1)} \tag{B.11}$$

B.2 D-HYDRO fixed weir scheme

The following is a cut-out from the technical reference manual of D-HYDRO (Deltares, 2023b).

6.7.2 Adjustment to momentum advection near, but not on the weir

Due to our subgrid modelling,the flow over a weir is discontinuous. In principle, this has is consequences for the discretization of all spatial operators near the weir and to this end the advection type near the weir is also adjusted by Algorithm (41). More precisely, all *faces belonging to cells that are adjacent to weirs, except for the faces that are associated with a weir themselves, with Algorithm (42) have their advection type set to* 4*. As can be seen in Algorithm (6), only inflowing cell-centered velocities are used in the expression for momentum advection for scheme* 4*. Doing so, the advection at faces adjacent to and upstream of the weir are not affected by the cell-centered velocities near the weir.*

Remark 6.7.2. Since the flow over a weir is discontinuous due to our subgrid modelling, one may need to discretize the spatial operators near the weir more rigorously.

6.7.3 Adjustments to the momentum advection on the weir: FixedWeirScheme

We assume that a face j *is located exactly* on top *of a fixed weir or not at all. Upstream of a fixed weir, a contraction zone exists. The cell-centered water level upstream of the face (*$L(j)$ *if* $u_j > 0$*) represents the far-field water level before the contraction zone. The water level at the cell-centered water level downstream of the face (*$R(j)$ *if* $u_j > 0$*) is used as a downwind approximation of the water level* on top *of the fixed weir. In other words, the discretization at a*

face j *represents the flow upstream of the weir at face* j*. This is the contraction zone, which is governed by energy conservation. The expansion zone downstream of the weir, is governed by momentum conservation and is directly resolved in the mesh without, in principle, further adjustments.*

Assume that at face j *is on top of a weir and that the flow is from the left* $L(j)$ *to the right neighboring cell* $R(j)$*. We require that:*

1. *Energy is conserved from cell* $L(j)$ *to* $R(j)$*.*
2. *The downstream water level* $\zeta_{R(j)}$ *should have no effect on the fixed weir in supercritical conditions. In this case the water height on top of the weir reached its minimum value of* $\frac{2}{3}E_j$*, where* E_j *is the far-field energy head above crest. Its computation will be discussed later.*

Energy conservation is expressed by means of Bernoulli's equation, i.e.

$$\frac{1}{2}u_{in_j}^2 + g\zeta_{L(j)} = \frac{1}{2}u_j^2 + g(z_{Cj} + h_{uj}), \tag{6.218}$$

where u_{in_j} *is a far-field velocity component in face-normal direction* $\boldsymbol{n}_j$ *and* z_{Cj} *is the crest level. For the water height at the weir* h_{uj} *a downwind approximation is used that obeys our second requirement:*

$$h_{uj} = \max(\zeta_{R(j)} - z_{Cj}, \frac{2}{3}E_j), \tag{6.219}$$

where E_j *is the far-field energy head above the crest. It is computed as*

$$E_j = \zeta_{L(j)} - z_{Cj} + \frac{1}{2g}u_{in_j}^2. \tag{6.220}$$

Remark 6.7.3. Equation (6.220) is only valid along streamlines and consequently we may only consider flows that are perpendicular to the weir (1D flows) or are uniform along both sides of the weir.

Substitution of Equation (6.219) in Equation (6.218), some rearrangement of terms and division by Δx_j *yields*

$$\frac{1}{2\Delta x_j}\left(u_j^2 - u_{in_j}^2\right) = -\frac{g}{\Delta x}\left(\zeta_{R(j)} - \zeta_{L(j)}\right) - \frac{g}{\Delta x}\max(0, \frac{2}{3}E_j - (\zeta_{R(j)} - z_{Cj})) \tag{6.221}$$

This equation if brought into the form that is solved in D-Flow FM by adding the acceleration term, which only serves to relax to our stationary subgrid expression of Equation (6.221)

$$\frac{du_j}{dt} + \frac{1}{2\Delta x_j}\left(u_j^2 - u_{in_j}^2\right) = -\frac{g}{\Delta x}\left(\zeta_{R(j)} - \zeta_{L(j)}\right) - \frac{g}{\Delta x}\max(0, \frac{2}{3}E_j - (\zeta_{R(j)} - z_{Cj})) \tag{6.222}$$

Remark 6.7.4. Although momentum diffusion over the wear is missing in Equation (6.222), it is actually included in D-Flow FM.

Recall that the spatial discretization is summarized as shown in Equation (6.26):

$$\frac{du_j}{dt} = -\frac{g}{\Delta x_j}\left(\zeta_{R(j)} - \zeta_{L(j)}\right) - \mathcal{A}_{ij}u_j - \mathcal{A}_{ej} - \frac{g\|\boldsymbol{u}_j\|}{C^2 h}u_j.$$

For the temporal discretization, see Equation (6.121). The terms for fixed weirs can then be put as, assuming $u_j > 0$*:*

$$\mathcal{A}_{ij} = \frac{1}{2\Delta x_j}u_j, \tag{6.223}$$

$$\mathcal{A}_{ej} = -\frac{1}{2\Delta x_j}u_{in_j}^2 + \frac{g}{\Delta x}\max(0, \frac{2}{3}E_j - (\zeta_{R(j)} - z_{Cj})). \tag{6.224}$$

Remark 6.7.5. Although bed friction is not included in Equation (6.221), it is included in D-Flow FM by means of Equation (6.26). Its actual computation will not be discussed at this occasion.

The terms of Equation (6.219), and Equation (6.223) and Equation (6.224) are prescribed partly *with Algorithm (43) and* partly *with Algorithm (44). Note that the latter also adjusts the cell-centered velocity vectors* $\boldsymbol{u}_c$*.*

B.3 Python script for alternative breach growth

The Python code that is used to calculate the alternative breach growths is shown here

```
"""
Created on Mon Jun  3 10:15:13 2024

@author: Ruben den Hertog
"""
from RoyalHaskoningFigure import FigureSettings as fs
from HandigeFuncties import HandigeFuncties as hf
import numpy as np
import matplotlib.pyplot as plt
import math
import warnings
warnings.filterwarnings("ignore", category=DeprecationWarning)

def calculate_damme_rate(vel,hRadius,m,c1,n):
    tau = 1000*9.81*((vel**2)*(n**2))/(hRadius**(1/3))
    rate = m*tau**0.5 + c1
    displacement = 2*rate
    print(vel)
    if displacement < 0:
        displacement = 0
    if vel < 0.2:
            displacement =0
    return displacement                              #in m/s

def calculate_verheij_a1_rate(vel,up,down,f1,f2,uc,ti,t0,z,hrad):
    g=9.81
    dbdt = f1* (hrad)*(vel/uc) * ((f2*g)/(math.log(10)*uc)) * (1/(1+((f2*g)/(3600*uc))*(ti-t0)))
    print('a1 ' , f1* (hrad)*(vel/uc))
    if vel < uc:
        dbdt=0
    return dbdt

def calculate_verheij_a2_rate(vel,f1,f2,uc,ti,t0):
    g=9.81
    dbdt = ((f1*vel**2)/(uc**2)) * ((f2*g)/(math.log(10)*uc)) * (1/(1+((f2*g)/(3600*uc))*(ti-t0)))
    print('a2 ', ((f1*vel**2)/(uc**2)))
    if vel < uc:
        dbdt=0
    return dbdt
```

```
41
42
43  def width_time_series(timesteps,breachwidth,vel,hRadius,up,down,z,f1,f2,uc,dt,m,c1,n):
44      Verheij_vdKnaap = np.zeros(len(timesteps))
45      Verheij_a1 = np.zeros(len(timesteps))
46      Verheij_a2 = np.zeros(len(timesteps))
47      VanDamme = np.zeros(len(timesteps))
48      VanDamme2 = np.zeros(len(timesteps))
49      m2 = 0.0002253
50      c12 = 0.008
51      for i in range(len(timesteps)-1):
52          t0 = 600
53          ti = i*dt
54          Verheij_vdKnaap[i] = breachwidth[i]
55          Verheij_a1[i+1] = Verheij_a1[i] + calculate_verheij_a1_rate(vel[i], up[i],
56                                              down[i], f1, f2, uc, ti, t0, z[i],hRadius[i])*(dt/3600)
57          Verheij_a2[i+1] = Verheij_a2[i] + calculate_verheij_a2_rate(vel[i],f1,f2,uc,ti,t0)*(dt/3600)
58          VanDamme[i+1] = VanDamme[i] + calculate_damme_rate(vel[i], hRadius[i],m,c1,n)*dt
59          VanDamme2[i+1] = VanDamme2[i] + calculate_damme_rate(vel[i], hRadius[i],m2,c12,n)*dt
60          if np.isnan(VanDamme[i+1]):
61              VanDamme[i+1] = 0
62          if np.isnan(VanDamme2[i+1]):
63                  VanDamme2[i+1] = 0
64          if np.isnan(Verheij_a1[i+1]):
65              Verheij_a1[i+1] = 0
66          if np.isnan(Verheij_a2[i+1]):
67              Verheij_a2[i+1] = 0
68      return Verheij_vdKnaap, Verheij_a1, Verheij_a2, VanDamme, VanDamme2
69
70  def plot_widths(paths, names, equation,upsidedown):
71      for i in range(len(paths)):
72          figW = fs('Dike Breach width',f'Dike Breach width {names[i]}',(8,4))
73          data, vars_pd, reftime = hf.read_his(paths[i])
74          dt=600
75          w = data.dambreak_crest_width.values
76          timesteps = np.linspace(0,len(w),len(w))
77          area = data.dambreak_flow_area.values
78          hrad = area/w
79          vel = abs(data.dambreak_normal_velocity.values*-1)
80          if upsidedown == True:
```

```
81              up = data.dambreak_s1dn.values
82              down = data.dambreak_s1up.values
83          else:
84              up = data.dambreak_s1up.values
85              down = data.dambreak_s1dn.values
86          z = data.dambreak_crest_level.values
87          f1 = 1.2
88          f2 = 0.04
89          uc = 0.2
90          m = 2.38E-5 #1.15E-5 2,38E-05
91          c1 = -1.77E-5 #3.6E-5#5.36E-5
92          n = 0.025
93          Verheij_vdKnaap, Verheij_a1, Verheij_a2, VanDamme, VanDamme2 = width_time_series(timesteps,w,vel,hrad,up,down,z,f1,f2,uc,dt,m,c1,n)
94          timesteps = (timesteps*600)/60/60/24
95          if equation[0] == True:
96              figW.plot(timesteps[0:-2],Verheij_vdKnaap[0:-2], 'Verheij-vdKnaap')
97          if equation[1] == True:
98              figW.plot(timesteps,Verheij_a1, 'Verheij-vdKnaap alternative 1')
99          if equation[2] == True:
100             figW.plot(timesteps,Verheij_a2, 'Verheij-vdKnaap alternative 2')
101         if equation[3] == True:
102             figW.plot(timesteps,VanDamme,'Van Damme alternative 1')
103         if equation[4] == True:
104             figW.plot(timesteps,VanDamme2,'Van Damme alternative 2')
105         figW.setAxis("Days after start simulation", "Breach Width [m]",[0,14],[0,350])
106
107         return VanDamme
```

B.4 Python algorithm to detect elevated elements

The Python code that is used to detect elevated elements in the Delft-FLS digital elevation model is shown here:

```
"""
Created on Mon Apr  8 10:11:42 2024

@author: Ruben den Hertog
"""
import numpy as np
import matplotlib.pyplot as plt
from scipy import ndimage
import pandas as pd
import geopandas as gpd
from shapely.geometry import Point

from pyproj import Transformer
from geopy.distance import geodesic
def rowCol_to_mat(filename,rowsBeforeData):
    matrix = np.loadtxt(filename,skiprows=rowsBeforeData)
    MatrixT = np.zeros([1057,1121])
    for i in range(1057):
        MatrixT[i,:] = matrix[1056-i,:]
    return MatrixT

filename = 'vik07.asc'
rowsBeforeData = 6
bedlevelCorrect = rowCol_to_mat(filename,rowsBeforeData)

print('finding elevated grid cells......')
th = 0.5
size = 3
#Grid cell identifier
#Links naar rechts
elevatedElements = {}
iD=1
for i in range(bedlevelCorrect.shape[0]):
    for j in range(bedlevelCorrect.shape[1]):
        #Grid cell a
         cellA = bedlevelCorrect[i,j]
         #grid cell b
         if j<bedlevelCorrect.shape[1]-2:
             cellB = bedlevelCorrect[i,j+1]
         else:
             break
         #step
         stepBlchange = cellA - cellB
         if stepBlchange < -th:
             richting = 'omhoog'
             nextStep = cellB - bedlevelCorrect[i,j+2]
             if nextStep > th:
                 print(f'Elevated element found at {i*100+404750,(j+1)*100+127650}')
                 elevatedElements[iD] = [iD,iD,(j+1)*100+127650,i*100+404750,'East',bedlevelCorrect[i,j+1],i,j+1,2]
                 iD = iD+1

#Boven naar onder
for j in range(bedlevelCorrect.shape[1]):
    for i in range(bedlevelCorrect.shape[0]):
        #Grid cell a
         cellA = bedlevelCorrect[i,j]
         #grid cell b
         if i<bedlevelCorrect.shape[0]-2:
             cellB = bedlevelCorrect[i+1,j]
         else:
             break
         #step
         stepBlchange = cellA - cellB
         if stepBlchange < -th:
             richting = 'omhoog'
             nextStep = cellB - bedlevelCorrect[i+2,j]
             if nextStep > th:
                 print(f'Elevated element found at {i*100+404750,(j+1)*100+127650}')
                 elevatedElements[iD] = [iD,iD,j*100+127650,(i+1)*100+404750,'North',bedlevelCorrect[i+1,j],i+1,j,1]
                 iD = iD+1

#plotting to check
plaatje = np.zeros([bedlevelCorrect.shape[0],bedlevelCorrect.shape[1]])
for value in elevatedElements.values():
    plaatje[value[6],value[7]] = 1
plt.imshow(plaatje, cmap='Reds')
plt.colorbar(label='Bedlevel values')
plt.gca().invert_yaxis()
plt.title('Bedlevel Colormap')
plt.ylim([180,420])
plt.xlim([0,780])
plt.show()

#%%
#Filter small elemetns
print('Filtering and labeling of fixed weir points......')
structure = np.ones((3, 3), dtype=bool)
labeled, ncomponents = ndimage.label(plaatje, structure)
filtered1 = np.zeros_like(labeled)
p=1
for i in range(1, ncomponents + 1):
    component_size = np.sum(labeled == i)
    if component_size >= size:
        filtered1[labeled == i] = 1
        p=p+1

#Delete intersecting elements
iD=1
intersection = {}
for i in range(filtered1.shape[0]-1):
    for j in range(filtered1.shape[1]-1):
        if filtered1[i,j] == 1:
```

```
            x = [-1,0,1]
            num = 0
            for n in x:
                for m in x:
                    num = num + filtered1[i+n,j+m]
            if num > 3:
                intersection[iD] = [i,j]
                iD=iD+1

#Delete intersections
for values in intersection.values():
    filtered1[values[0],values[1]] = 0

#find endpoints
endpoints = {}
iD=1
for i in range(filtered1.shape[0]-1):
    for j in range(filtered1.shape[1]-1):
        if filtered1[i,j] == 1:
            x = [-1,0,1]
            num = 0
            for n in x:
                for m in x:
                    num = num + filtered1[i+n,j+m]
            if num == 2:
                endpoints[iD] = [j*100+127650,i*100+404750]
                iD=iD+1

#Label elements
structure = np.ones((3, 3), dtype=bool)
labeled, ncomponents = ndimage.label(filtered1, structure)
filtered = np.zeros_like(labeled)
p=1
for i in range(1, ncomponents + 1):
    component_size = np.sum(labeled == i)
    if component_size >= size:
        filtered[labeled == i] = p
        p=p+1


plt.imshow(filtered, cmap='Reds')
plt.colorbar(label='Bedlevel values')
plt.gca().invert_yaxis()
plt.title('Bedlevel Colormap')
plt.ylim([180,420])
plt.xlim([0,780])
plt.show()
#Create Fixed weir point dictionary
elevatedElementsNew = elevatedElements.copy()
for key, values in elevatedElements.items():
    values[0] = filtered[values[6],values[7]]
    if filtered[values[6],values[7]] == 0:
```

```
        del elevatedElementsNew[key]
    else:
        elevatedElementsNew[key] = elevatedElements[key]

elevatedElementsSorted = dict(sorted(elevatedElementsNew.items(), key=lambda item: (item[1][0], item[1][2], item[1][3],item[1][8])))

elementShapes = {}
no = 100000000000000
for key, values in elevatedElementsSorted.items():
    noN = values[0]
    x_proj = values[2]
    y_proj = values[3]
    if noN != no:
        elId = 1
        no = noN
    if values[4] == 'North':
        y_proj = values[3]+25
    elif values[4] == 'East':
        x_proj = values[2]+25
    elementShapes[key] = [values[0],elId,values[2],values[3],x_proj,y_proj,values[5]]
    elId = elId + 1

#%%
print('Sorting line points.....')
def c_c(x,y):
    # Create a transformer to convert from EPSG:3857 to EPSG:4326
    transformer = Transformer.from_crs("EPSG:28992", "EPSG:4326")

    # Convert to EPSG:4326
    lon, lat = transformer.transform(x, y)
    return lon,lat

#order points to proximity
elementstoOrder = {}
i=0
for values in elementShapes.values():
    i=i+1
    elementstoOrder[(c_c(values[4],values[5]))] = (values[0],[values[0],elId,values[2],values[3],values[4],values[5],values[6]])
    if i%100 == 0:
        print(i)

def sort_points_by_distance(points):
    # Convert the dictionary to a list of tuples
    points_list = list(points.items())

    # Group points by line_id
    lines = {}
    for point, data in points_list:
        line_id = data[0]
        if line_id not in lines:
            lines[line_id] = []
        lines[line_id].append((point, data))
```

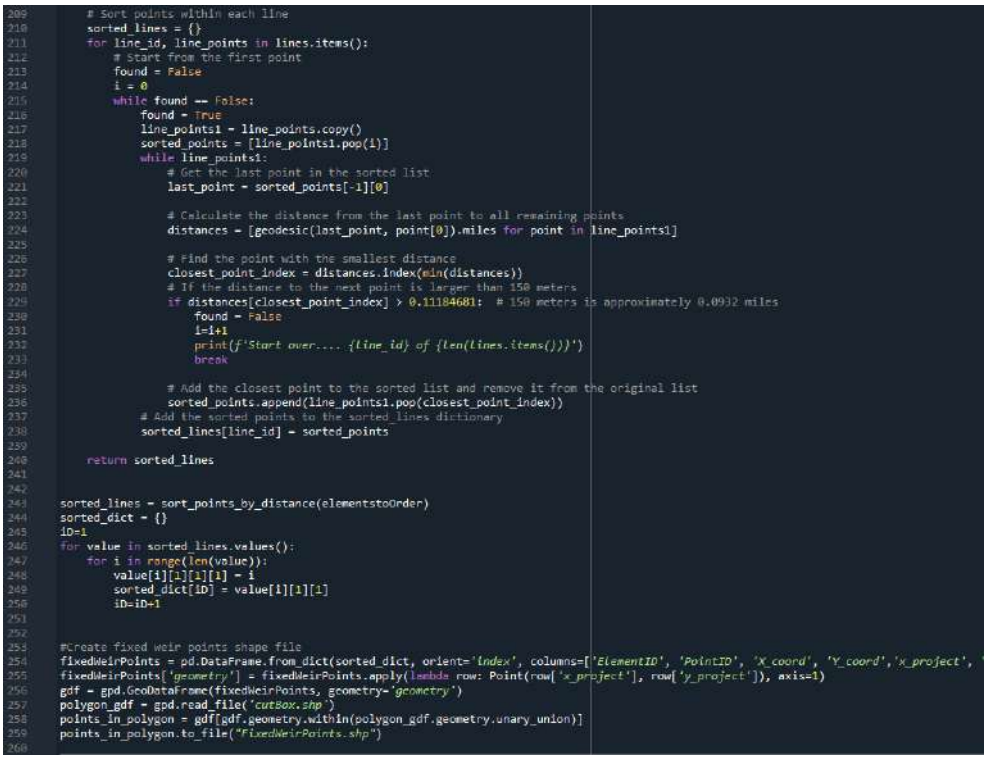

```
    # Sort points within each line
    sorted_lines = {}
    for line_id, line_points in lines.items():
        # Start from the first point
        found = False
        i = 0
        while found == False:
            found = True
            line_points1 = line_points.copy()
            sorted_points = [line_points1.pop(i)]
            while line_points1:
                # Get the last point in the sorted list
                last_point = sorted_points[-1][0]

                # Calculate the distance from the last point to all remaining points
                distances = [geodesic(last_point, point[0]).miles for point in line_points1]

                # Find the point with the smallest distance
                closest_point_index = distances.index(min(distances))
                # If the distance to the next point is larger than 150 meters
                if distances[closest_point_index] > 0.11184681:  # 150 meters is approximately 0.0932 miles
                    found = False
                    i=i+1
                    print(f'Start over.... {line_id} of {len(lines.items())}')
                    break

                # Add the closest point to the sorted list and remove it from the original list
                sorted_points.append(line_points1.pop(closest_point_index))
            # Add the sorted points to the sorted_lines dictionary
            sorted_lines[line_id] = sorted_points

    return sorted_lines


sorted_lines = sort_points_by_distance(elementstoOrder)
sorted_dict = {}
ID=1
for value in sorted_lines.values():
    for i in range(len(value)):
        value[i][1][1][1] = i
        sorted_dict[ID] = value[i][1][1]
        ID=ID+1


#Create fixed weir points shape file
fixedWeirPoints = pd.DataFrame.from_dict(sorted_dict, orient='index', columns=['ElementID', 'PointID', 'X_coord', 'Y_coord','x_project', '
fixedWeirPoints['geometry'] = fixedWeirPoints.apply(lambda row: Point(row['x_project'], row['y_project']), axis=1)
gdf = gpd.GeoDataFrame(fixedWeirPoints, geometry='geometry')
polygon_gdf = gpd.read_file('cutBox.shp')
points_in_polygon = gdf[gdf.geometry.within(polygon_gdf.geometry.unary_union)]
points_in_polygon.to_file("FixedWeirPoints.shp")
```

C Extra modeling results

This appendix shows a selection of modelling results, on which conclusions of this research are based, but was not shown in the main body.

C.1 HYDRO_D43_1998 at Heteren

This appendix shows simulations performed with HYDRO_D43_1998 for the breach location at Heteren.

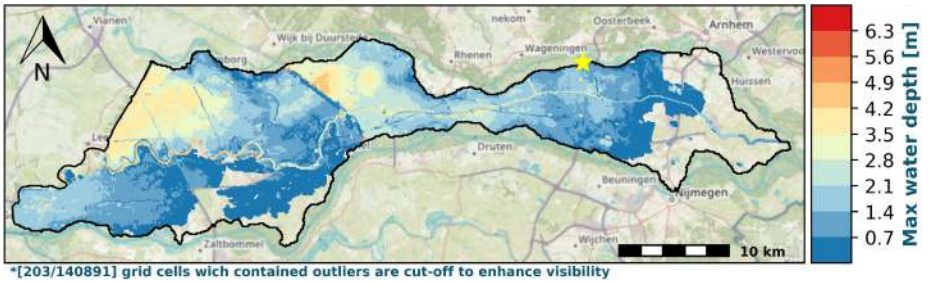

(A) Maximum inundation [m]

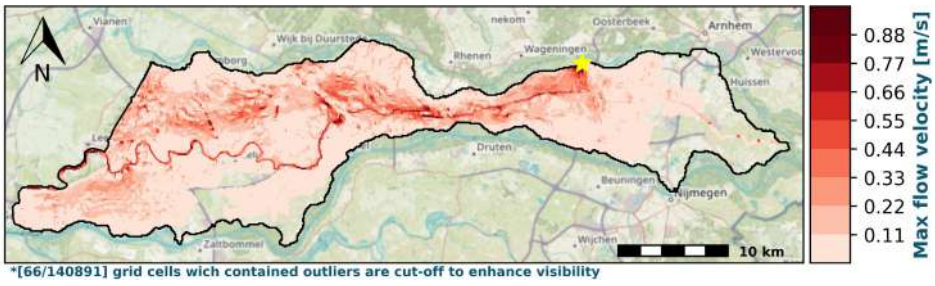

(B) Maximum flow velocity [m/s]

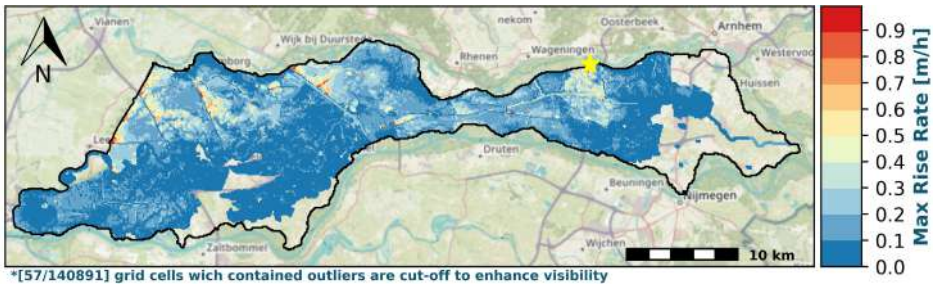

(C) Maximum Rise rate [m/h]

(D) Arrival time [h]

FIGURE C.1: HYDRO_D43_1998 at Heteren [Yellow star = breach location]]

C.2 Water level boundary VS simulated river

This appendix shows the impact of a higher breach discharge caused by a water level boundary on the river axis, as opposed to breach discharge resulting from a 2D river simulation. For both schematisations, breach discharge is computed by D-HYDRO. This is significantly lower than the breach discharge in Delft_D43_1998 which is computed by Delft-FLS.

C.2.1 Breach location Bemmel

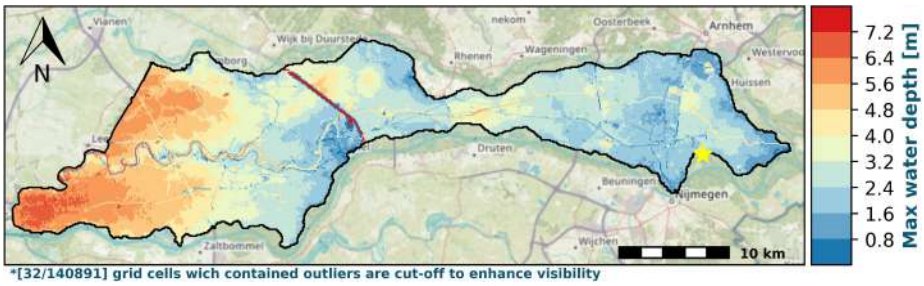

(A) Water level boundary at river axis

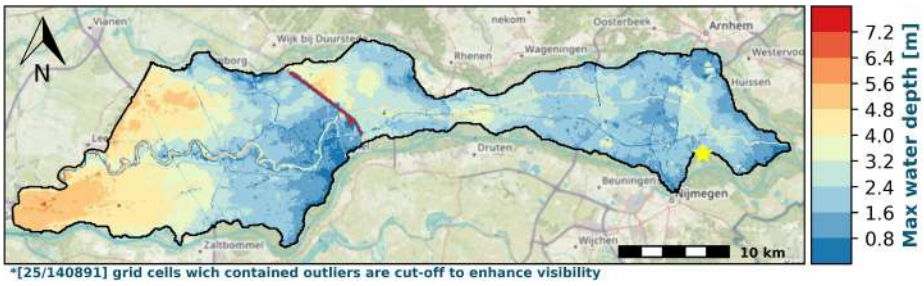

(B) HYDRO_D43_1998

FIGURE C.2: Maximum inundation at Bemmel [Yellow star = breach location]]

(A) Water level boundary at river axis

(B) HYDRO_D43_1998

FIGURE C.3: Maximum flow velocity at Bemmel [Yellow star = breach location]]

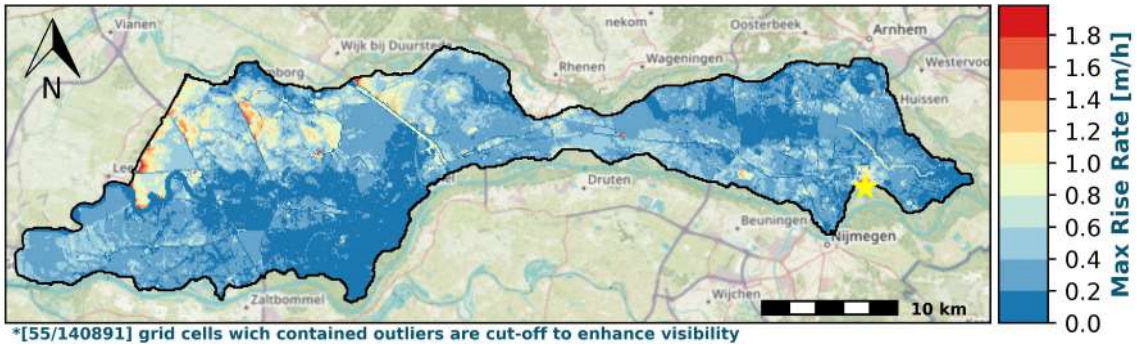

(A) Water level boundary at river axis

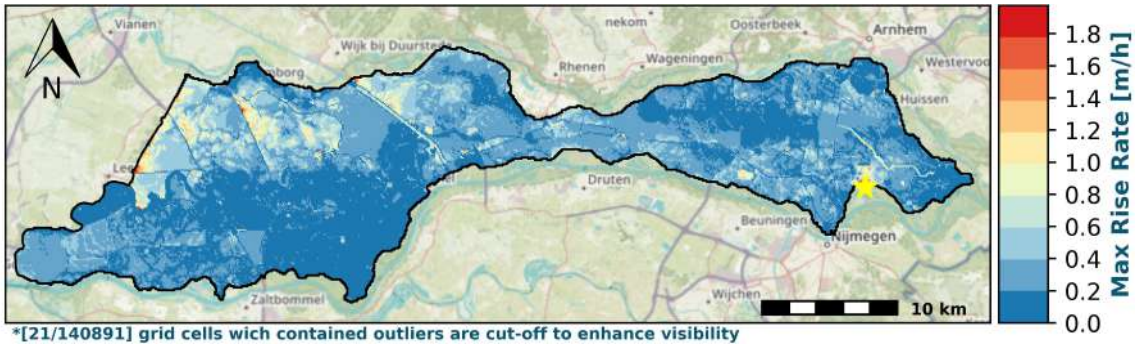

(B) HYDRO_D43_1998

FIGURE C.4: Maximum rise rate at Bemmel [Yellow star = breach location]]

(A) Water level boundary at river axis

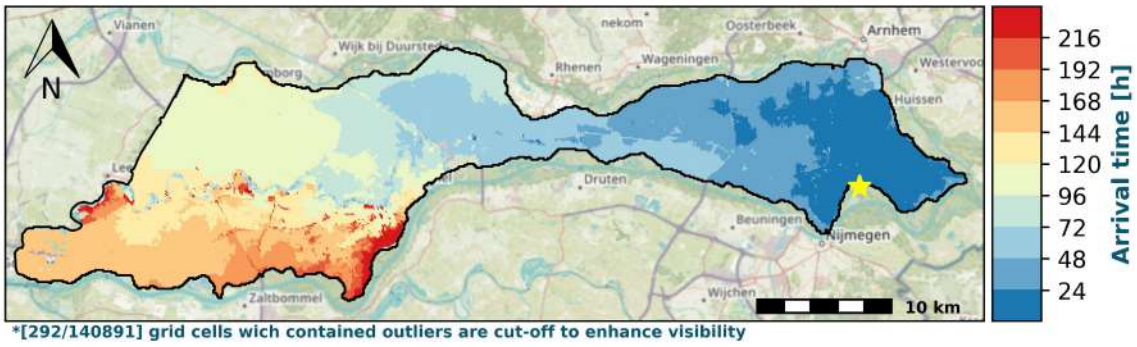

(B) HYDRO_D43_1998

FIGURE C.5: Arrival time at Bemmel [Yellow star = breach location]]

C.2.2 Breach location Tiel

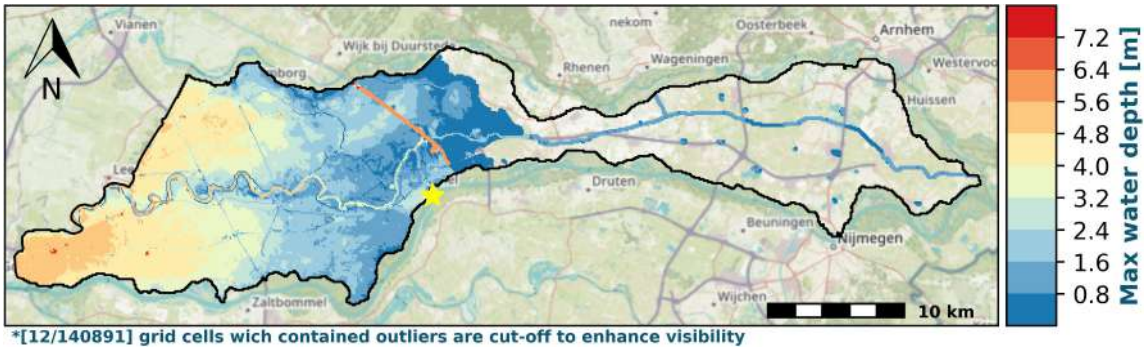

(A) Water level boundary at river axis

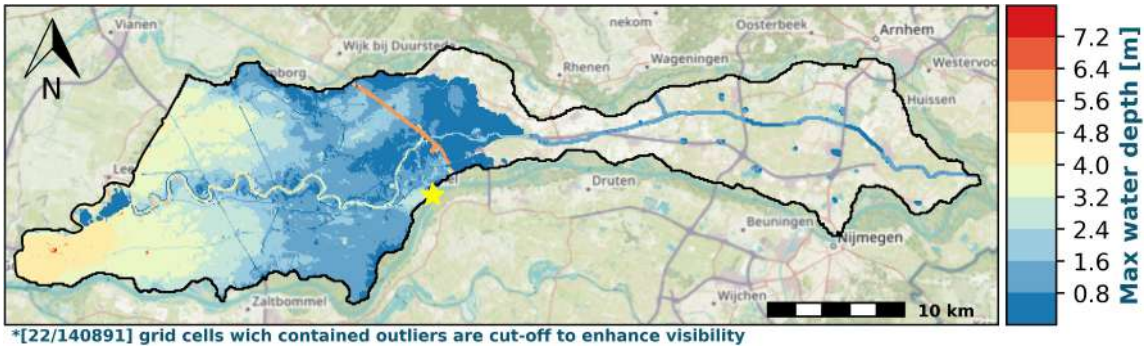

(B) HYDRO_D43_1998

FIGURE C.6: Maximum inundation at Tiel [Yellow star = breach location]]

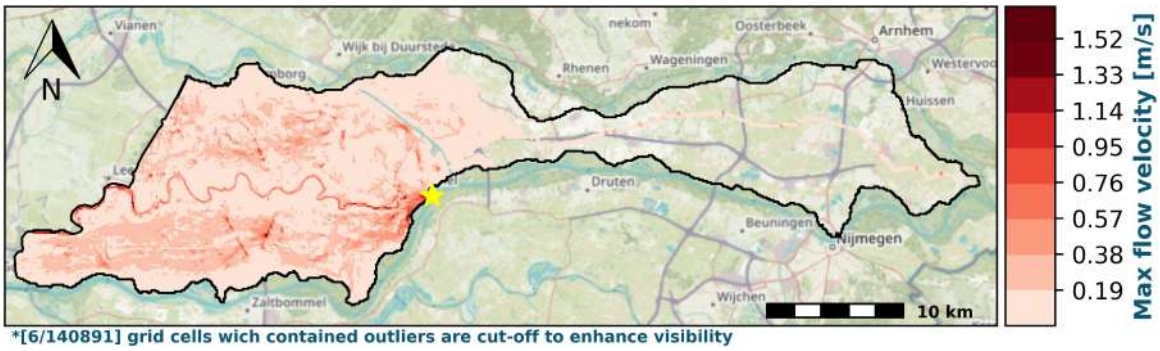

(A) Water level boundary at river axis

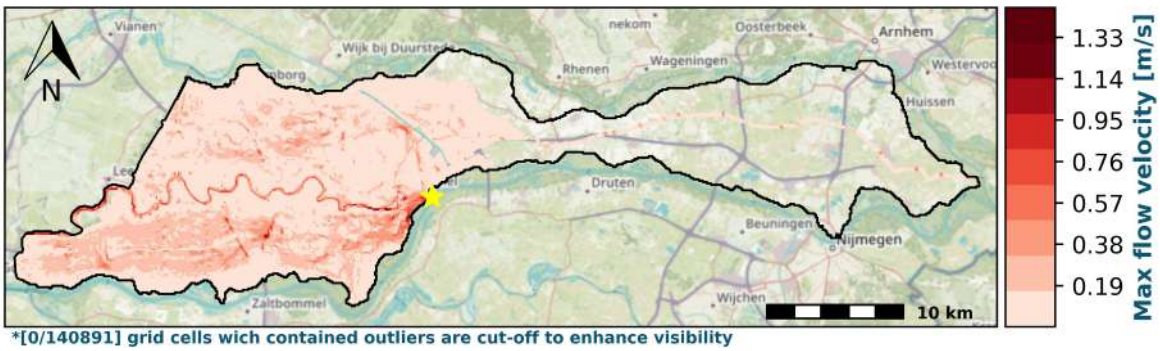

(B) HYDRO_D43_1998

FIGURE C.7: Maximum flow velocity at Tiel [Yellow star = breach location]]

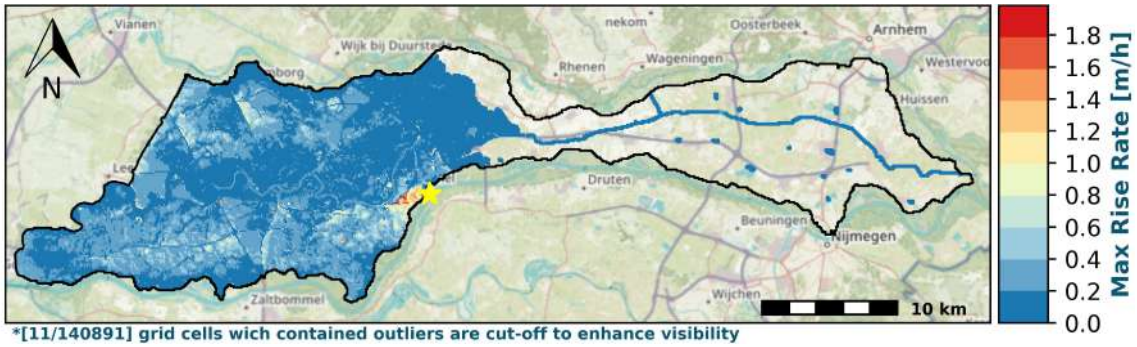

(A) Water level boundary at river axis

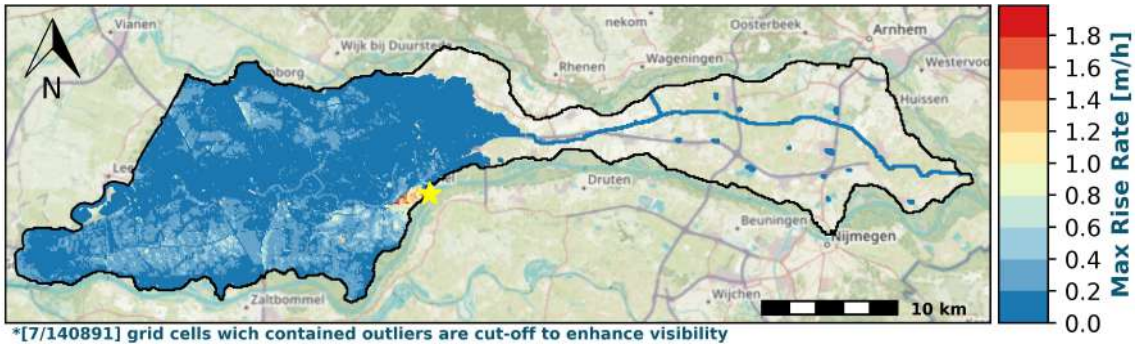

(B) HYDRO_D43_1998

FIGURE C.8: Maximum rise rate at Tiel [Yellow star = breach location]]

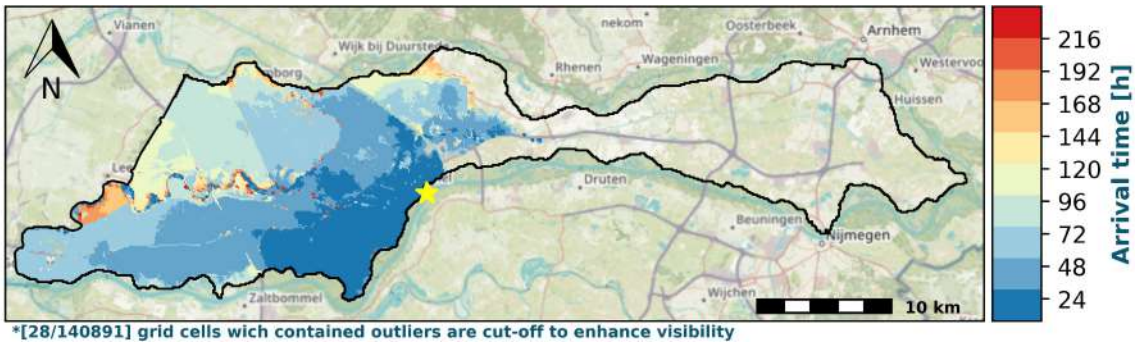

(A) Water level boundary at river axis

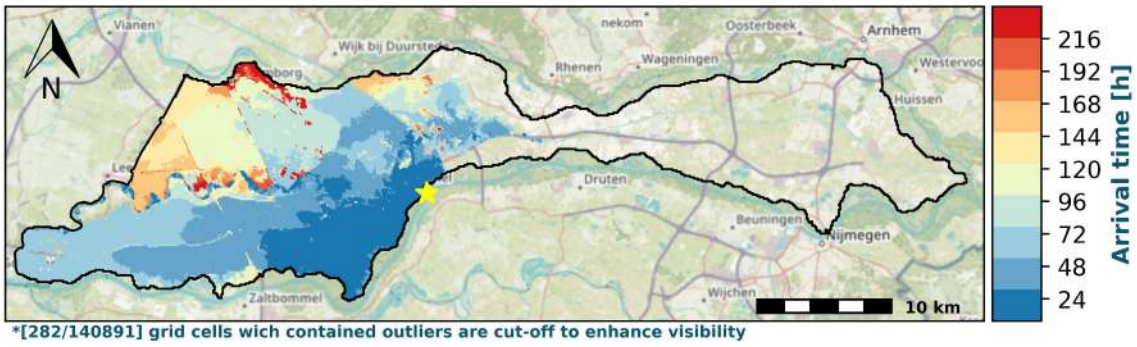

(B) HYDRO_D43_1998

FIGURE C.9: Arrival time at Tiel [Yellow star = breach location]]

C.2.3 Breach location Heteren

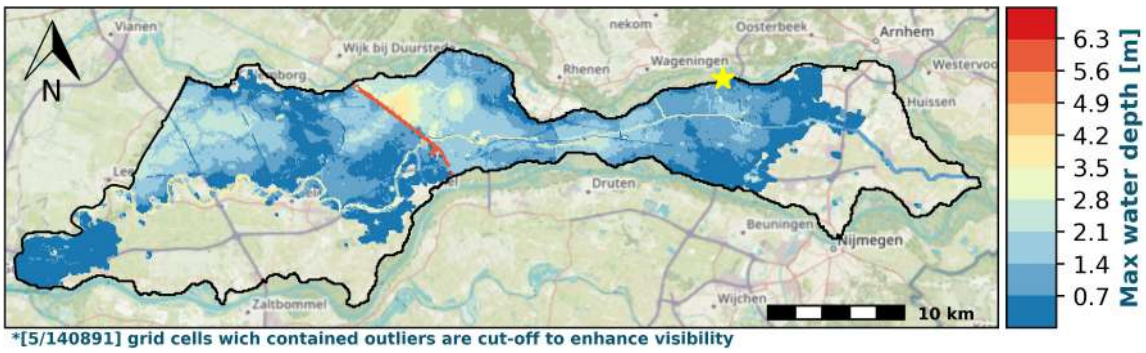

(A) Water level boundary at river axis

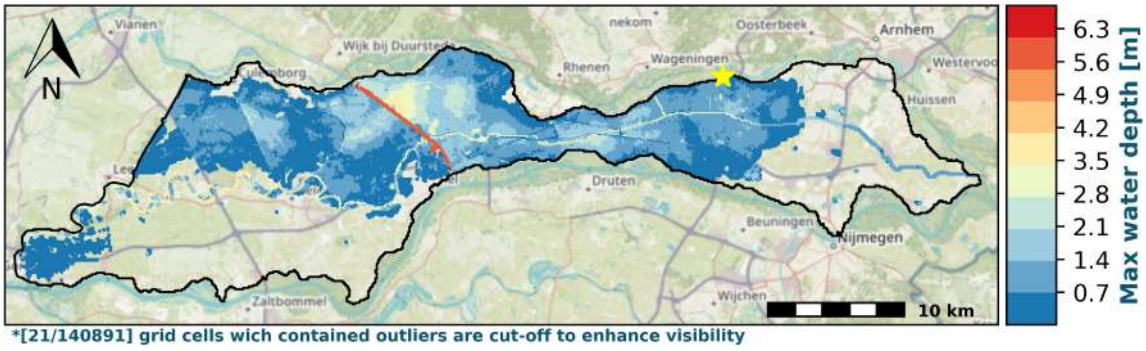

(B) HYDRO_D43_1998

FIGURE C.10: Maximum inundation at Heteren [Yellow star = breach location]]

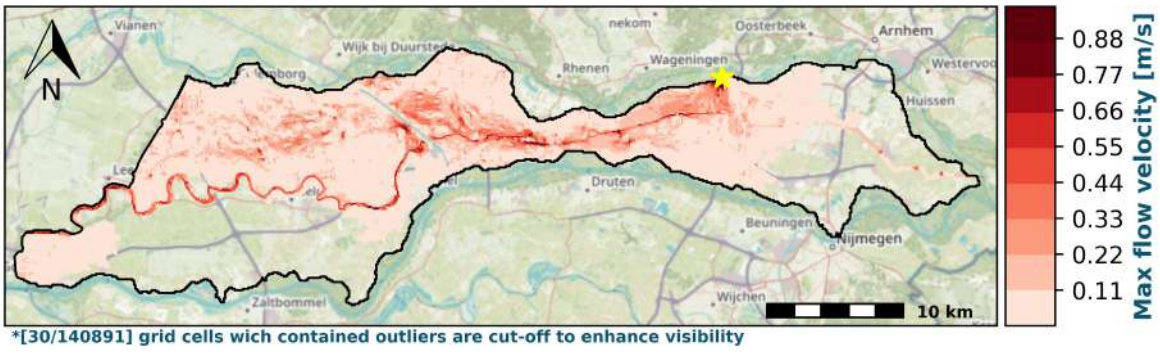

(A) Water level boundary at river axis

(B) HYDRO_D43_1998

FIGURE C.11: Maximum flow velocity at Heteren [Yellow star = breach location]]

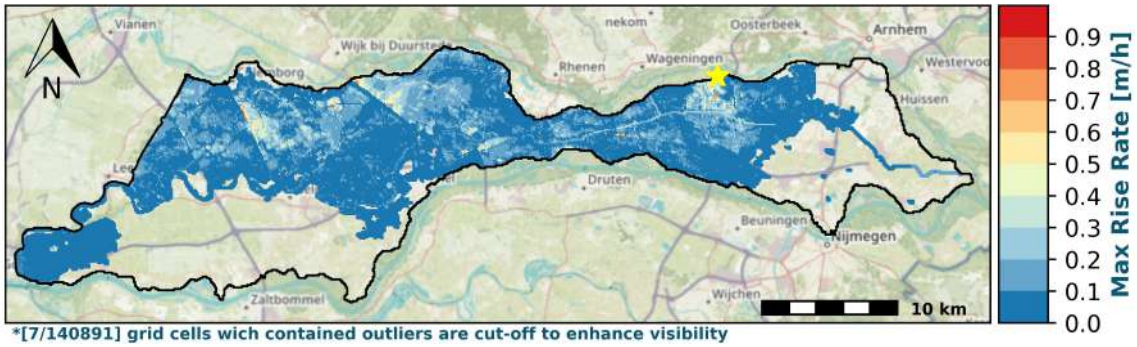

(A) Water level boundary at river axis

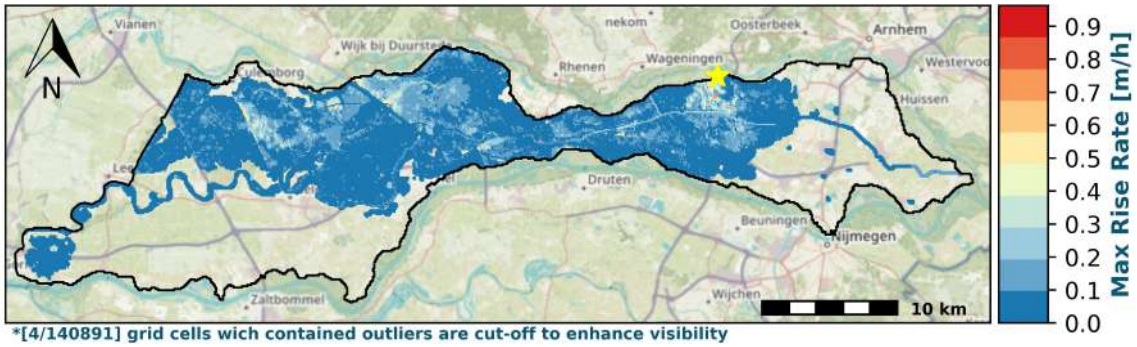

(B) HYDRO_D43_1998

FIGURE C.12: Maximum rise rate at Heteren [Yellow star = breach location]]

(A) Water level boundary at river axis

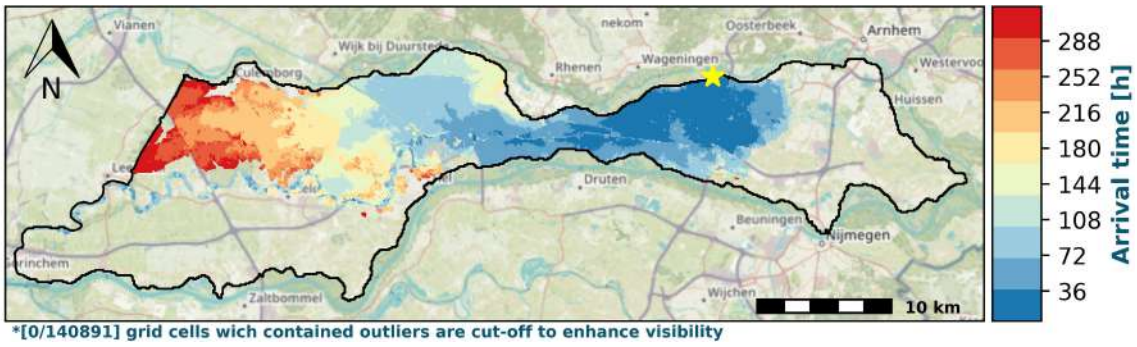

(B) HYDRO_D43_1998

FIGURE C.13: Arrival time at Heteren [Yellow star = breach location]]

C.3 Fixed weirs model runs without changed elevation

This appendix shows simulations performed with a schematisation, including fixed weirs. The elevation of underlying grid cells is not changed.

C.3.1 Breach location Bemmel

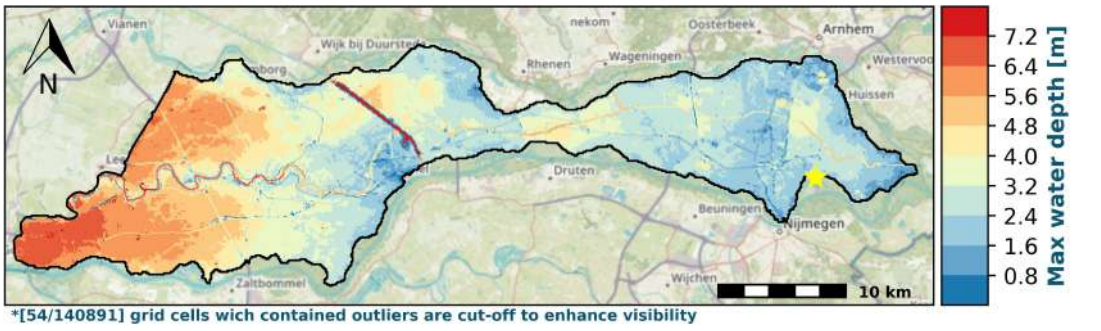

(A) Maximum inundation [m]

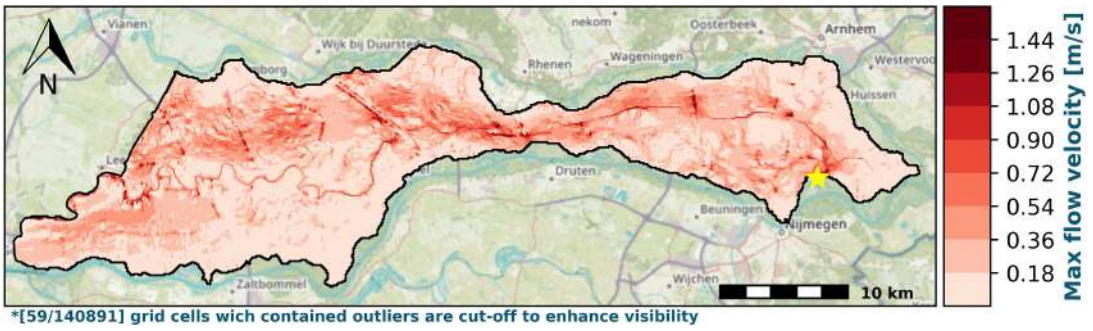

(B) Maximum flow velocity [m/s]

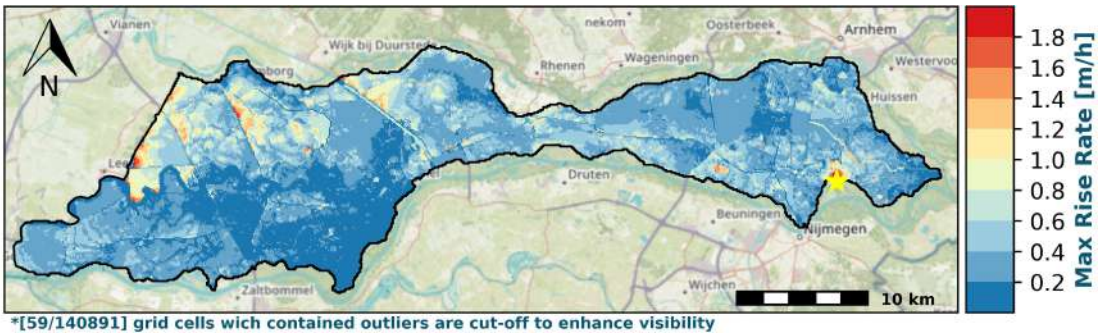

(C) Maximum Rise rate [m/h]

(D) Arrival time [h]

FIGURE C.14: Fixed weir without elevation change Bemmel [Yellow star = breach location]

C.3.2 Breach location Heteren

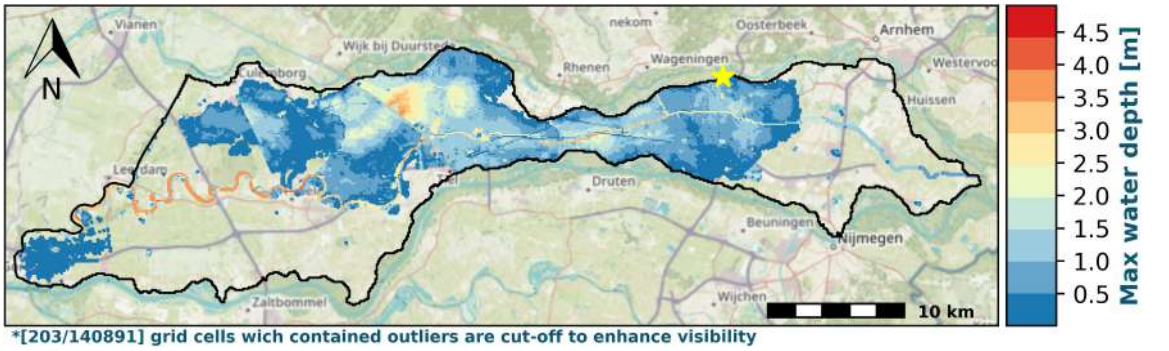

(A) Maximum inundation [m]

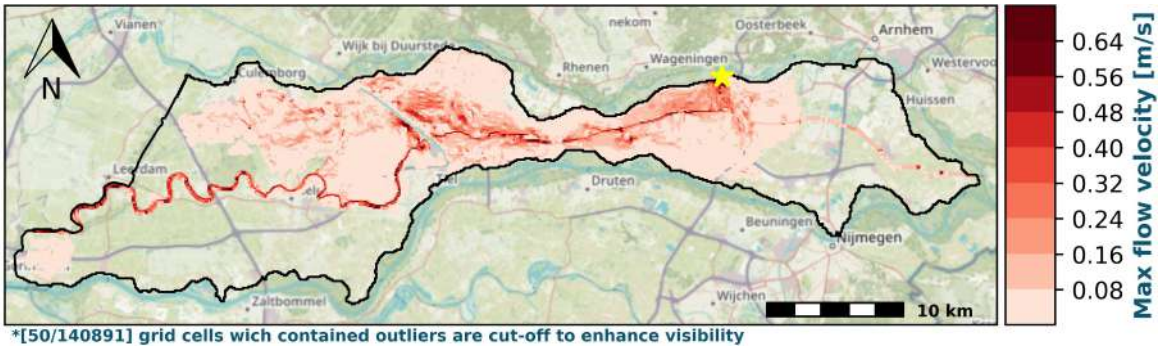

(B) Maximum flow velocity [m/s]

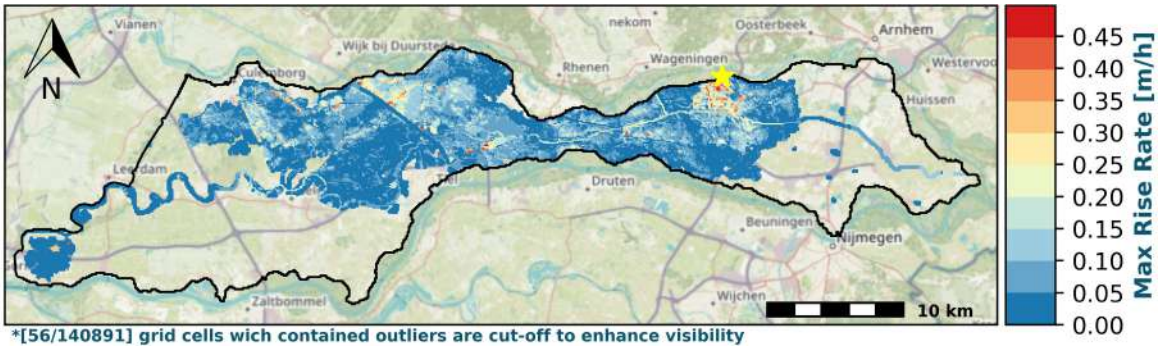

(C) Maximum Rise rate [m/h]

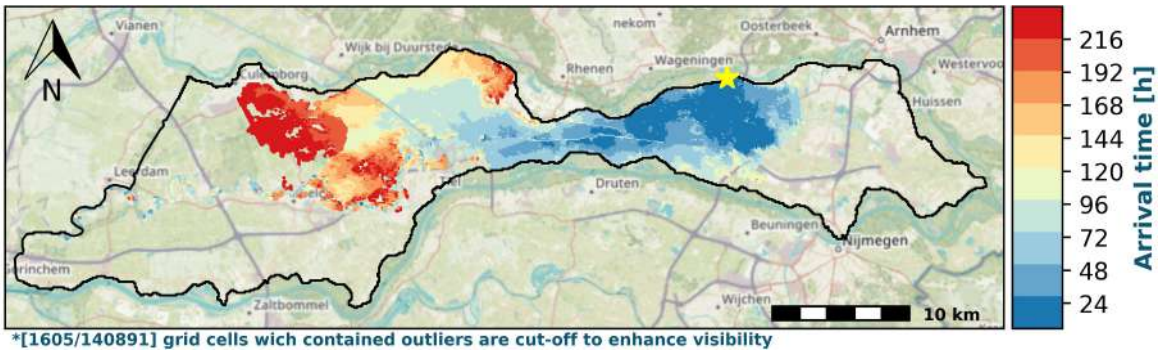

(D) Arrival time [h]

FIGURE C.15: Fixed weir without elevation change model run at Heteren [Yellow star = breach location]]

C.4 Fixed weirs model runs with changed elevation

This appendix shows simulations performed with a schematisation, including fixed weirs. The elevation of underlying grid cells is changed.

C.4.1 Breach location Bemmel

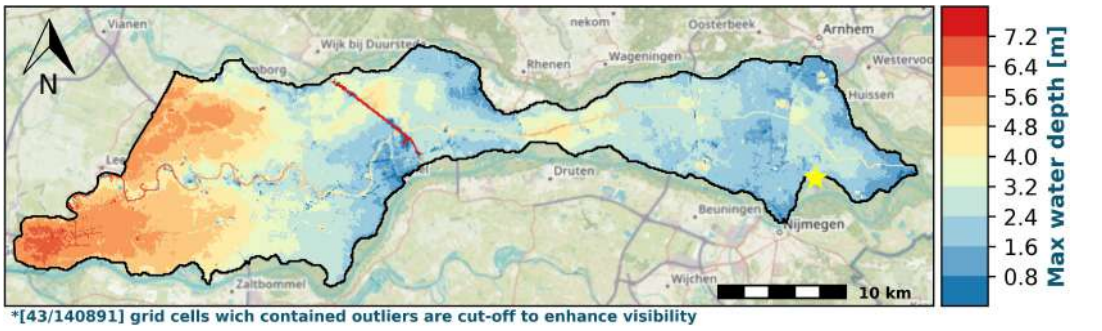

(A) Maximum inundation [m]

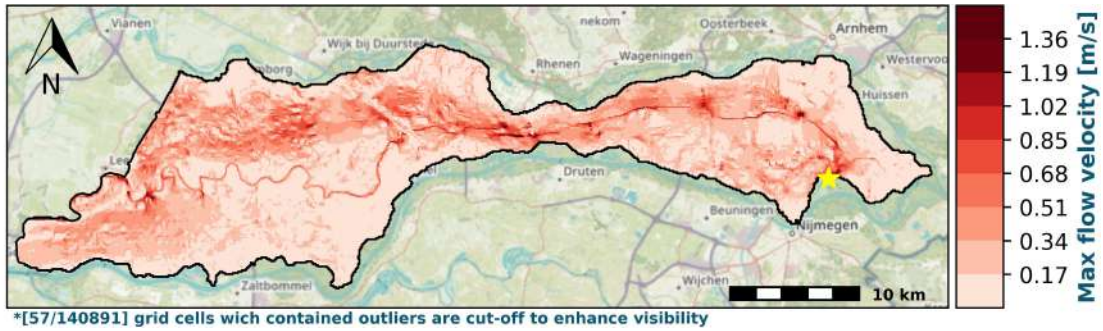

(B) Maximum flow velocity [m/s]

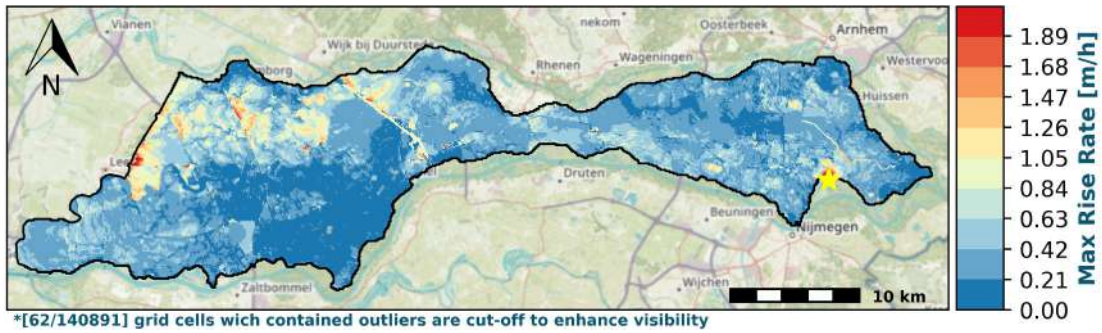

(C) Maximum Rise rate [m/h]

(D) Arrival time [h]

FIGURE C.16: Fixed weir with elevation change at Bemmel [Yellow star = breach location]]

C.4.2 Breach location Heteren

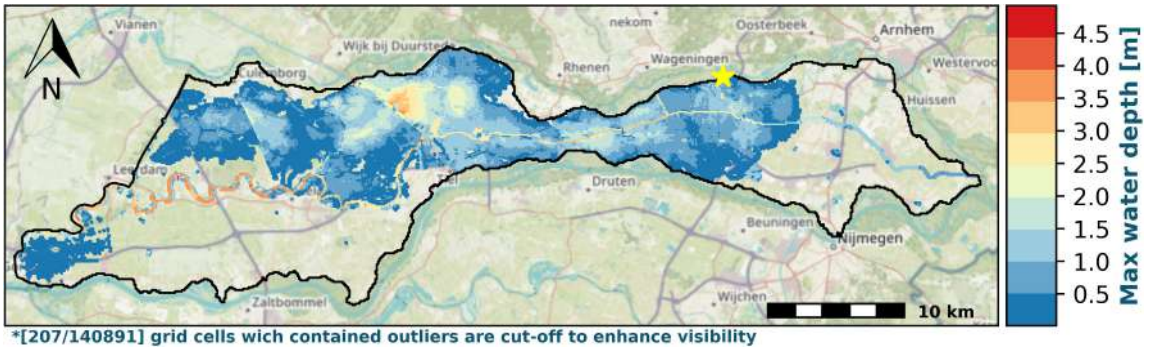

(A) Maximum inundation [m]

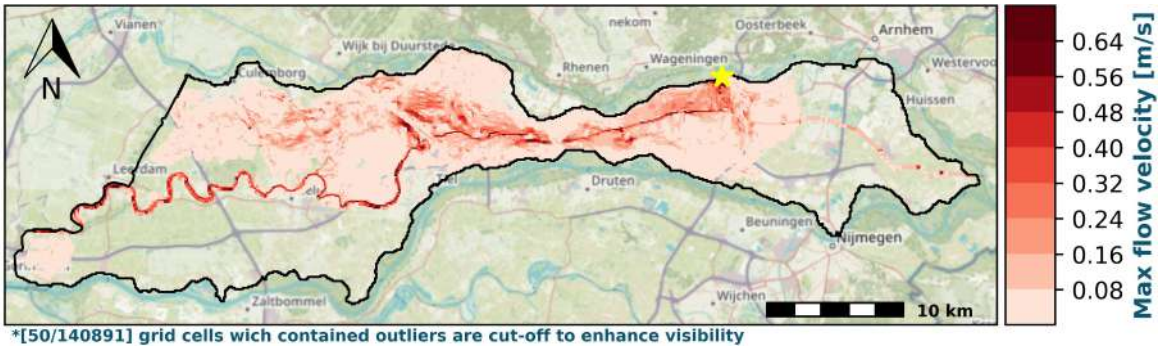

(B) Maximum flow velocity [m/s]

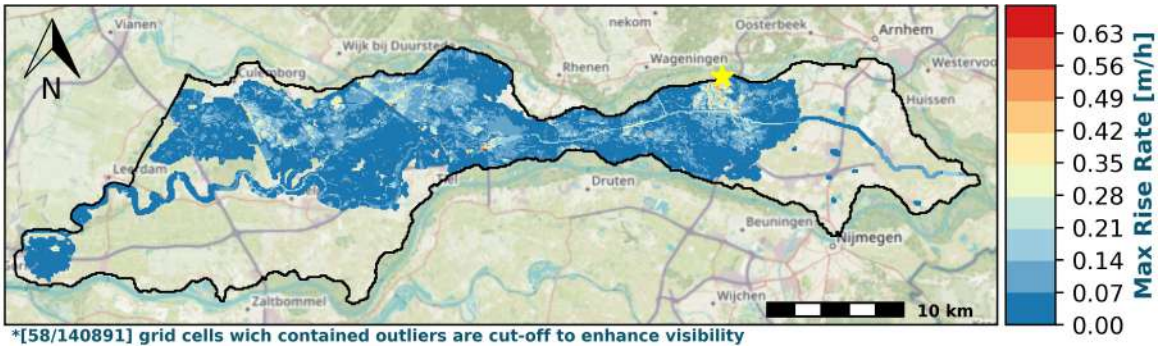

(C) Maximum Rise rate [m/h]

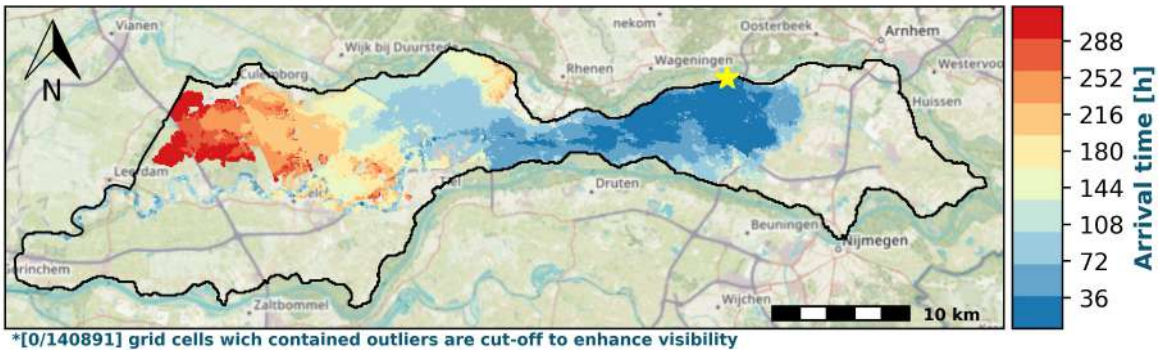

(D) Arrival time [h]

FIGURE C.17: Fixed weir with elevation change model run at Heteren [Yellow star = breach location]]

C.5 Detailed Linge grid

This appendix shows simulations performed with a schematisation, including a detailed grid around the Linge.

C.5.1 Breach location Bemmel

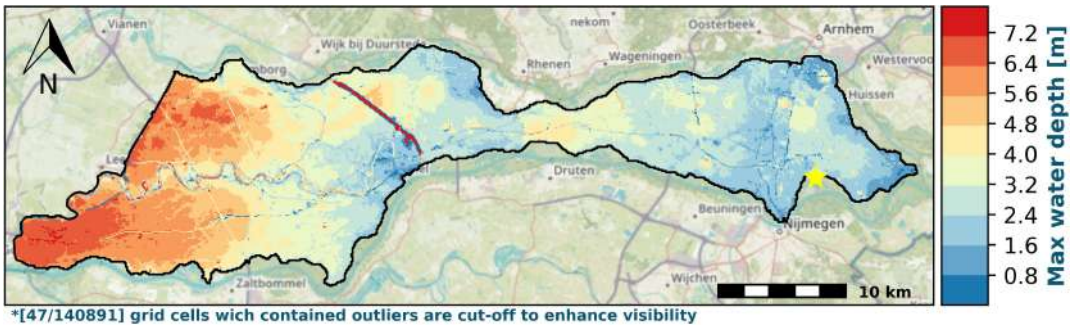

(A) Maximum inundation [m]

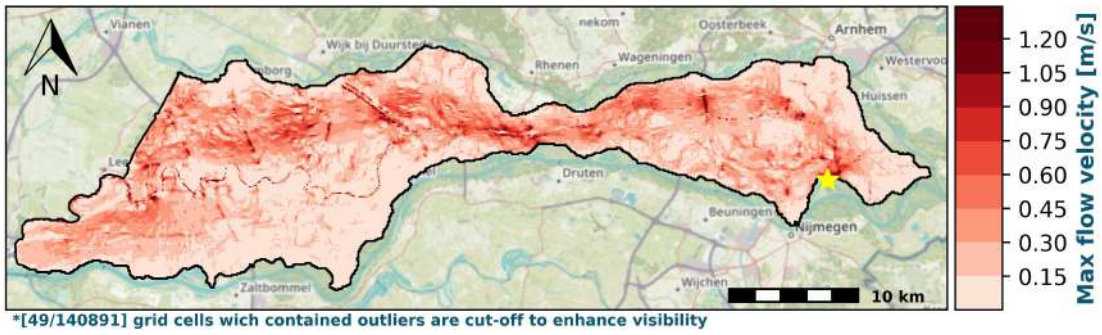

(B) Maximum flow velocity [m/s]

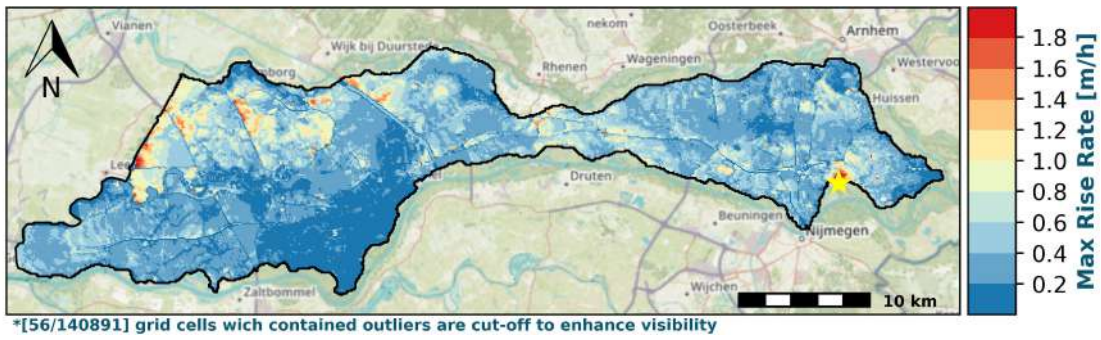

(C) Maximum Rise rate [m/h]

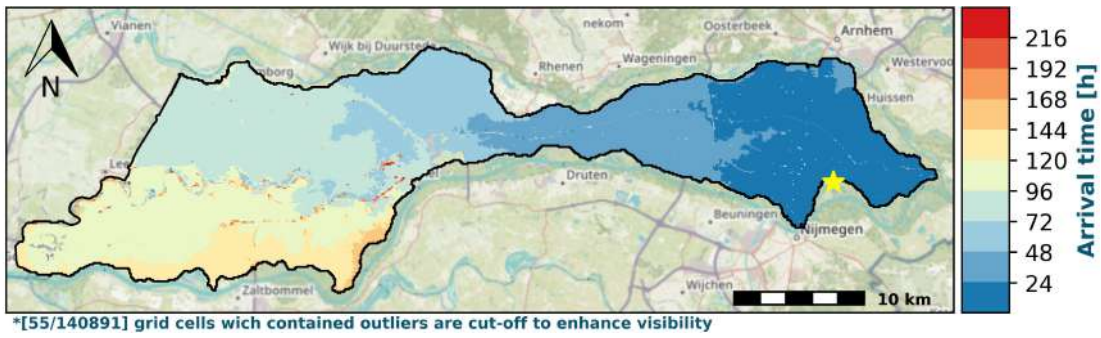

(D) Arrival time [h]

FIGURE C.18: Detailed Linge grid model run at Bemmel [Yellow star = breach location]]

C.5.2 Breach location Tiel

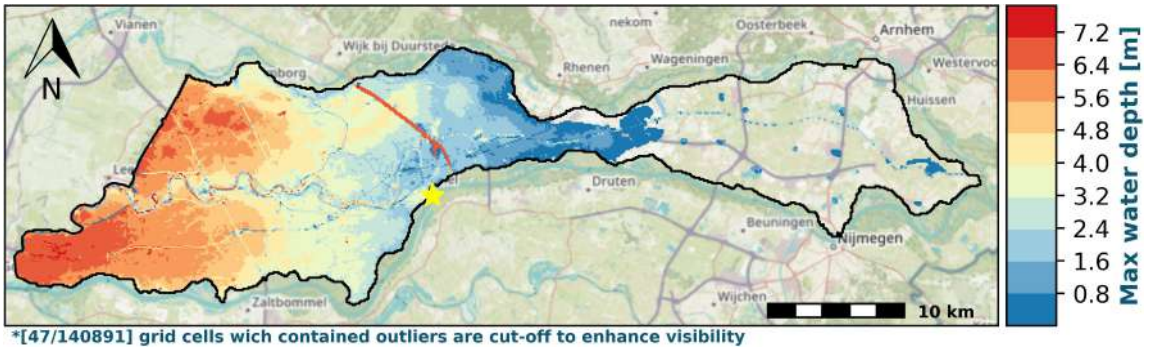

(A) Maximum inundation [m]

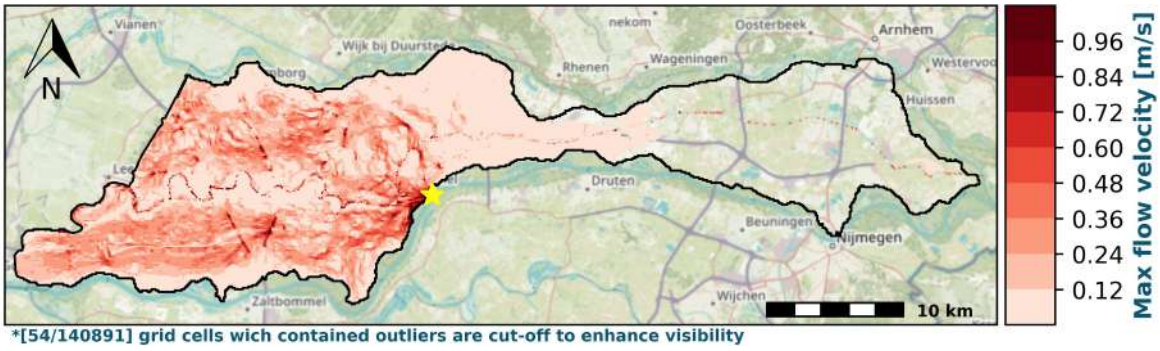

(B) Maximum flow velocity [m/s]

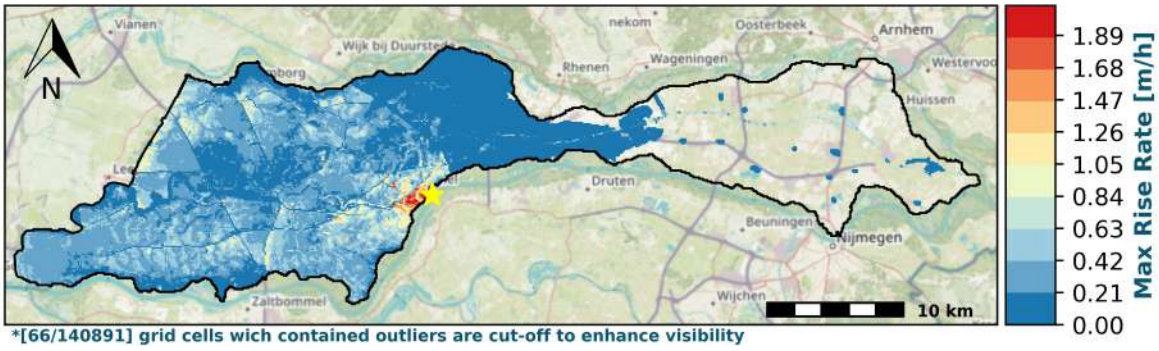

(C) Maximum Rise rate [m/h]

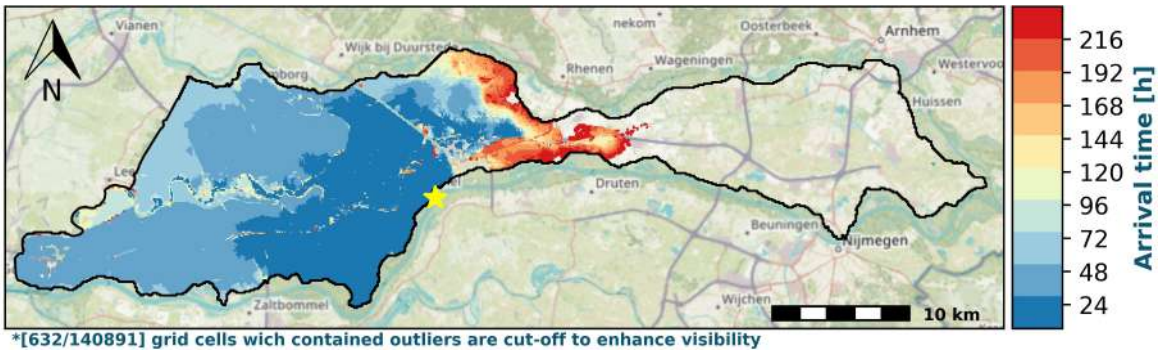

(D) Arrival time [h]

FIGURE C.19: Detailed Linge grid model run at Tiel [Yellow star = breach location]]

C.5.3 Breach location Heteren

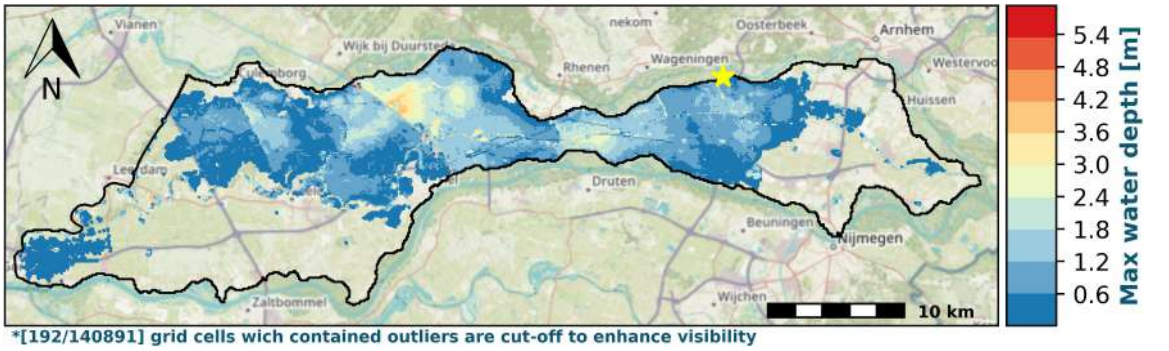

(A) Maximum inundation [m]

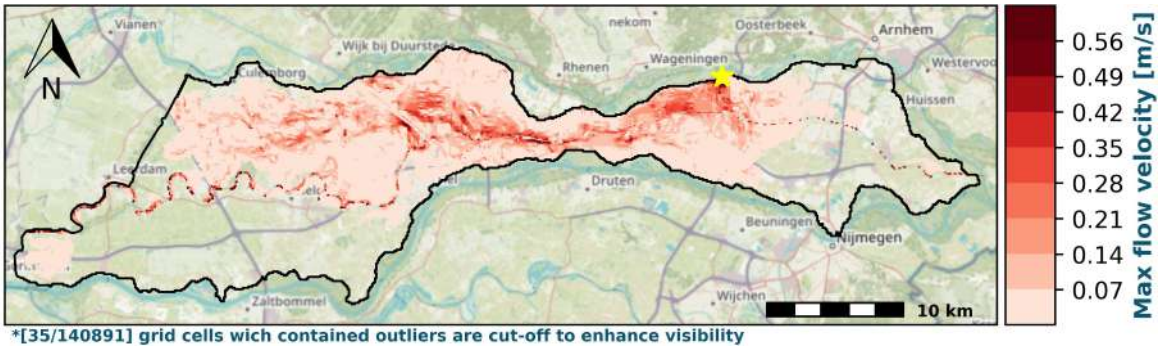

(B) Maximum flow velocity [m/s]

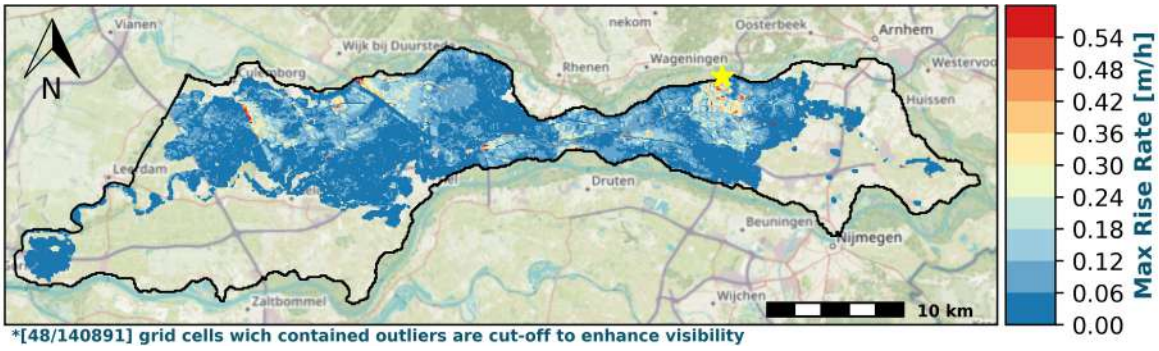

(C) Maximum Rise rate [m/h]

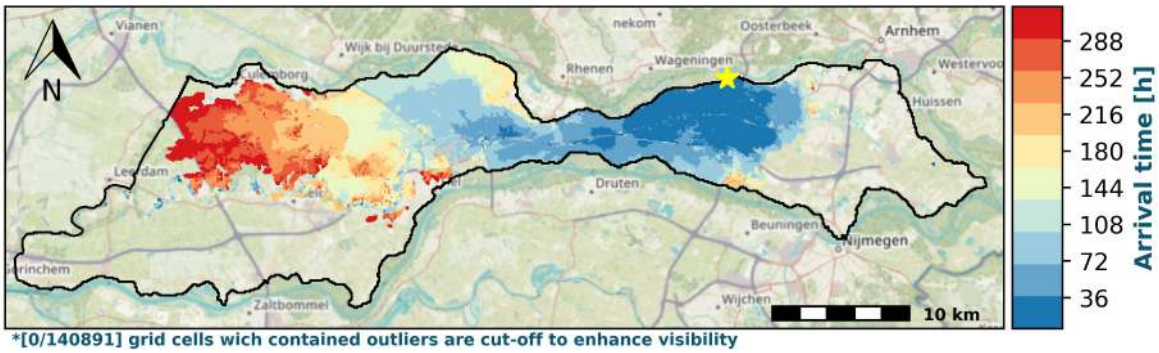

(D) Arrival time [h]

FIGURE C.20: Detailed Linge grid model run at Heteren [Yellow star = breach location]]